

AD A 097206

LEVEL IV

12

RADC-TR-80-377

Interim Report  
January 1981



## ACOSS SIX (ACTIVE CONTROL OF SPACE STRUCTURES)

The Charles Stark Draper Laboratory, Inc.

Sponsored by  
Defense Advanced Research Projects Agency (DoD)  
ARPA Order No. 3654

APPROVED FOR PUBLIC RELEASE; DISTRIBUTION UNLIMITED

The views and conclusions contained in this document are those of the authors and should not be interpreted as necessarily representing the official policies, either expressed or implied, of the Defense Advanced Research Projects Agency or the U.S. Government.

DTIC FILE COPY

ROME AIR DEVELOPMENT CENTER  
Air Force Systems Command  
Griffiss Air Force Base, New York 13441

DTIC  
ELECTE  
APR 2 1981  
S D

D

81 4 U1 024

This report has been reviewed by the RADC Public Affairs Office (PA) and is releasable to the National Technical Information Service (NTIS). At NTIS it will be releasable to the general public, including foreign nations.

RADC-TR-80-377 has been reviewed and is approved for publication.

APPROVED:

*Richard W. Carman*  
RICHARD W. CARMAN  
Project Engineer

APPROVED:

*Frank Rehm*

FRANK J. REHM  
Technical Director  
Surveillance Division

FOR THE COMMANDER:

*John P. Huss*  
JOHN P. HUSS  
Acting Chief, Plans Office

If your address has changed or if you wish to be removed from the RADC mailing list, or if the addressee is no longer employed by your organization, please notify RADC (OCSE) Griffiss AFB NY 13441. This will assist us in maintaining a current mailing list.

Do not return this copy. Retain or destroy.

ACOSS SIX (ACTIVE CONTROL OF SPACE STRUCTURES)

R. R. Strunce  
J. G. Lin  
D. R. Hegg  
R. K. Pearson  
J. P. Govignon  
T. C. Henderson

Contractor: The Charles Stark Draper  
Laboratory, Inc.

Contract Number: F30602-80-C-0096

Effective Date of Contract: 14 February 1980

Contract Expiration Date: 13 February 1981

Short Title of Work: ACOSS Six

Program Code Number: OE20

Period of Work Covered: Feb 80 - Jul 80

Principal Investigator: Robert Strunce  
Phone: 617-258-1547

Project Engineer: Richard Carman  
Phone: 315-330-3148

Approved for public release; distribution unlimited.

This research was supported by the Defense Advanced Research Projects Agency of the Department of Defense and was monitored by Richard Carman (OCSE), Griffiss AFB NY 13441 under Contract F30602-80-C-0096.

Accession For	
NTIS GRA&I	<input checked="" type="checkbox"/>
DTIC TAB	<input type="checkbox"/>
Unannounced	<input type="checkbox"/>
Justification	
By _____	
Distribution/	
Availability Codes	
Dist	Avail and/or Special
A	

DTIC  
ELECTE  
S D  
APR 2 1981  
D

## UNCLASSIFIED

SECURITY CLASSIFICATION OF THIS PAGE (When Data Entered)

(19) REPORT DOCUMENTATION PAGE		READ INSTRUCTIONS BEFORE COMPLETING FORM	
1. REPORT NUMBER RADC/TR-80-377	2. GOVT ACCESSION NO. AD-A097 306	3. RECIPIENT'S CATALOG NUMBER 9	
4. TITLE (and Subtitle) ACOSS SIX (ACTIVE CONTROL OF SPACE STRUCTURES)		5. TYPE OF REPORT & PERIOD COVERED Interim Report 14 Feb 80 - 15 Jul 80	
6. AUTHOR(s) R. Strunce Ronald, K. Pearson G. Lin Jacques, P. Govignon R. Hegg T. C. Henderson		7. PERFORMING ORGANIZATION NAME AND ADDRESS The Charles Stark Draper Laboratory, Inc. Cambridge MA 02139	
8. CONTROLLING OFFICE NAME AND ADDRESS Defense Advanced Research Projects Agency 1400 Wilson Blvd Arlington VA 22209		9. PROGRAM ELEMENT, PROJECT, TASK AREA & WORK UNIT NUMBERS 62301E 36540106 (17) 41	
10. MONITORING AGENCY NAME & ADDRESS (if different from Controlling Office) Rome Air Development Center (OCSE) Griffiss AFB NY 13441		11. REPORT DATE January 1981	
12. NUMBER OF PAGES 153		13. SECURITY CLASS. (of this report) UNCLASSIFIED	
14. DECLASSIFICATION/DOWNGRADING SCHEDULE N/A			
15. DISTRIBUTION STATEMENT (of this Report)			
Approved for public release; distribution unlimited.			
16. DISTRIBUTION STATEMENT (of the abstract entered in Block 20, if different from Report)			
Same			
17. SUPPLEMENTARY NOTES RADC Project Engineer: Richard Carman (OCSE)			
18. KEY WORDS (Continue on reverse side if necessary and identify by block number)			
Output Feedback Structural Vibration Control Draper Model #2		Modern Modal Control Structural Damping Augmentation Control Spillover Observation Spillover	
19. ABSTRACT (Continue on reverse side if necessary and identify by block number)			
This is the Charles Stark Draper Laboratory, Inc., Interim Technical Report on its Active Control of Space Structures study. The theoretical research documented in this report addresses control law design methodologies relevant to control of large space structures. Emphasis is on model reduction, design methods for determining reduced-order compensators, and criteria for determining overall closed-loop system stability. A simple but realistic evaluation model (Draper Model #2) is			

408386

bpg

**UNCLASSIFIED**

**SECURITY CLASSIFICATION OF THIS PAGE(When Data Entered)**

presented which will be used to assess performance and sensitivity of the various active structural control methods.

**UNCLASSIFIED**

**SECURITY CLASSIFICATION OF THIS PAGE(When Data Entered)**

#### ACKNOWLEDGMENT

The work reported herein was performed by the Charles Stark Draper Laboratory, Inc. (CSDL) under Contract F30602-80-C-0096. The research was supported by the Advanced Research Projects Agency of the Department of Defense, and was monitored by the Rome Air Development Center. This interim report covers the time period from 14 February 1980 to 15 July 1980. The technical monitors of this program are Lt. Col. A. Herzberg and Mr. R. Carman.

The Program Manager is Dr. Keto Soosaar and the Principal Investigator is Mr. Robert Strunce. This study was performed within the Advanced Systems Department headed by Mr. David Hoag. The contributors to this report are: Mr. Robert Strunce (Sections 1, 10), Dr. Daniel R. Hegg (Section 2), Dr. Jiguang G. Lin (Sections 3, 4, 5, 6), Mr. Ronald K. Pearson (Section 7), Mr. Jacques P. Govignon (Section 8), and Mr. Timothy C. Henderson (Section 9). Assistance from the following persons for helpful discussions is gratefully acknowledged: Dr. N. Harris McClamroch (Section 2), Dr. Timothy L. Johnson (Sections 3, 4, 7), Dr. Yu-Hwan Lin (Section 6), Mr. Robert B. Preston (Section 5), Mr. Glen Kissel (Section 6), and Mr. Yeung Yam (Section 4).

## TABLE OF CONTENTS

<u>Section</u>		<u>Page</u>
1	1.0 INTRODUCTION AND SUMMARY .....	1
	1.1 Introduction .....	1
	1.2 Research Scope .....	2
	1.3 Summary of Principal Results .....	3
2	SUBOPTIMAL OUTPUT FEEDBACK - EXTENDED KOSUT METHOD .....	6
	2.1 Introduction .....	6
	2.2 Notation .....	7
	2.3 New Results for Centralized Controllers .....	10
	2.4 New Results for Decentralized Controllers .....	14
	2.5 Proofs of Theoretical Results .....	29
	2.6 Conclusion .....	33
3	STABILITY MARGINS FOR FIXED-ORDER COMPENSATORS .....	36
	3.0 Abstract .....	36
	3.1 Closed-Loop Dynamic Equations with Observer-Based Fixed-Order Compensators .....	37
	3.2 Symmetrization of Closed-Loop Stiffness Matrices .....	40
	3.3 Closed-Loop Stability Conditions for a Two-Mode Example .....	42
4	AGGREGATE MODEL DEVELOPMENT .....	48
	4.0 Abstract .....	48
	4.1 Aggregation of Vibration Modes with Respect to Actuator and Sensor Influences .....	49
	4.2 Ideas for Specifying the Nonunique Aggregation Transformation .....	55
	4.3 Aggregation of Vibration Modes Also with Respect to Tracking and Disturbance Rejection .....	60
5	PARETO-OPTIMAL CONTROL .....	64
	5.0 Abstract .....	64
	5.1 Applicability of Multiple-Objective Optimization Methods to the Design of Vibration Controllers .....	65
	5.2 Application to Draper Tetrahedral Model of LSS .....	71

TABLE OF CONTENTS (Cont.)

<u>Section</u>		<u>Page</u>
6	GENERAL REQUIREMENTS FOR STABILIZATION .....	73
6.0	Abstract .....	73
6.1	General Conditions for Closed-Loop Stabilization by Output Feedback Control .....	74
6.2	Closed-Loop Stabilization with "Modal Dashpots" and "Modal Springs" .....	79
6.3	Prevention of Control and Observation Spillover by Synthesis of Actuator and Sensor Influences .....	81
7	STOCHASTIC OUTPUT FEEDBACK CONTROL .....	85
7.1	Introduction .....	85
7.2	Minimum Various Fixed Form Output Feedback Compensator .....	85
7.3	A Lower Bound on the Optimal SOFC Cost .....	88
7.4	Suboptimal SOFC Compensators .....	89
7.5	Conclusions .....	92
8	CALCULATION OF OPTICAL LINE-OF-SIGHT .....	95
8.1	Introduction .....	95
8.2	Results .....	95
8.3	Application to the Test Case #2 .....	101
9	DRAPER MODEL #2 .....	102
9.1	Introduction .....	102
9.2	Structural Design .....	102
9.3	Structural Analysis .....	117
9.4	System Performance .....	117
9.5	Parameter Variations .....	131
9.6	System Disturbances and Tolerances .....	133
10	PRELIMINARY ASSESSMENT OF DRAPER MODEL .....	140
10.1	Introduction .....	140
10.2	Steady State LOS Error .....	140
10.3	Sinusoidal Disturbance Impact on LOS Error .....	141
10.4	Modal Damping Requirements .....	143
10.5	Summary .....	143

## SECTION 1

### INTRODUCTION AND SUMMARY

#### 1.1. Introduction

This interim report is submitted in partial fulfillment of documentation requirements for the study: Active Control of Space Structures-Six (ACOSS Six). For the successful control of large space structures (LSS), it is recognized by the LSS community at large that the fundamental problem is the design of a finite-dimensional compensator to control an infinite dimensional system (1). To date, numerous theoretical contributions towards "solving" this problem have been made; however, the resolution of this problem requires further theoretical research which must be validated through appropriate design, analysis and experimentation. As a result of our endeavors, together with exposure to a broad spectrum of knowledge provided by the LSS community, it is our judgment that the technical issues in LSS control technology include the following:

- (1) LSS Modeling accuracy should be known to within some specified bounds. Modeling errors will limit achievable control system performance. These errors may be introduced through initially assumed structural properties or the truncation process implicit in the finite-element method. In space, LSS parameters may vary as a function of thermal gradients, configuration changes, or depletion of consumables. The more stringent the mission performance requirements, the greater the LSS model fidelity required.
- (2) Upper Atmosphere Models must be improved and verified by appropriate experiments. Accurate knowledge of the external forces (e.g., earth magnetic and gravitational fields, solar wind and radiation pressure, drag) acting upon a LSS is necessary to satisfy precision control requirements.
- (3) System Identification is necessary for the purpose of LSS structural model verification. Parameter identification techniques must be developed such that modal frequencies, damping ratios, and mode shapes can be accurately determined. Consideration must be given to the type of sensors, onboard processing requirements, data reduction, post-processing requirements, and control law configuration.
- (4) Sensor and Actuator specifications must be determined in order to assess the applicability of existing hardware, as well as to provide new directions in research and development.
- (5) Control Law Design Methodology must address the following:
  - (a) The model reduction process which reduces the high-dimensional finite-element model to a lower order design model.

- (b) The design method for determining reduced-order compensators.
- (c) The criteria for determining overall closed-loop system stability.
- (d) Direct digital design methodologies and implementation techniques.
- (e) Sensor and actuator placement techniques which yield maximum observability and controllability.
- (f) Sensor and actuator dynamics.
- (g) The dynamic interaction of the attitude, vibration, and shape control laws.

The theoretical research documented in the present report addresses control law design methodologies with particular emphasis on model reduction, design methods for determining reduced-order compensators, and criteria for determining overall closed-loop system stability.

## 1.2 Research Scope

### 1.2.1 Scope of Theoretical Research

The enabling technology necessary for successful active control of large precision space structures requires mastery of at least the following principal topics:

- (1) Reduction of high-order, high-fidelity structural models to lower-order models suitable for the design of feedback controllers.
- (2) Design of fixed-order compensators which ensures stability for the total closed-loop system.
- (3) Analytical techniques for determining overall closed-loop system stability (including robustness).

The theoretical results documented in this report address these topics. Given a finite-element modal representation of a LSS, a technique which aggregates the vibration modes with respect to actuator and sensor influences has been developed (Section 4). By proper selection of the aggregation transformation, this reduced-model may be made to approximate the open-loop performance of the LSS more accurately than methods utilizing direct modal truncation. New results relative to the extended Kosut design approach to multivariable output feedback controller design are presented in Section 2. The stochastic output feedback controller (Section 7) is formulated as the zero-order limit of the minimum variance fixed-order output feedback compensator. Section 5 discusses pareto-optimal control (multiple-objective optimization) with respect to the design of LSS vibration controllers. Stability margins for observer-based, fixed-order compensators is investigated in Section 3. The general conditions for LSS closed-loop stabilization by output feedback control are derived (see Section 6).

### 1.2.2 Scope of Applications Research

In order to assess performance, sensitivity, and hardware requirements of the various active structural control methods, a simple but realistic evaluation model is necessary. Section 9 describes such a model (Draper Model #2) which is based on realistic sizes and masses. This model contains a simple optical system with unclassified performance measures and tolerances. A line-of-sight (LOS) performance measure (Section 8) is available for evaluation purposes. Section 10 presents preliminary results of a sinusoidal disturbance (see Section 9) impact on the LOS performance.

### 1.3 Summary of Principal Results

#### 1.3.1 Results from Theoretical Research

Previously reported results relating to the algebraic consistency of, and the structure of solutions to, the Kosut gain equation are substantially improved (Section 2). Conditions for design-model-independence of free parameters occurring in such solutions are given. The nature and extent of performance degradation to be expected due to decentralizing the feedback information structure is obtained. Stable designs obtained by the extended Kosut method are shown to be robust. Major theoretical problems that need to be addressed are: (1) Characterization of systems for which the extended Kosut approach leads to a stable closed-loop design (at the design model level); (2) Synthesize a systematic procedure for assigning values to the free parameters (where available) so as to improve stability and/or performance of the full-order system incorporating the reduced-order controller.

The stability margins for fixed-order compensators (Section 3) was investigated. The observer-based fixed-order compensator was assumed since it is representative of the most general case. The objective was to find a procedure which would determine the gain matrices such that the full-order, closed-loop system remained stable. If the resulting equations could be solved analytically, then explicit stability conditions could be given. Due to the complexity of these equations, an analytical closed-form expression is not apparent at this time.

A standard approach to LSS model reduction is to truncate the open-loop modal representation directly by neglecting certain modes. The aggregate model development (Section 4) provides a technique for aggregating the vibration modes (state variables) with respect to actuator and sensor influences. The aggregation is accomplished by a similarity transformation which can be implemented by Gaussian elimination or Gram-Schmidt orthogonalization procedures. By proper choice of the aggregation transformation, the resulting model may be reduced to a lower order while retaining an approximate open-loop performance equivalent to that of the full-order model. Since the aggregation transformation is nonunique, several approaches were examined which utilized this nonuniqueness for imposing additional properties on the aggregate design model. The feasibility of these approaches was also analyzed.

Pareto optimality (Section 5) is a practical notion of "multiple-objective" optimality that is useful to control designers faced with multiple disparate performance objectives. A design is Pareto optimal if none of the multiple objectives can be further improved without degrading any other. The application of Pareto-optimal control to the design of LSS vibration controllers provides the control designer with a systematic procedure for making efficient design tradeoffs. The underlying multiple-objective design problems relevant to LSS active control are shown via Canavin's modal dashpot concept and Aubrun's low authority control theory. Favorable results were obtained by Pareto optimal designs on the 12-mode Draper tetrahedral model. Efficient tradeoffs between high damping and low output feedback gains were demonstrated.

General conditions for closed-loop LSS stabilization (Section 6) by output feedback control were developed. If these conditions are satisfied by proper design, asymptotic stability of the closed-loop LSS system is ensured. The resulting theorems are applicable to the general case of LSS that contain not only stable elastic modes but also rigid-body modes and unstable modes. A specific output feedback control design technique is also presented for integrated control of elastic and rigid-body modes which increases both the damping and frequency of selected modes. This controller is closed-loop asymptotically stable as well as robust with respect to modal truncation and parameter variations. A technique is presented for synthesis of actuator influences such that control spillover to selected modes is prevented. It is subsequently shown that this concept is readily extendable to placement of actuators which minimizes control spillover.

The minimum variance fixed form output feedback compensator has been proposed as a possible solution to the problem of designing reduced-order controllers for plants of large dimensions. The zero-order limit of this compensator is the stochastic output feedback controller (Section 7). A detailed discussion of the stochastic output feedback controller and its relation to several other compensator formulations such as the minimum order dual observer based compensator and the Levine-Athans-Johnson reduced-order compensator is presented. Lower and upper bounds on the optimal stochastic output feedback controller cost are derived. These bounds should be useful in preliminary evaluations of subsequent controller performance. These bounds may also provide useful starting estimates in iteratively computing the optimal gains. Presently, this computation represents the major theoretical problem with the stochastic output feedback controller.

### 1.3.2 Results from Applications Research

The Draper model #2 (Sections 8, 9) was evaluated with respect to the sinusoidal disturbances given in Section 9. The preliminary results (Section 10) show that the addition of damping to individual modes is not sufficient to suppress a sinusoidal disturbance impact on the steady-state LOS amplitude error.

LIST OF REFERENCES

1. Strunce, R.R., Hegg, D.R., Lin, J.G. and Henderson, T.C., Final Report, Actively Controlled Structures Theory, Vol. 1, Charles Stark Draper Laboratory Report R-1338, December 1979.

## SECTION 2

### SUBOPTIMAL OUTPUT FEEDBACK - EXTENDED KOSUT METHOD

#### 2.1 Introduction

##### 2.1.1 Synopsis of Previous Research

The Kosut approach to multivariable output feedback controller design was originally developed [1] as an alternative to optimal output feedback approaches [2] in which an acceptable solution to the strongly coupled nonlinear equations for the feedback gains was seldom obtainable [3]. By accepting suboptimal values for the control system performance measure, equations for the feedback gains were obtained that could be solved without iteration. Part of the price paid for the resultant simplicity of the design procedure was the lack of a guarantee for stability of the closed-loop system. As a result, the method found only limited application [4].

Recently, a fresh look at the Kosut approach was taken to determine its feasibility for use as a design tool for controllers of large flexible spacecraft [5]. It was immediately recognized that certain assumptions on which the method is based are incompatible with corresponding properties of reduced-order modal models that are needed for controller design with large-scale systems; in particular, the state-to-output observation matrix in the reduced-order model must have maximum rank. It was observed that this restriction on the design technique is not in fact necessary. The linear equation for the feedback gain matrix can be solved in all cases; in particular, when this equation is rank-deficient, the general solution for the feedback gains contains free parameters proportional in number to the rank-deficiency. It was demonstrated how such free parameters can be selected so as to improve the performance of the full-order closed-loop system relative to what would be possible if the rank restriction on the observation matrix were retained [6]. As part of a parallel investigation, the Kosut approach incorporating the above extensions was compared to other representative multivariable controller design approaches in the context of a specific example having certain of the principal features of a large flexible spacecraft model [5,7]. In spite of the lack of a guarantee for stability of the closed-loop design model, the performance of the example system incorporating a Kosut controller compared very favorably with that using other controller designs. Finally, an algorithm for the numerical solution of rank-deficient linear equations was developed [8] to enable application of the extended Kosut approach to high-order design models.

##### 2.1.2 Summary of New Results

New results relative to the extended Kosut design approach appearing in the present report are briefly summarized. A general criterion for stability of a closed loop system - at the design model level - for output feedback systems is given in terms of the basic parameters of the full-order

structural model, including sensor and actuator parameters, and the feedback gain matrix. A simple and useful, but undesirably restrictive, sufficient condition for stability is also given. Robustness of stability is established for designs obtained by the extended Kosut method in the situation that only rate sensing is used. In addition, certain previously reported results are improved. In particular, conditions are given under which free parameters occurring in the feedback gain matrix do not influence the stability of the design model. Under such conditions, a decision on their selection can be based solely on considerations of stability and performance of the full-order closed-loop system. Also, a simplified proof is given of the general algebraic consistency of the linear equation for the feedback gains [6].

It has been noted previously [5] that the essential nature of the Kosut design approach, including extensions, is not fundamentally altered when a decentralized information structure is imposed in the feedback path. A closer look at the differences in detail, however, suggests a much more satisfactory way of representing and understanding the general solution to the rank-deficient gain equation. A modified representation for the general solution is presented that is more readily related to the classical algebraic theory of linear spaces. The algorithm for numerical solution of such equations is correspondingly modified. A much clearer understanding of the impact of decentralization is revealed by a study of its implications upon performance for a specific system. Performance of the two-mass oscillator system incorporating several decentralized Kosut designs is examined. Specific limitations on system performance are observed when compared with corresponding centralized designs.

The section is concluded with a brief statement of important questions that remain to be resolved regarding the extended Kosut approach.

## 2.2 Notation

In order to be self-contained, the notation to be used is briefly summarized. It is assumed that the structural dynamics of systems to be discussed can be adequately represented by a finite-element model:

$$\ddot{Mq} + Kq = f \quad (2-1)$$

where  $q \equiv (q_1, \dots, q_n)^T$  is the vector of generalized physical coordinates,  $M:n \times n$  is the (positive definite) mass matrix,  $K:n \times n$  is the (positive semidefinite) stiffness matrix, and  $f \equiv (f_1, \dots, f_n)^T$  is the vector of forces applied to the structure. Equation (2-1) may be transformed to an equivalent representation in modal coordinates:

$$\ddot{\eta} + \Omega^2\eta = \Phi^T f \equiv \Phi^T B_A u \quad (2-2)$$

where  $\Omega^2:n \times n$  is the diagonal matrix containing squares of the natural frequencies  $\omega_1^2, \dots, \omega_n^2$ ,  $\Phi:n \times n$  is the nonsingular matrix whose columns are the structural mode shapes  $\phi^1, \dots, \phi^n$ , normalized such that

$$\Phi^T M \Phi = I_n, \quad \Phi^T K \Phi = \Omega^2 \quad (2-3)$$

$B_A:n \times m$  is the actuator influence matrix for the control  $u \equiv (u_1, \dots, u_m)^T$ , and  $\eta \equiv (\eta_1, \dots, \eta_n)^T$  is the vector of modal coordinates defined by

$$q = \Phi \eta \quad (2-4)$$

Superscript "T" denotes matrix transpose, and the notation  $I_n$  denotes the  $n \times n$  identity matrix. The linear measurement equation has the form:

$$y = C_p q + C_v \dot{q} \quad (2-5)$$

where  $y \equiv (y_1, \dots, y_\ell)^T$  is the vector of system outputs, and  $C_p:\ell \times n$ ,  $C_v:\ell \times n$  are the displacement and rate measurement coefficient matrices, respectively.

The structural model (2-2) may be placed in a convenient state space form as follows. Without loss of generality, it can be assumed that the components of  $\eta$  have been reordered so that the first  $N$  ( $N \leq n$ ) of them are the selected critical modes  $\eta_C \equiv (\eta_1, \dots, \eta_N)^T$ , and that the remainder are residual modes  $\eta_R \equiv (\eta_{N+1}, \dots, \eta_n)^T$ . Corresponding submatrices  $\Omega_C^2:N \times N$ ,  $\Omega_R^2:(n-N) \times (n-N)$  of  $\Omega^2$  and  $\Phi_C:n \times N$ ,  $\Phi_R:n \times (n-N)$  of  $\Phi$  are defined similarly. With  $x \stackrel{\Delta}{=} (\eta_C, \dot{\eta}_C, \eta_R, \dot{\eta}_R)$  as a state vector, the structural model (2-2), (2-4), (2-5) becomes:

$$\dot{x} = Ax + Bu \quad (2-6)$$

$$y = Cx \quad (2-7)$$

where

$$A \triangleq \begin{bmatrix} 0 & I_N & & \\ -\Omega_C^2 & 0 & & \\ & & 0 & \\ & & & I_{n-N} \\ 0 & & & \\ & & -\Omega_R^2 & 0 \end{bmatrix}, \quad B \triangleq \begin{bmatrix} 0 \\ \Phi_C^T B_A \\ 0 \\ \Phi_R^T B_A \end{bmatrix}$$

$$C \triangleq \begin{bmatrix} C_P \Phi_C & C_V \Phi_C & C_P \Phi_R & C_V \Phi_R \end{bmatrix}.$$

Using residual mode truncation as the model reduction process, a reduced-order model with the state  $x_C \triangleq (\eta_C, \dot{\eta}_C)$  is obtained:

$$\dot{x}_C = A_C x_C + B_C u \quad (2-8)$$

$$y_C = C_C x_C \quad (2-9)$$

where

$$A_C \triangleq \begin{bmatrix} 0 & I_N \\ -\Omega_C^2 & 0 \end{bmatrix}, \quad B_C \triangleq \begin{bmatrix} 0 \\ \Phi_C^T B_A \end{bmatrix},$$

$$C_C \triangleq \begin{bmatrix} C_P \Phi_C & C_V \Phi_C \end{bmatrix}.$$

## 2.3 New Results for Centralized Controllers

### 2.3.1 Stability and Robustness for Output Feedback Designs

#### 2.3.1.1 General Criteria for Stability

As noted previously, one of the principal objections to the use of the extended Kosut method for controller design is the absence of any useful conditions which guarantee closed-loop stability even at the design model level. The approach taken to developing such conditions has been to try to discover an appropriate subclass of the systems (2-8), (2-9) being considered for which the extended Kosut approach leads to a stable closed-loop system at the design model level.

The first result characterizes the eigenvalues of the closed-loop design model for general output feedback systems in terms of fundamental model parameters.

**Theorem 2-1.** Assume that the reduced-order model (2-8), (2-9) is connected by an output feedback law:  $u = Gy_C$ . Then the eigenvalues of the closed-loop system are the roots of the  $(2N)$ th degree polynomial equation:

$$\det \left\{ \Phi_C^T \left[ -\lambda^2 M + \lambda B_A G C_V - (K - B_A G C_P) \right] \Phi_C \right\} = 0 \quad \square \quad (2-10)$$

The proof is given in Section 2.5. A remark about Equation (2-10) is appropriate. Since the mode shapes  $\phi^1, \dots, \phi^n$  are linearly independent, the matrix  $\Phi_C \equiv [\phi^1; \dots; \phi^N] : n \times N$  has maximum rank. It does not follow that equation (2-10) can be replaced with the  $(2n)$ th degree polynomial equation:

$$\det \left[ -\lambda^2 M + \lambda B_A G C_V - (K - B_A G C_P) \right] = 0 \quad (2-11)$$

The latter equation is easily recognized as the closed loop characteristic equation for the full-order structural model (2-1), (2-5) connected with the output feedback law  $u = Gy$ . (Set  $\lambda = i\omega$  in equation (2-11) to obtain an equivalent, more familiar, form.) Equation (2-11) has  $2(n - N)$  more solutions than equation (2-10).

A simple, but useful, sufficient condition for closed-loop design model stability is based on Theorem 2-1. For clarity, the result is presented for the case where rate sensors only are used ( $C_P = 0$ ).

Corresponding results for the general case are easily obtained.

Theorem 2-2. Assume a closed-loop structure as in Theorem 2-1 with  $C_p = 0$ . Suppose that there exist  $\delta_i > 0$ ,  $i = 1, \dots, N$  such that  $\Phi_{CA}^T B_A G C_V \Phi_C = \text{diag}(-\delta_i)$ . Then the closed-loop system is stable.  $\square$

The proof is given in Section 2.5. This result is useful for establishing robustness of stability.

Specializing from general output feedback systems to those designed using the extended Kossut method, one may ask under what conditions the feedback gain matrix generated by that method satisfies the hypotheses of Theorem 2-2. This question has not been answered in general. It should be evident, however, that Theorem 2-2 is by no means necessary for design model stability; it is in fact a quite restrictive condition. This may be seen by examining the condition in the context of the two-mass oscillator example worked out previously [5; Sec. 6]. In that case,  $\Phi_{CA}^T B_A G C_V \Phi_C = (\phi^2)^T G \phi^2$ , a scalar (hence diagonal), where

$$G = G(\sigma; \varepsilon, \delta) = \begin{bmatrix} -\sigma + \varepsilon \frac{\phi_2^2}{\phi_1^2} & -\varepsilon \\ -\delta & -\sigma + \delta \frac{\phi_1^2}{\phi_2^2} \end{bmatrix}$$

The stability condition of Theorem 2-2 reduces here to the condition that  $G$  be negative definite, which requires [10] that:

$$\sigma - \varepsilon \frac{\phi_2^2}{\phi_1^2} > 0$$

and

$$\sigma \left[ \sigma - \varepsilon \frac{\phi_2^2}{\phi_1^2} - \delta \frac{\phi_1^2}{\phi_2^2} \right] > 0.$$

However, it was seen [5; Sec. 6] that this closed-loop design model  $A_C + B_C G C_C$  is independent of the free parameters  $\varepsilon$  and  $\delta$ , and is in fact stable as long as  $\sigma > 0$ .

### 2.3.1.2 Robustness of Stability for the Extended Kosut Method

The robustness question is examined in two parts. First, the sensitivity of the design model closed-loop eigenvalues is examined relative to changes in the feedback gain matrix. This is applicable to any output feedback system. Second, the sensitivity of the gains generated by the extended Kosut method is examined relative to changes in the fundamental structural model parameters. For clarity, it is again assumed that rate sensing only is used ( $C_p = 0$ ).

Theorem 2-3. Assume a closed-loop structure as in Theorem 2-1 with  $C_p = 0$ .

The mapping which assigns to each output feedback gain matrix the set of closed-loop eigenvalues is continuous.  $\square$

The proof is given in Section 2.5. The significance of Theorem 2-3 is as follows. Suppose that for a particular gain  $G_0$  the system is stable. Then the corresponding eigenvalues  $\lambda^0 \equiv (\lambda_1^0, \dots, \lambda_{2N}^0)$  lie in the Cartesian product of the sets  $\operatorname{Re}(\lambda_i) < 0$ , an open set in real Euclidean  $2N$ -space.

Theorem 2-3 says that there is an open set containing  $G_0$  in the space of  $m \times l$  real matrices for which the corresponding eigenvalues also satisfy  $\operatorname{Re}(\lambda_i) < 0$ ,  $i = 1, \dots, 2N$ . It should be noted that Theorem 2-3 is essentially without significance if at least one stable set of eigenvalues cannot be found (cf. Theorem 2-2).

For the following result, it is assumed that structural model reduction is by truncation (equations (2-8), (2-9)), and that a specific reference system and a specific suboptimal performance measure for the extended Kosut method (minimum error excitation) have been chosen. The mapping described is then well defined.

Theorem 2-4. Assume  $C_p = 0$ . The mapping which assigns to each mass-stiffness matrix pair in Equation (2-1) the extended-Kosut feedback gain matrix (Moore-Penrose inverse particular solution [8]) is continuous.  $\square$

The proof is given in Section 2.5. Together with Theorem 2-3, this result shows that if a stable design can be achieved by the extended Kosut method, then stability is retained under appropriately small changes in the fundamental structural model parameters.

### 2.3.2 Refinement of Previously Reported Results

Extensions to the Kosut method reported previously [5] are based on the existence and properties of solutions  $G: m \times l$  to the Kosut gain equation:

$$G \left( C_C P C_C^T \right) = F^* P C_C^T \quad (2-12)$$

where  $F^*:m \times 2N$  is the state feedback gain for the stable reference system used in the suboptimal design, and  $P:2N \times 2N$  is the positive definite Lagrange multiplier matrix obtained from the Liapunov equation:

$$(A_C + B_C F^*)P + P(A_C + B_C F^*)^T + I_{2N} = 0 \quad (2-13)$$

It was shown [5; para. 6.2.3.3] that Equation (2-12) is solvable regardless of the rank of  $C_C$  (equivalently, rank of  $C_C P C_C^T$ ), and that in the rank-deficient case (say, rank  $C_C = r < \ell \leq 2N$ ), the general solution has the form:

$$G(\Gamma) = G_0 + \Gamma S \quad (2-14)$$

where  $G_0$  is a particular solution of Equation (2-12),  $\Gamma$  is a matrix whose  $m \cdot (\ell-r)$  non-zero elements are free parameters, and  $S$  is an appropriate non-singular matrix.

In a detailed design example, it was observed that the eigenvalues of the closed-loop design model were independent of the (two) free parameters in the feedback gain matrix. Since the performance (as contrasted with the stability) of the design model is not of practical interest, it was possible to base the selection of free parameter values solely on full-order system performance considerations. The question arises as to what conditions characterize this "independence" in general. To begin, a very simple sufficient condition can be stated.

Fact 2-5. Assume a closed-loop structure as in Theorem 2-1; refer to Equation (2-14). If  $B_C \Gamma S C_C = 0$ , then the eigenvalues of the closed-loop design model are independent of the free parameter matrix  $\Gamma$ .  $\square$

The proof is self-evident, since both  $G(\Gamma)$  and  $G_0$  generate the same closed-loop system matrix. It is worth observing that this condition (in fact, even the stronger condition:  $\Gamma S C_C = 0$ ) has been satisfied in all numerical examples studied to date. The following theorem fully characterizes the independence condition.

Theorem 2-6. Assume a closed-loop structure as in Theorem 2-1; refer to Equation (2-14). The eigenvalues of the closed-loop design model are independent of the free parameter matrix  $\Gamma$  if and only if  $A_C + B_C G(\Gamma) C_C$  and  $A_C + B_C G_0 C_C$  are similar; i.e., if and only if there exists a nonsingular matrix  $Q:2N \times 2N$  such that:

$$[A_C + B_C G(\Gamma) C_C]Q - Q[A_C + B_C G_0 C_C] = 0. \quad \square$$

The proof is given in Section 2.5. The full implications of this freedom of choice in selecting a feedback gain matrix with the extended Kosut method have not yet been uncovered. Performance improvements for low-order vibrating systems have already been demonstrated [5,6]. It is worth observing, however, that the question of effective use of available freedom of choice in selections of feedback gains is an important, and largely unexplored, question for general multivariable feedback systems [13;p.51].

Proof of the general algebraic consistency of Equation (2-12) has been considerably simplified (cp. [6;Theorem 2], [5;Theorem 6-6]). Since this is a principal result, the streamlined proof is of interest. Details are given in Section 2.5.

## 2.4 New Results for Decentralized Controllers

### 2.4.1 New Perceptions Suggested by Decentralization

The discussion of decentralization in this section of the report is restricted to the nature of the information structure in the sensor-to-actuator feedback connection. Totally decentralized systems which include decentralized plant structures are not treated. Specifically, it is assumed that the information for driving a given actuator is derived from a (possibly proper) subset of all available sensors, and that the collection of sensors in this subset is (in general) different from one actuator to another. In symbols, the sensor combinations for transmission to each actuator are generated from the state vector as follows:

$$y^i = C^i x, \quad C^i : \ell_i \times 4N ; \quad i = 1, \dots, m \quad (2-15)$$

Equation (2-15) replaces Equation (2-7) in a decentralized full-order model. The feedback connection is made by:

$$u_i = g_i^T y^i, \quad g_i : \ell_i \times 1 ; \quad i = 1, \dots, m \quad (2-16)$$

Remark: In the special case that the components of each  $y^i$  are selections from the components of a fixed vector  $y \equiv (y_1, \dots, y_\ell)^T$ , Equation (2-16) may be written in the form  $u = Gy$ , where  $u \equiv (u_1, \dots, u_m)^T$ , and  $G \equiv [g_{ij}]$  has the property that  $g_{ij} = 0$  if the component  $y_j$  of the fixed vector  $y$  is not also a component of the output vector  $y^i$  associated with  $u_i$ . In general, however, this situation will not necessarily exist.

The Kosut gain equations corresponding to Equation (2-12) for a controller with decentralized feedback structure are [5]:

$$g_i^T \left( C_C^i P C_C^i \right)^T = F_i^* P C_C^i \quad , \quad i = 1, \dots, m \quad (2-17)$$

where  $F_i^*: 1 \times N$  are the rows of  $F^*$ , and  $C_C^i: \ell_i \times 2N$  are the matrices corresponding to Equation (2-15) for a reduced-order model. The structure of solutions to algebraically consistent equations of the form (2-17) may be expressed in the following form.

Theorem 2-7. Let  $A: \lambda \times v$ ,  $b: 1 \times v$  be matrices for which the equation  $xA = b$  has a solution  $x_0$ . Denote  $r \triangleq \text{rank } (A)$ . The general solution of this equation has the form:

$$x = x_0 + \gamma^T S \quad (2-18)$$

where the  $\lambda - r$  row vectors of  $S: (\lambda - r) \times \lambda$  form a basis for the null space of  $A$  (viewed as a mapping of  $E^\lambda$  into  $E^v$ ), and the  $(\lambda - r)$ -vector  $\gamma$  is arbitrary.  $\square$

The proof is given in Section 2.5. This result immediately suggests an appropriate reformulation of previously reported solution structures for homogeneous matrix equations [cf. 5, Theorem 6-3; 6, Theorem 3; 8, Theorem 3-9] which sharpens the statement and identifies the true nature of the "S" matrix.

Theorem 2-8. Let  $A: \lambda \times v$  be a matrix. Denote  $r \triangleq \text{rank } (A)$ . The general solution of the equation  $XA = \underset{\mu}{0}$  has the form  $X = \Gamma S$ , where the  $\lambda - r$  row vectors of  $S: (\lambda - r) \times \lambda$  form a basis for the null space of  $A$  (viewed as a mapping from  $E^\lambda$  into  $E^v$ ), and the matrix  $\Gamma: \mu \times (\lambda - r)$  is arbitrary.  $\square$

This result shows that the last  $\lambda - r$  rows of the  $S$  matrix in Theorem 6-3 of [5] and the last  $\ell - r$  rows of the  $U^T$  matrix in Theorem 3-9 of [8] correspond simply to different choices of a basis for the null space of  $A$ .

Step 4 of the algorithm for numerical solution of the Kosut gain equation [8, Sec. 3.5] should now be modified so as to be consistent with Theorem 2-8.

Step 4 (revised). Find the general solution.

(a) Select an  $m \times (\lambda - r)$  matrix  $\Gamma$  of free parameters.

(b) Choose row  $l$ -vectors  $s_1, \dots, s_{l-r}$  that form a basis for the null space of  $A$  and form the matrix

$$S \triangleq \begin{bmatrix} s_1 \\ \vdots \\ s_{l-r} \end{bmatrix}.$$

(One possible choice is the set of vectors obtained by transposing columns  $r+1, \dots, l$  of the matrix  $U$  from Step 1(a)).

(c) Compute the homogeneous solution  $X_c \triangleq PS_c$ .

(d) Compute the general solution  $X = X_p + X_c$ , using the results of Steps 3(b) and 4(c).  $\square$

Step 4(b) makes explicit the fact that there is considerable freedom in choosing the matrix  $S$  (although not complete arbitrariness). Specific approaches to exploiting this freedom of choice await further investigation.

#### 2.4.2 Performance Implications of Decentralization

There are a number of reasons why a decentralized information structure might be incorporated in a physical system. For a very large structure with many sensors, the computational burden of incorporating information from all of the sensors in the determination of control signals to each actuator may far outweigh the advantages when a centralized processing unit is used. If numerous processing units are distributed throughout the structure, it may not be feasible to transmit information from all the sensors to each processing unit. On the other hand, there are cases in which the only relevant information is that from nearby sensors (e.g., in the case of shape control), in which case information from all the sensors at each processing unit would be largely unnecessary. Whatever the reasons, however, it is important to take these information structure constraints explicitly into account in the mathematical model used for controller design and evaluation. In general, one would expect some loss in performance (by whatever measure) as the price of operating with restrictions on the internal information structure for determining control signals.

A clear picture of such performance implications does not emerge from the design equations themselves. In fact, the gain equations (2-17) for the decentralized controller have exactly the same mathematical structure as the gain equation (2-12) for the centralized controller. Hence, all the results obtained for the latter (e.g., algebraic consistency, structure of general solution) apply to the former. Therefore, some design calculations were made on a specific representative system (the two-mass oscillator example [5])

to get at least a snapshot of the nature of performance degradation, if any, associated with decentralization of the controller. The oscillator was assumed to have one force actuator and one rate sensor associated with each mass [5; Fig. 2-2]. Each of three possible types of decentralization in the feedback structure was studied: (a) fully decentralized:  $u_1 = u_1(y_1)$ ,  $u_2 = u_2(y_2)$ ; (b) partially decentralized with actuator 1 localized:  $u_1 = u_1(y_1)$ ,  $u_2 = u_2(y_1, y_2)$ ; (c) partially decentralized with actuator 2 localized:  $u_1 = u_1(y_1, y_2)$ ,  $u_2 = u_2(y_2)$ . The reference system for the Kosut design was taken as determined in previous examples [5]. Hence  $F^*$ , and also  $P$ , [cf. Equation (2-13)] are as previously computed:

$$F^* = \begin{bmatrix} F_1^* \\ \hline \hline F_2^* \end{bmatrix} = \begin{bmatrix} 0.066389774 & 0.51609641 \\ -0.028241581 & -0.21954252 \end{bmatrix},$$

$$P = \begin{bmatrix} 1.1373892 & -0.5 \\ -0.5 & 7.4375655 \end{bmatrix}.$$

#### 2.4.2.1 Fully Decentralized Design

Recall that the state vector for the reduced-order model [cf. Equation (2-8)] is  $x_C \triangleq (\eta_2, \dot{\eta}_2)$ , that residual mode ( $\eta_1$ ) dynamics are being ignored, and that Equation (2-4) relates the physical and modal coordinates. The specifications for this configuration may be stated:  $y^1 = \dot{q}_1$ ,  $y^2 = \dot{q}_2$ . Accordingly, the matrices  $C_C^i$  corresponding to Equation (2-15) for the reduced-order system are:

$$C_C^1 \triangleq \begin{bmatrix} 0 & \phi_1^2 \end{bmatrix}, \quad C_C^2 \triangleq \begin{bmatrix} 0 & \phi_2^2 \end{bmatrix}.$$

Since each  $C_C^i$  has maximum rank, each of the gain equations (2-17) has a unique solution. The solutions are:

$$g_1 = -\sigma^0 = g_2$$

where  $\sigma^0 = 0.59708155$  is the reference-system-dependent parameter occurring in the solution of Equation (2-12) for the centralized design [5, Eq.(6-43)].

Referring to the remark following Equation (2-16), we may write the feedback connection as  $u = Gy_C$ , where

$$G \triangleq \begin{bmatrix} g_1^T & 0 \\ 0 & g_2^T \end{bmatrix} = \begin{bmatrix} -\sigma^0 & 0 \\ 0 & -\sigma^0 \end{bmatrix}$$

The closed loop design model has the same characteristic polynomial as in the centralized case:

$$\lambda^2 + \sigma^0(\phi^2 \phi^2) \lambda + \omega_2^2$$

It is stable, with  $\omega = \omega_2$  (open-loop critical mode frequency), and  $\zeta = 0.1$  (design objective). Note that, in contrast to the corresponding centralized design, there are no free parameters in the solution for the feedback gains.

The matrices  $C^1$  of Equation (2-15) for the full-order system:

$$C^1 \triangleq \begin{bmatrix} 0 & \phi_1^2 & 0 & \phi_1^1 \end{bmatrix}, \quad C^2 \triangleq \begin{bmatrix} 0 & \phi_2^2 & 0 & \phi_2^1 \end{bmatrix}$$

are used to connect the reduced-order controller to the full-order system via Equation (2-16). The characteristic polynomial for the closed-loop full-order system is

$$\begin{aligned} \det & \left( A + B \begin{bmatrix} g_1^T C^1 \\ g_2^T C^2 \end{bmatrix} - \lambda I_{4N} \right) \\ & = \left[ \lambda^2 + \sigma^0(\phi^2 \phi^2) \lambda + \omega_2^2 \right] \left[ \lambda^2 + \sigma^0(\phi^1 \phi^1) \lambda + \omega_1^2 \right] - \lambda^2 \sigma^0 (\phi^2 \phi^1)^2 \end{aligned}$$

Dynamic characteristics of this system are:

$$\text{Mode 1 (critical): } \omega_{2C} = 2.5851902 \text{ sec}^{-1}$$

$$\zeta_{2C} = 0.099939961$$

$$\text{Mode 1 (residual): } \omega_{1C} = 0.54704429 \text{ sec}^{-1}$$

$$\zeta_{1C} = 0.34631083$$

Some effects of decentralization on overall system performance can be seen by comparing the time response in Figure 2-1 and the frequency response in Figure 2-2 with the corresponding plots for the centralized design [5; Figs. 6-7 and 6-8, respectively]. Noticeable degradation does occur, and is traceable to the reduction in damping of the residual mode. Nonetheless, the degradation is not nearly as severe as that occurring when the sensor on the outer mass of the two-mass system is deactivated while retaining a centralized information structure on the remaining available sensor [5; Figs. 6-13 and 6-14, respectively].

#### 2.4.2.2 Partially Decentralized Design: Actuator 1 Localized

The specifications for this configuration may be stated:  $y^1 = \dot{q}_1$ ,  $y^2 = (\dot{q}_1, \dot{q}_2)^T$ . The related matrices  $C_C^i$  corresponding to Equation (2-15) for the reduced-order system are:

$$C_C^1 \triangleq \begin{bmatrix} 0 & \phi_1^2 \end{bmatrix}, \quad C_C^2 \triangleq \begin{bmatrix} 0 & \phi^2 \end{bmatrix}$$

Solutions to the gain equations (2-17) are as follows:

$$g_1 = -\sigma^0, \quad g_2^T(\delta) = \begin{bmatrix} \phi_1^2 \\ -\delta & -\sigma^0 + \delta \phi_1^2 / \phi_2^2 \end{bmatrix}$$

where  $\delta$  is a free parameter. An equivalent feedback connection of form  $u = Gy_C$  exists and is:

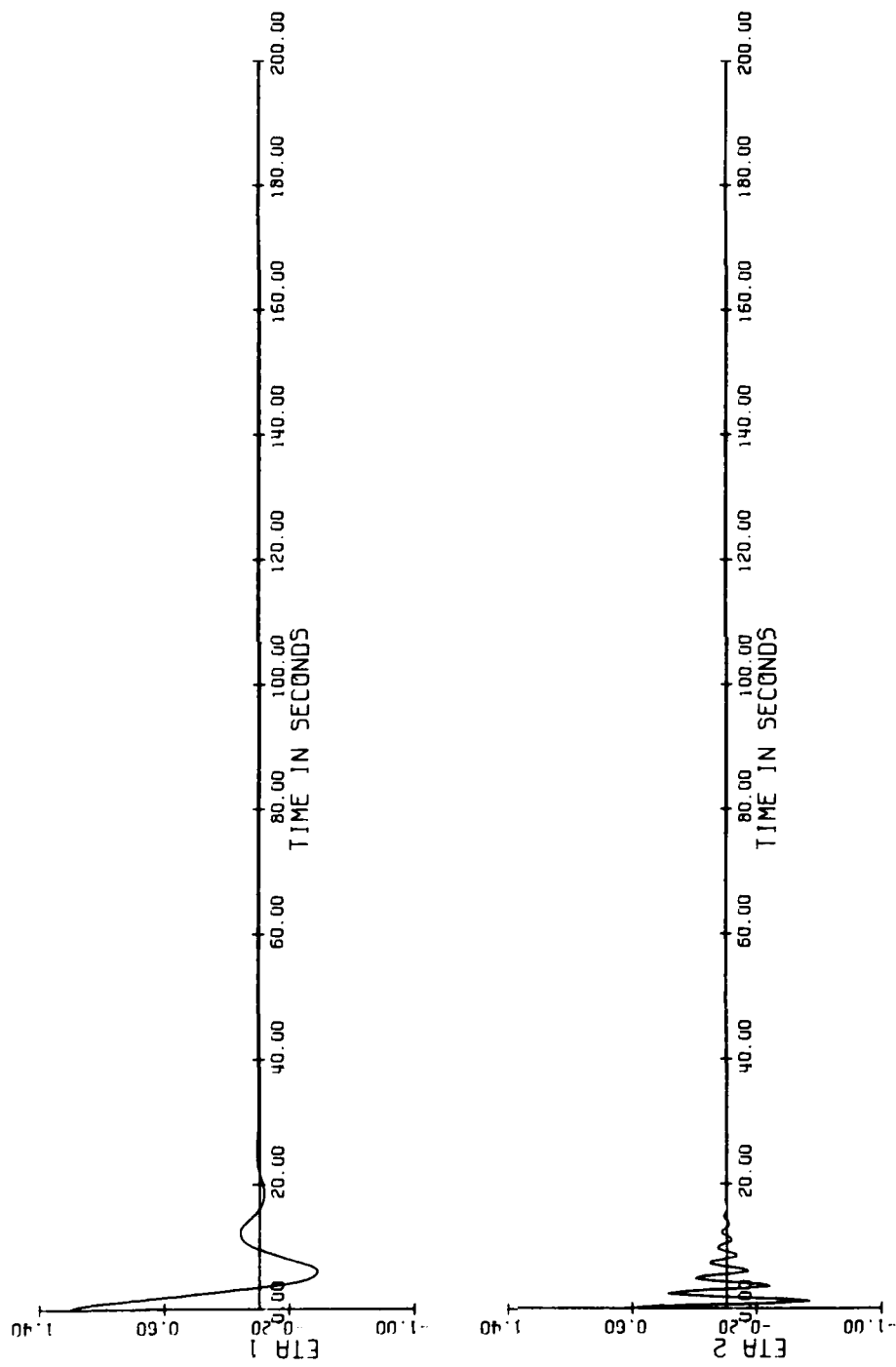
$$G(\delta) \triangleq \begin{bmatrix} g_1^T & 0 \\ \hline \hline & \hline \hline \\ g_2^T(\delta) & \end{bmatrix} = \begin{bmatrix} -\sigma^0 & 0 \\ -\delta & -\sigma^0 + \delta \phi_1^2 / \phi_2^2 \end{bmatrix}$$

The characteristic polynomial for the closed-loop design model is the same as that for the preceding design; in particular, it is independent of the free parameter  $\delta$ .

The matrices  $C^i$  of Equation (2-15) for the full-order system are:

$$C^1 \triangleq \begin{bmatrix} 0 & \phi_1^2 & 0 & \phi_1^1 \end{bmatrix}, \quad C^2 \triangleq \begin{bmatrix} 0 & \phi^2 & 0 & \phi^1 \end{bmatrix}$$

SYSTEM: Q101      I.C.     $Q_2(0) = 1$ .



TIME: 18:25:21.2    DATE: 09/09/80 (80/253)  
TIME: 18:25:21.2    DATE: 09/09/80 (80/253)  
Figure 2-1. Modal response to initial conditions  $q_1(0) = \dot{q}_1(0) = 0$ ,  $q_2(0) = 1$   
(fully decentralized controller).

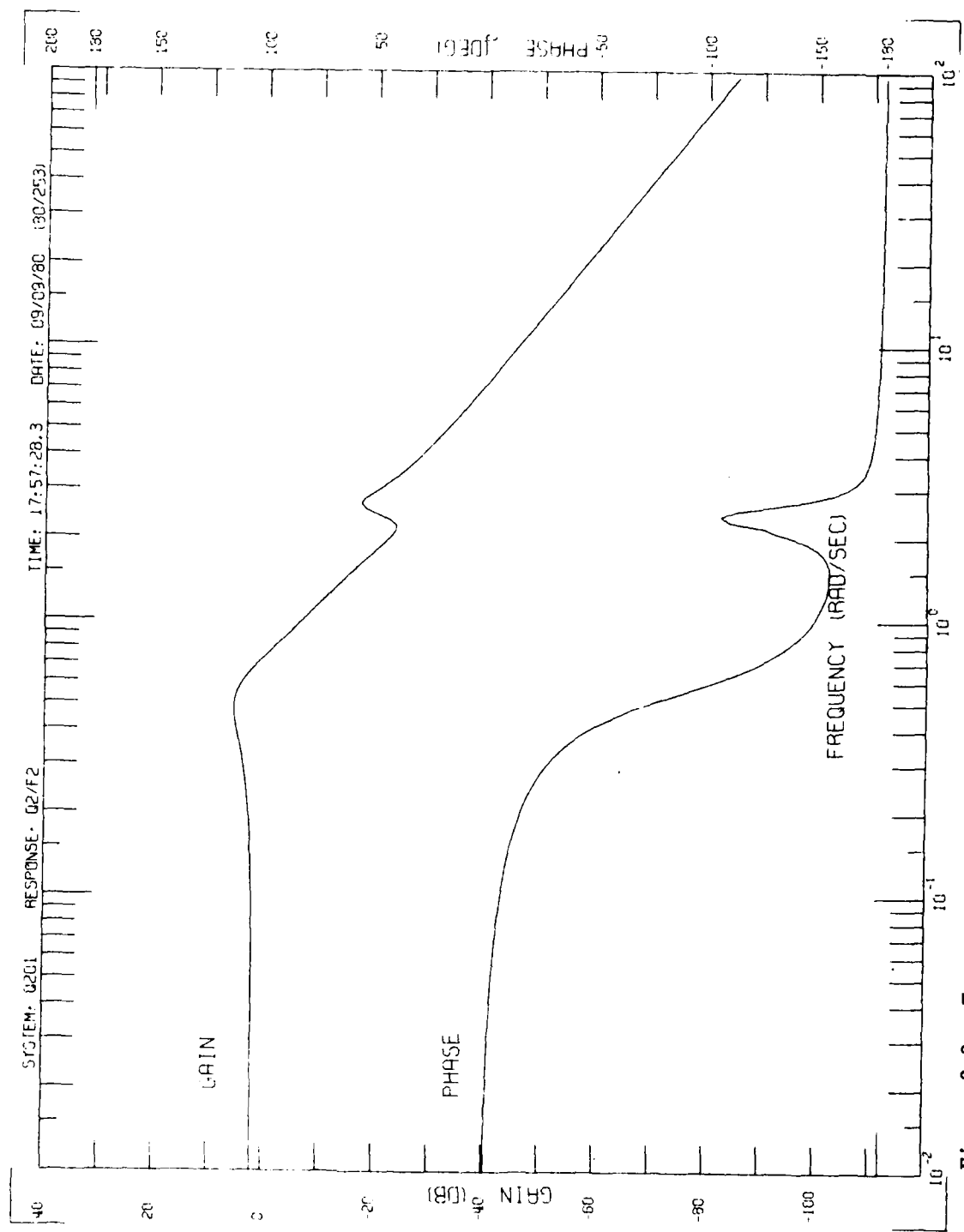


Figure 2-2. Frequency response of  $q_2$  to periodic disturbance  $f_2(t) = \sin \omega t$  (fully decentralized controller).

To assist in determining an appropriate value for the free parameter, the modal closed-loop equations are developed:

$$\ddot{\eta}_2 + \sigma^0(\phi^2 \phi^2) \dot{\eta}_2 + \omega_2^2 \eta_2 = \left[ -\sigma^0(\phi^2 \phi^1) - \delta \det \Phi \right] \dot{\eta}_1 \quad (2-19)$$

$$\ddot{\eta}_1 + \left[ \sigma^0(\phi^1 \phi^1) + \delta \det \Phi \left( \frac{\phi^1}{\phi_2^2} \right) \right] \dot{\eta}_1 + \omega_1^2 \eta_1 = \left[ -\sigma^0(\phi^2 \phi^1) \right] \dot{\eta}_2 \quad (2-20)$$

Several possibilities for selecting  $\delta$  are as follows: (a) choose  $\delta$  so that the coefficient of  $\dot{\eta}_1$  in Equation (2-19) vanishes; (b) choose  $\delta$  so that the coefficient of  $\dot{\eta}_1$  in Equation (2-20) attains some desired value; or (c) some combination of (a) and (b). Selection (a) eliminates the effect on the critical mode of residual mode dynamics, whereas selection (b) approximates a specification for the residual mode damping. Past design examples have indicated that failure to damp the residual mode strongly and adversely affects the full system performance, and that the spillover effect admitted by Equation (2-19) is a lesser concern. Since selection (a) will not affect residual mode damping, whereas selection (b) will tend to reduce the spillover problem indicated by Equation (2-19), selection (b) is made. Thus:

$$\delta^0 \triangleq \frac{2\zeta_{1D}\omega_1 - \sigma^0(\phi^1 \phi^1)}{\det \Phi \left( \frac{\phi^1}{\phi_2^2} \right)} = 0.33580542$$

where  $\zeta_{1D}$  is chosen to be  $1/\sqrt{2}$ . The gain values then become:

$$G(\delta^0) = \begin{bmatrix} -0.59708155 & 0 \\ -0.33580542 & -1.3864866 \end{bmatrix}$$

With this connection, the dynamic characteristics of the system are:

$$\text{Mode 2 (critical): } \omega_{2C} = 2.5914658 \text{ sec}^{-1}$$

$$\zeta_{2C} = 0.10021320$$

$$\text{Mode 1 (residual): } \omega_{1C} = 0.54571957 \text{ sec}^{-1}$$

$$\zeta_{1C} = 0.70633967$$

Performance of this design is so close to that of the corresponding centralized design that no degradation can be observed from the plots. Figures 2-3 and 2-4 may be compared with the corresponding plots for the centralized system [5; Figs. 6-7 and 6-8, respectively]. Consequently, Figures 2-3 and 2-4 may themselves be viewed as representing the centralized system time and frequency response, respectively, for the purposes of the comparisons in this section.

#### 2.4.2.3 Partially Decentralized Design: Actuator 2 Localized

The specifications for this configuration may be stated:  $y^1 = (\dot{q}_1, \dot{q}_2)^T$ ,  $y^2 = \dot{q}_2$ . The related matrices  $C_C^1$  corresponding to Equation (2-15) for the reduced-order system are:

$$C_C^1 \triangleq \begin{bmatrix} 0 & \phi^2 \end{bmatrix}, \quad C_C^2 \triangleq \begin{bmatrix} 0 & \phi_2^2 \end{bmatrix}$$

Solutions to the gain equation (2-17) are as follows:

$$g_1^T(\epsilon) = \begin{bmatrix} \phi_2^2 & -\epsilon \\ -\sigma^0 + \epsilon \phi_2^2 / \phi_1^2 & -\epsilon \end{bmatrix}, \quad g_2 = -\sigma^0$$

where  $\epsilon$  is a free parameter. An equivalent feedback connection of form  $u = Gy_C$  is:

$$G(\epsilon) \triangleq \begin{bmatrix} g_1^T(\epsilon) \\ \hline \hline 0 & g_2^T \end{bmatrix} = \begin{bmatrix} \phi_2^2 & -\epsilon \\ -\sigma^0 + \epsilon \phi_2^2 / \phi_1^2 & -\epsilon \\ 0 & -\sigma^0 \end{bmatrix}$$

The characteristic polynomial for the closed-loop design model is the same as for the fully decentralized design; it is also independent of the free parameter  $\epsilon$ .

The matrices  $C^1$  of Equation (2-15) for the full-order system are:

$$C^1 \triangleq \begin{bmatrix} 0 & \phi^2 & 0 & \phi^1 \end{bmatrix}, \quad C^2 \triangleq \begin{bmatrix} 0 & \phi_2^2 & 0 & \phi_2^1 \end{bmatrix}$$

SYSTEM: 0102      I.C.  $Q_2(0) = 1.$

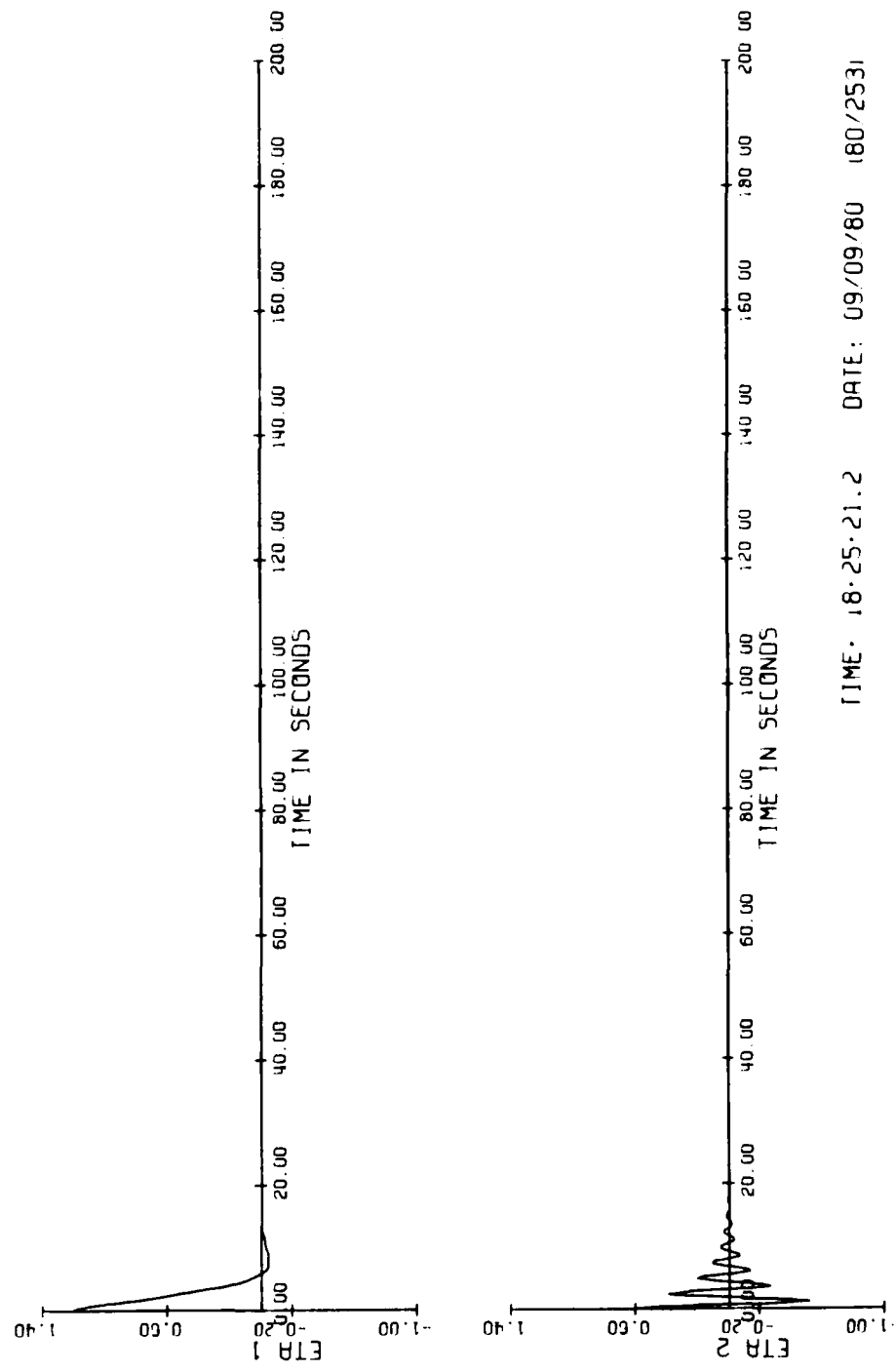


Figure 2-3. Modal response to initial conditions  $q_1(0) = q_1'(0) = q_2(0) = q_2'(0) = 1$   
(partially decentralized controller: actuator 1 localized).

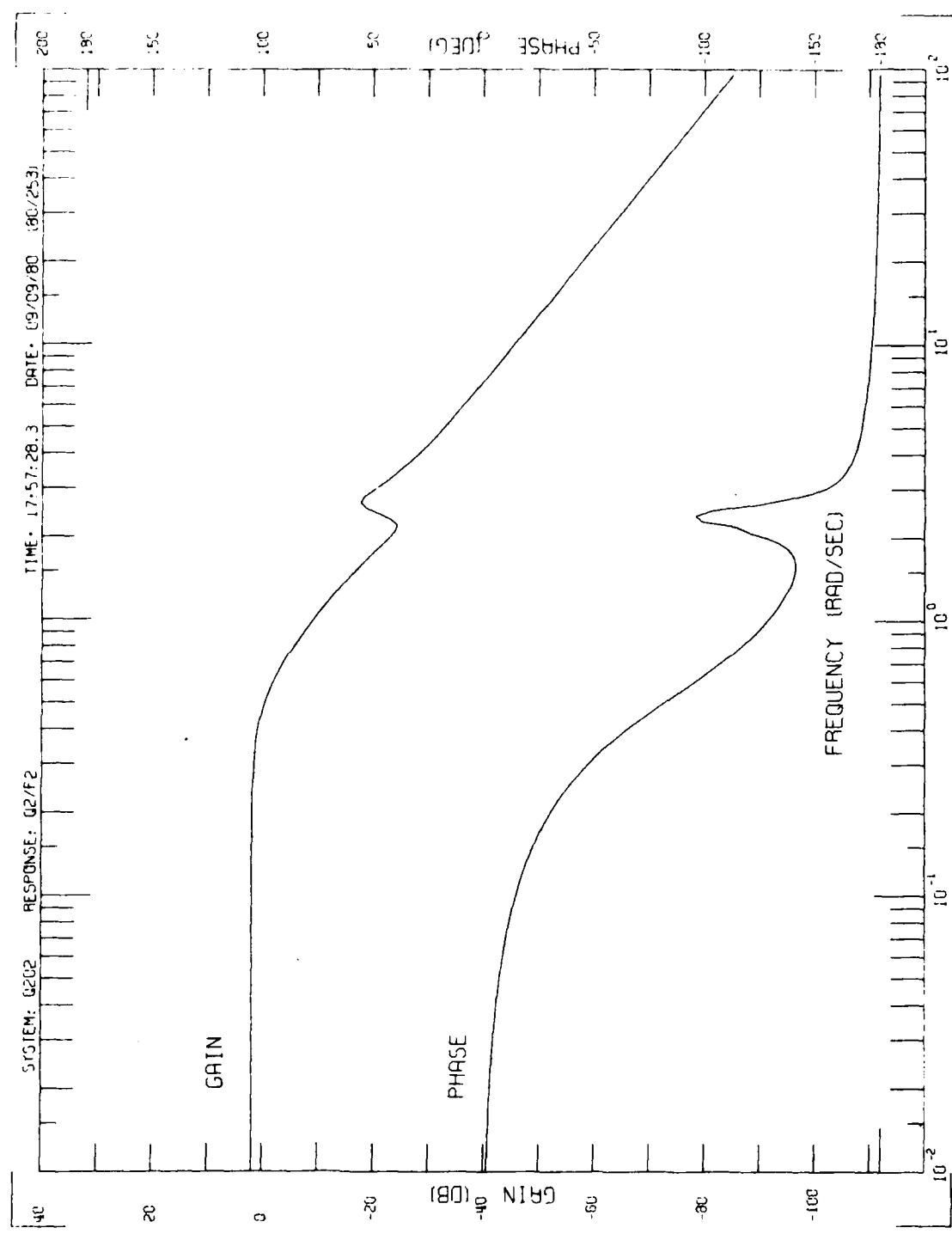


Figure 2-4. Frequency response of  $q_2$  to periodic disturbance  $f_2(t) = \sin \omega t$   
(partially decentralized controller: actuator 1 localized).

The modal closed-loop equations (to help select  $\epsilon$ ) are:

$$\begin{aligned}\ddot{\eta}_2 + \sigma^0(\phi^2 \phi^2) \dot{\eta}_2 + \omega_2^2 \eta_2 &= \left[ -\sigma^0(\phi^2 \phi^1) + \epsilon \det \Phi \right] \dot{\eta}_1 \\ \ddot{\eta}_1 + \left[ \sigma^0(\phi^1 \phi^1) - \epsilon \det \Phi \left( \frac{\phi_1^1}{\phi_1^2} \right) \right] \dot{\eta}_1 + \omega_1^2 \eta_1 &= \left[ -\sigma^0(\phi^2 \phi^1) \right] \dot{\eta}_2\end{aligned}\quad (2-21)$$

Following the same arguments as in the preceding section, the parameter  $\epsilon$  is chosen so that the coefficient of  $\dot{\eta}_1$  in Equation (2-21) has the desired value  $\zeta_{1D} \triangleq 1/\sqrt{2}$ :

$$\epsilon^0 \triangleq \frac{2\zeta_{1D}\omega_1 - \sigma^0(\phi^1 \phi^1)}{\det \Phi \left( \frac{\phi_1^1}{\phi_1^2} \right)} = 0.92785918$$

The gain values then become:

$$G(\epsilon^0) = \begin{bmatrix} -0.99178405 & -0.92785918 \\ 0 & -0.59708155 \end{bmatrix}$$

With this connection, the dynamic characteristics of the system are:

$$\begin{aligned}\text{Mode 2 (critical): } \omega_{2C} &= 2.5683141 \text{ sec}^{-1} \\ \zeta_{2C} &= 0.098354234\end{aligned}$$

$$\begin{aligned}\text{Mode 1 (residual): } \omega_{1C} &= 0.55063889 \text{ sec}^{-1} \\ \zeta_{1C} &= 0.71291349\end{aligned}$$

The only performance degradation relative to the centralized design observable from the plots is in the frequency domain, and is quite minor. The frequency response shows slightly higher magnitudes near  $\omega = \omega_2$  (open-loop critical mode frequency), and slightly higher phase shifts for  $\omega \geq \omega_2$ . Figures 2-5 and 2-6 may be compared with the corresponding plots for the centralized system [5; Figs. 6-7 and 6-8, respectively].

SYSTEM: Q103 I.C. Q2(0) = 1.

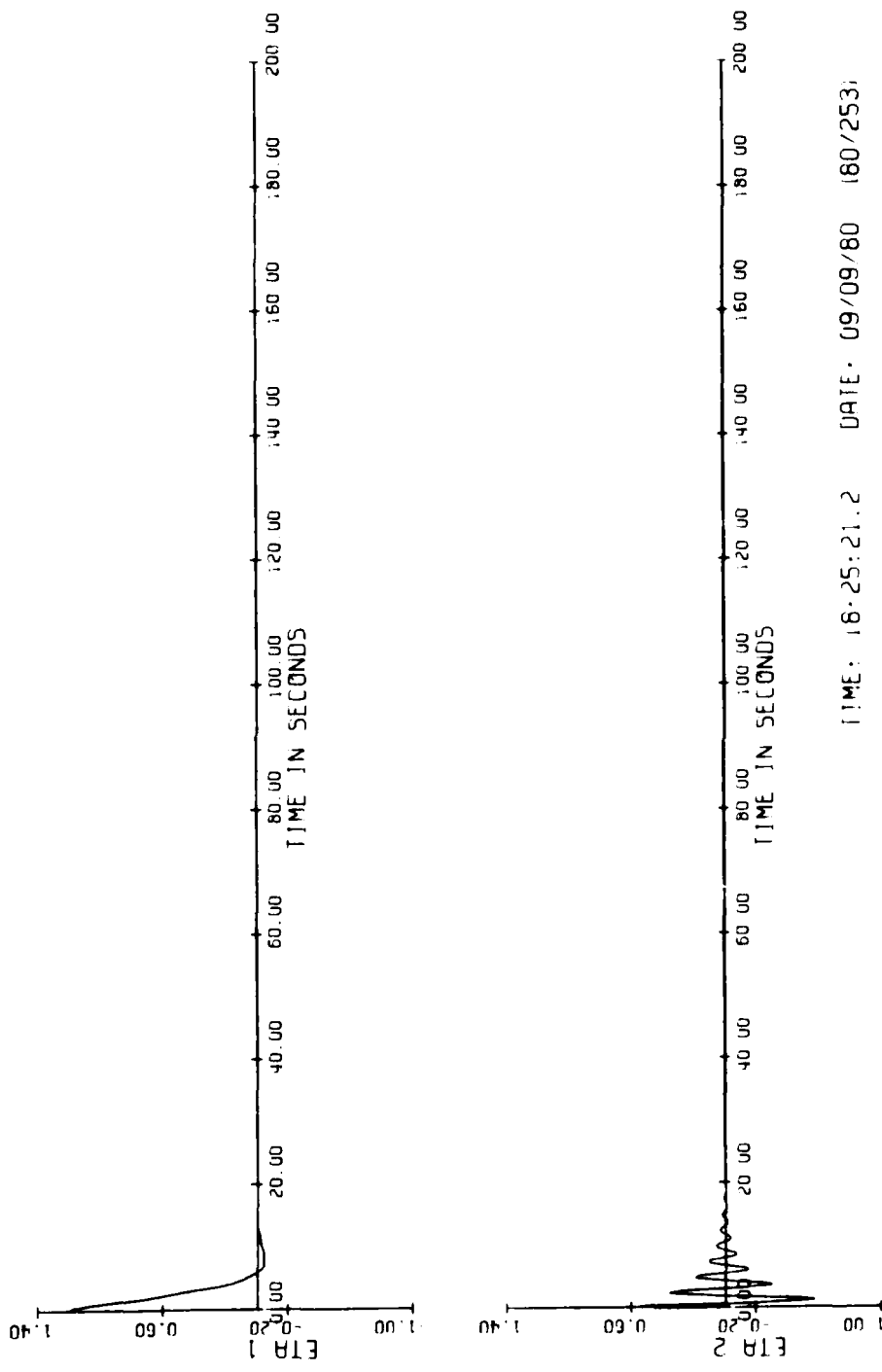


Figure 2-5. Modal response to initial conditions  $q_1(0) = \dot{q}_1(0) = q_2(0) = \dot{q}_2(0) = 1$   
(partially decentralized controller: actuator 2 localized).

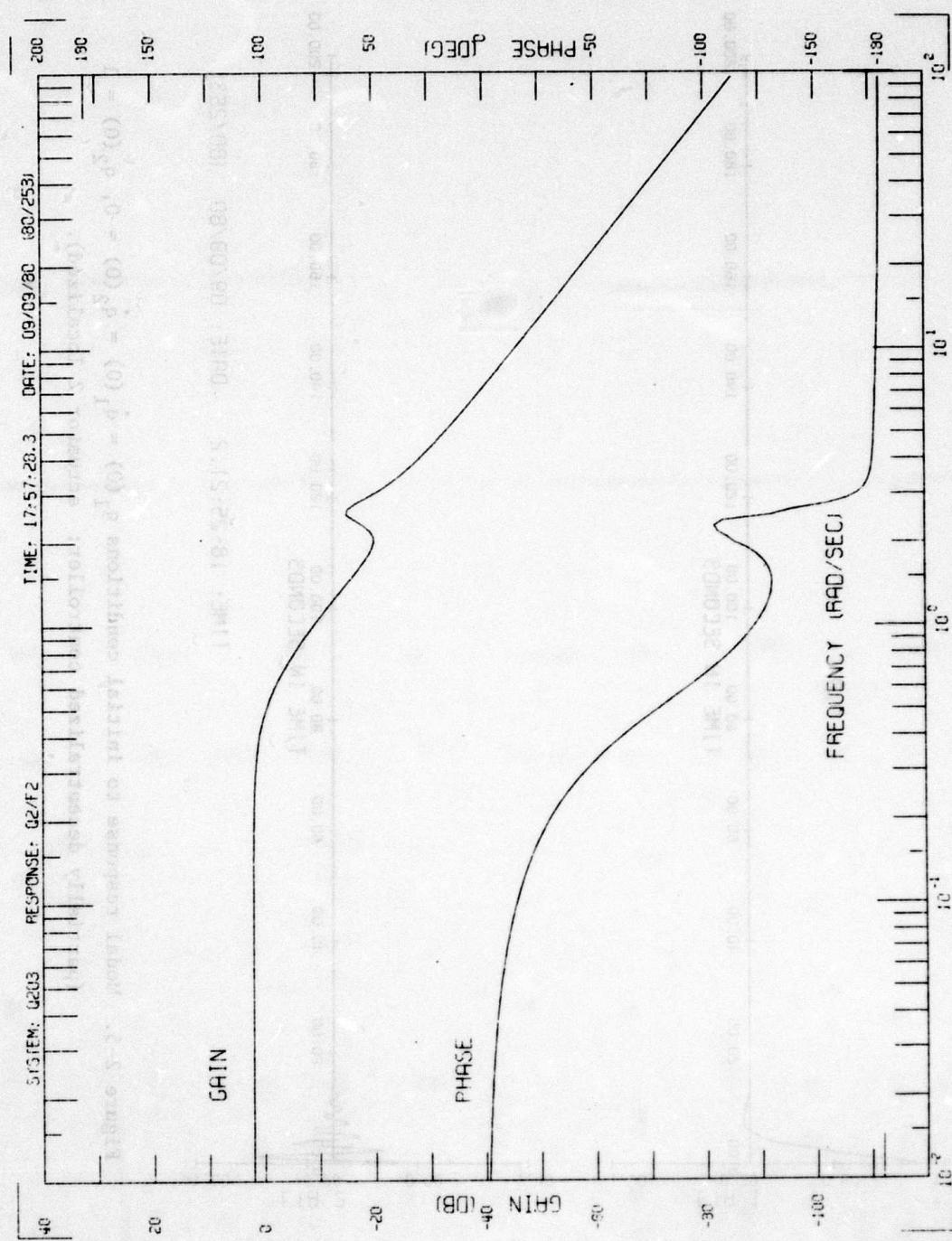


Figure 2-6. Frequency response of  $q_2$  to periodic disturbance  $f_2(t) = \sin \omega t$   
(partially decentralized controller: actuator 2 localized).

#### 2.4.2.4 Remarks on Performance Comparisons

A summary of the design studies on the two-mass oscillator example for all of the centralized and decentralized designs discussed in this section is shown in Table 2-1. Data for the centralized designs was previously reported [5,7].

Broad conclusions regarding the effects on performance of decentralizing the feedback information structure cannot be drawn from these few designs on such a low-order system. However, several observations are worth noting. First, noticeable performance degradation did occur, and the degree of degradation increased as the degree of decentralization increased. Second, the worst performance degradation (for the fully decentralized configuration) was not as bad as one might have expected. Finally, the design flexibility due to the free parameters occurring in the designs with partial, but less than total, decentralization was sufficient to eliminate (nearly) all performance degradation.

#### 2.5 Proofs of Theoretical Results

The proof of Theorem 2-1 depends on the following two facts.

Fact 1.  $\Phi_C^T M \Phi_C = I_N, \quad \Phi_C^T K \Phi_C = \Omega_C^2$

Proof. It follows from a block matrix representation of Equation (2-3) that  $(\phi^1)^T M \phi^j = \delta_{ij}$ , and  $(\phi^1)^T K \phi^j = \omega_1^2 \delta_{ij}$ ,  $i, j = 1, \dots, n$ , where  $\delta_{ij}$  is the Kronecker indicator function:

$$\delta_{ij} \triangleq \begin{cases} 1, & i = j \\ 0, & i \neq j \end{cases}$$

In particular, these relations hold for  $i, j = 1, \dots, N$ . ■

Fact 2. (Rosenbrock [9]). If  $A, B, C, D$  are matrices, with  $A, D$  being square and  $A$  nonsingular, then:

$$\det \begin{bmatrix} A & B \\ -C & D \end{bmatrix} = \det A \det (-CA^{-1}B + D)$$

Table 2-1. Principal closed-loop system parameters.

DESIGN	FEEDBACK INFORMATION STRUCTURE	NUMBER OF FREE PARAMETERS	EFFECTIVE GAIN G ( $u = Gy_c$ )	CLOSED-LOOP DYNAMICS		
				MODE 2	MODE 1	$\omega$ (sec $^{-1}$ )
Centralized	$u_1 = u_1(y_1, y_2)$	2	$\begin{bmatrix} -0.6437 & -0.1096 \\ -0.2961 & -1.293 \end{bmatrix}$	0.09999	2.589	0.5463
	$u_2 = u_2(y_1, y_2)$					
Fully Decentralized	$u_1 = u_1(y_1)$	0	$\begin{bmatrix} -0.5971 & 0 \\ 0 & -0.5971 \end{bmatrix}$	0.09994	2.585	0.5470
	$u_2 = u_2(y_2)$					
Partially Decentralized - Actuator 1 Localized	$u_1 = u_1(y_1)$	1	$\begin{bmatrix} -0.5971 & 0 \\ -0.3358 & -1.386 \end{bmatrix}$	0.1002	2.591	0.5457
	$u_2 = u_2(y_1, y_2)$					
Partially Decentralized - Actuator 2 Localized	$u_1 = u_1(y_1, y_2)$	1	$\begin{bmatrix} -0.9918 & -0.9279 \\ 0 & -0.5971 \end{bmatrix}$	0.09835	2.568	0.7129
	$u_2 = u_2(y_2)$					
Centralized (no sensor on $m_2$ )	$u_1 = u_1(y_1)$	0	$\begin{bmatrix} -0.5971 & 0 \\ -0.2540 & 0 \end{bmatrix}$	0.1002	2.580	0.07270
	$u_2 = u_2(y_1)$					

Proof of Theorem 2-1. The closed-loop system matrix for the model (2-8), (2-9) under the connection  $u = Gy_C$  is:

$$A_C + B_C G C_C = \begin{bmatrix} 0_N & I_N \\ -\Omega_C^2 + \Phi_{C_A}^T G C_P \Phi_C & \Phi_{C_A}^T G C_V \Phi_C \end{bmatrix}$$

It is easily seen from the properties of determinants that the vanishing of  $\det(A_C + B_C G C_C)$  is equivalent to the condition:  $\det[-\Omega_C^2 + \Phi_{C_A}^T G C_P \Phi_C] = 0$ . This proves result (2-10) for the case  $\lambda = 0$ . For  $\lambda \neq 0$ , the matrix  $-\lambda I_N$  is nonsingular. Using Fact 2 and the properties of determinants leads to:

$$\det(A_C + B_C G C_C - \lambda I_{2N}) = (-1)^N \lambda^N \left(\frac{1}{\lambda}\right)^N \det\left\{-\lambda^2 I_N + \Phi_{C_A}^T [B_A G(\lambda C_V + C_P)] \Phi_C - \Omega_C^2\right\}$$

Result (2-10) follows by an application of Fact 1. ■

Proof of Theorem 2-2. Denote  $\Delta \triangleq \text{diag}(-\delta_i)$ . Using Theorem 2-1 and Fact 1, the eigenvalues of the closed-loop system are seen to be the roots of:

$$0 = \det\left(-\lambda^2 I_N + \lambda \Delta - \Omega_C^2\right) = (-1)^N \prod_{i=1}^N \left(\lambda^2 + \delta_i \lambda + \omega_i^2\right)$$

Since each  $\delta_i > 0$ , all eigenvalues have negative real parts. ■

Proof of Theorem 2-3. Denote by  $G \xrightarrow{\gamma} (\lambda_1, \dots, \lambda_{2N})$  the mapping described in the theorem. The function  $\gamma$  is a composition  $\gamma_3 \circ \gamma_2 \circ \gamma_1$  of the following three mappings: (1)  $G \xrightarrow{\gamma_1} \Phi_{C_A}^T G C_V \Phi_C$ ; (2)  $z \xrightarrow{\gamma_2} p_z(\cdot)$ , where  $p_z(\lambda) \triangleq \det(\lambda^2 I_N + \lambda z + \Omega_C^2)$ ; and (3)  $p(\cdot) \xrightarrow{\gamma_3} (\lambda_1, \dots, \lambda_{2N})$ , the roots of  $p(\lambda) = 0$ . It can be shown that  $\gamma_1$ ,  $\gamma_2$ , and  $\gamma_3$  are continuous; hence  $\gamma$  is continuous. Continuity of  $\gamma_3$  is based on the well-known root-coefficient relations for polynomial equations [11]. ■

Proof of Theorem 2-4. Denote by  $(M, K) \xrightarrow{\beta} G$  the mapping described in the theorem. The function  $\beta$  is a composition  $\beta_3 \circ \beta_2 \circ \beta_1$  of the following three mappings: (1)  $(M, K) \xrightarrow{\beta_1} (\Omega^2, \Phi)$ , where  $\Omega^2 \equiv \text{diag}(\omega_1^2, \dots, \omega_n^2)$ ,  $\omega_i^2$  being the roots of  $\det(-\omega_i^2 M + K) = 0$ , and  $\Phi \equiv [\phi^1 \mid \dots \mid \phi^n]$ ,  $\phi^i$  being the solutions of  $(-\omega_i^2 M + K)\phi = 0$  such that Equation (2-3) holds; (2)  $(\Omega^2, \Phi) \xrightarrow{\beta_2} (A_C, B_C, C_C)$ , the latter matrices being defined by Equations (2-8), (2-9); and (3)  $(A_C, B_C, C_C) \xrightarrow{\beta_3} G \equiv (F^* P C_C^T) (C_C^P C_C^T)^+$ , where  $F^*$  is the state feedback gain for the Kosut reference system, and  $P$  is the solution of Equation (2-13). The superscript " $+$ " denotes the Moore-Penrose inverse [8]. It can be shown that  $\beta_1$ ,  $\beta_2$ , and  $\beta_3$  are continuous; hence  $\beta$  is continuous. ■

The proof of Theorem 2-6 is self-evident from the following general result.

Fact 3. Two square matrices are similar if and only if they have the same set of eigenvalues.

Proof. (Only if) This is a well-known result [12; p.144].

(If) Since both matrices have the same set of eigenvalues, they are each similar to the same Jordan block matrix. Since similarity is an equivalence relation, the matrices in question are similar to each other.

Simplified proof of Theorem 6-6 of [5; Sec. 6].

Denote  $E \triangleq \begin{bmatrix} C_C \\ \cdots \\ F^* \end{bmatrix}$ . Since the rank of a matrix is equal to the number of

its linearly independent rows:  $\text{rank}(C_C^P C_C^T) \leq \text{rank}(E C_C^T)$ . Conversely, suppose that this inequality is strict. Denote  $r \triangleq \text{rank}(E C_C^T)$ . Using the fact that  $\text{rank}(C_C^P C_C^T) = \text{rank}(C_C)$  when  $P$  is positive definite, it follows that  $\text{rank}(C_C) < r$ . But then it follows easily [12] that  $\text{rank}(E C_C^T) \leq \min\{\text{rank}(E), \text{rank}(C_C^T)\} < r$ , which contradicts the definition of  $r$ . Hence,  $\text{rank}(C_C^P C_C^T) \geq \text{rank}(E C_C^T)$ . ■

The proof of Theorem 2-7 is based on the following well-known result from linear algebra [12].

Fact 4. Let  $\mathcal{A}$  be a linear transformation defined on a vector space  $X$ . Then:

$$\dim [\text{Range } (\mathcal{A})] + \dim [\text{Null } (\mathcal{A})] = \dim (X)$$

Proof of Theorem 2-7. Define the map  $x \xrightarrow{\mathcal{A}} xA$  on the row-space  $E^\lambda$ . Since  $\text{rank } (\mathcal{A}) = \text{rank } (A) = r$ , it follows from Fact 4 that  $\text{Null } (\mathcal{A})$ , the null space of  $\mathcal{A}$ , has dimension  $\lambda-r$ . If  $r = \lambda$ , then  $\text{Null } (\mathcal{A}) = 0$  and  $x_0$  is unique. Otherwise,  $r < \lambda$ , so there exist row vectors  $s_1, \dots, s_{\lambda-r}$  that form a basis for  $\text{Null } (\mathcal{A})$ . Denote  $S \triangleq [s_1^T \mid \dots \mid s_{\lambda-r}^T]^T$ . Let  $x \in E^\lambda$  satisfy  $xA = b$ . Then  $(x - x_0) \in \text{Null } (\mathcal{A})$ , so there exist constants  $\gamma \equiv (\gamma_1, \dots, \gamma_{\lambda-r})^T$  such that

$$x - x_0 = \sum_{i=1}^{\lambda-r} \gamma_i s_i = \gamma^T S$$

Conversely, any vector of form (2-18) satisfies the equation  $xA = b$ . ■

## 2.6 Conclusion

A capsule summary of the results reported in this section may be stated as follows. First, certain previously reported results relating to the algebraic consistency of, and the structure of solutions to, the Kosut gain equation are substantially improved. Moreover, conditions for design-model-independence of free parameters occurring in such solutions are given. Second, a clearer idea of the nature and extent of performance degradation to be expected due to decentralizing the feedback information structure is obtained. Finally, stable designs obtained by the extended Kosut method are shown to be robust.

However, some substantial open questions, both in theory and in application methods, must be resolved before the extended Kosut approach can become a competitive method for large space structure controller design.

### Major theoretical problems:

1. Characterize systems for which the extended Kosut approach leads to a stable closed-loop design (at the design model level).
2. Synthesize a systematic procedure for assigning values to free parameters (when available) so as to improve performance of the full-order system incorporating the reduced-order controller.

### Major applications problems

1. Develop the algorithm for solving the Kosut gain equation [8] into an effective design tool.
2. Compare the extended Kosut method with several other representative design methods on more sophisticated structural models.

### LIST OF REFERENCES

1. Kosut, R.L., Suboptimal Control of Linear Time-Invariant Systems Subject to Control Structure Constraints, IEEE Trans. Automatic Control, Vol. AC-15, pp. 557-563, October 1970.
2. Levine, W.S. and Athans, M., On the Determination of the Optimal Constant Output Feedback Gains for Linear Multivariable Systems, IEEE Trans. Automatic Control, Vol. AC-15, pp. 44-48, February 1970.
3. Bingulac, S.P., Cuk, N.M., and Calovic, M.S., Calculation of Optimum Feedback Gains for Output-Constrained Regulators, IEEE Trans. Automatic Control, Vol. AC-20, pp. 164-166, February 1975.
4. Petkovski, Dj. B. and Rakic, M., On the Calculation of Optimum Feedback Gains for Output-Constrained Regulators, IEEE Trans. Automatic Control, Vol. AC-23, p. 760, August 1978.
5. Lin, J.G., Lin, Y.H., Hegg, D.R., Johnson, T.L., and Keat, J.E., Theory of Design Methods, Interim Technical Report, Actively Controlled Structures Theory, Volume 1, Charles Stark Draper Laboratory Report R-1249, April 1979.
6. Hegg, D.R., Extensions of Suboptimal Output Feedback Control with Application to Large Space Structures, Proc. AIAA Guidance and Control Conference, Danvers, Mass., August 10-12, 1980.
7. Lin, J.G., Hegg, D.R., Lin, Y.H., and Keat, J.E., Output Feedback Control of Large Space Structures: An Investigation of Four Design Methods, Proc. Second VPI&SU/AIAA Symposium on Dynamics and Control of Large Flexible Spacecraft, Blacksburg, Va., June 21-23, 1979.
8. Strunce, R.R., Hegg, D.R., Lin, J.G., and Henderson, T.C., Final Report, Actively Controlled Structures Theory, Vol. 1, Charles Stark Draper Laboratory Report R-1338, December 1979.
9. Rosenbrock, H.H., State-space and Multivariable Theory. New York: Wiley, 1970.
10. Bellman, R., Introduction to Matrix Analysis, second edition. New York: McGraw-Hill, 1970.

11. MacDuffee, C.C., Theory of Equations. New York: Wiley, 1954.
12. Thrall, R.M. and Tornheim, L., Vector Spaces and Matrices. New York: Wiley, 1957.
13. Wonham, W.M., Linear Multivariable Control: a Geometric Approach, second edition. New York: Springer-Verlag, 1979.

## SECTION 3

### STABILITY MARGINS FOR FIXED-ORDER COMPENSATORS

#### 3.0 Abstract

In order that a theory can be developed for establishing an upper bound on closed-loop stability when evaluating a fixed-order compensator with higher-order evaluation models of large space structures, the closed-loop dynamic equations were derived first (see Subsection 3.1). As an initial effort, the common observer-based fixed-order controllers were considered; the design of such compensators was assumed to be based only on a reduced-order model formed by truncating all but a fixed number of vibration modes. The resultant closed-loop dynamic equations were then put into the standard second-order matrix form in two different ways, all having a certain form of effective damping and stiffness matrices.

The closed-loop effective stiffness matrices were not symmetric; their symmetrization was then studied, so that standard stability conditions on second-order dynamics could be applied. Two steps were proposed: symmetrizing transformation of the coordinates and orthonormalizing transformation of the new eigenvectors. (See Subsection 3.2.) The closed-loop dynamic equations were then put in a modal form similar to the open-loop case. Determining the closed-loop stability and its margin would then be a straightforward matter after carrying out this two-step procedure, say, by a computer. Analytic expressions for the closed-loop stability conditions (with higher-order evaluation models), however, were not easy to derive.

The stability of the closed-loop system having a fixed-order compensator could be looked at directly in the frequency domain. In other words, the shortest distance of the closed-loop poles to the imaginary axis of the complex plane could determine the upper bound of closed-loop stability. An example was worked out analytically in detail (see Subsection 3.3) to demonstrate that it would be very difficult to obtain an analytical expression of closed-loop stability margins from this viewpoint even for a structure as simple as having only two elastic modes.

### 3.1 Closed-Loop Dynamic Equations with Observer-Based Fixed-Order Compensators

Assume that an open-loop modal representation of the large space structures, in the form

$$\begin{cases} \ddot{\eta} + (G + D)\dot{\eta} + \Omega^2\eta = \beta u \\ y = P\eta + V\dot{\eta} \end{cases} \quad (3-1)$$

is available, and that the critical modes are the low-frequency ones while the residual modes are of high frequencies.  $G$  and  $D$  are gyroscopic and damping matrices respectively;  $\Omega$  is a diagonal matrix of natural frequencies. Let  $\ell$ ,  $m$ ,  $n$ ,  $n_c$ , and  $n_r$  denote the numbers of outputs, inputs, modes, critical modes, and residual modes, respectively. Consider the following partitioning.

$$\begin{aligned} \eta &= \begin{bmatrix} \eta_c \\ \eta_r \end{bmatrix}, \quad \Omega^2 = \begin{bmatrix} \Omega_c^2 & 0 \\ 0 & \Omega_r^2 \end{bmatrix} \quad (3-2) \\ G &= -G^T = \begin{bmatrix} G_{cc} & -G_{cr} \\ -G_{cr}^T & G_{rr} \end{bmatrix}, \quad D = D^T = \begin{bmatrix} D_{cc} & D_{cr} \\ D_{cr}^T & D_{rr} \end{bmatrix} \\ \beta &= \begin{bmatrix} \beta_c \\ \beta_r \end{bmatrix}, \quad P = [P_c \ P_r], \quad V = [V_c \ V_r] \quad (3-3) \end{aligned}$$

We presume that the parameters of the full model are available, but that the design is to be based essentially on the critical-mode part of the model. The feedback controls that will be considered are of the form

$$u = K\dot{\eta}_c + L\ddot{\eta}_c \quad (3-4)$$

where

$$\ddot{\hat{\eta}}_c + (G_{cc} + D_{cc})\dot{\hat{\eta}}_c + \Omega_c^2 \hat{\eta}_c = \beta_c u + H(y - P_c \hat{\eta}_c - V_c \dot{\hat{\eta}}_c) \quad (3-5)$$

In (3-5),  $\hat{\eta}_c$  has the form of an observer for  $\eta_c$ . Note that it is driven by the output,  $y$ , which contains  $\eta_r$ , and is thus not actually an observer of  $\eta_c$  in the formal sense. Evidently, (3-5) involves only the critical mode parameters. The free design parameters are the gain matrices  $K$ ,  $L$ , and  $H$ , and we want to know if they can be chosen by a procedure so that (3-1), (3-4), (3-5) yield a stable closed-loop system, particularly when  $G$  and  $D$  are very small.

The reason for assuming this form is that it is representative of a range of practical schemes for finding gains. Note, for instance, that  $K$ ,  $L$ , could be designed on the basis of an LQ control problem, and that  $H$  could be designed on the basis of a Kalman filtering problem or as a model matched filter for the critical modes. However, these methods have not been shown to lead in general to closed-loop stability, and more refined conditions on their application are needed.

The standard coordinates for the closed-loop dynamics are  $\hat{\eta}_c$  and

$$e \equiv \eta_c - \hat{\eta}_c \quad (3-6)$$

We write these in second-order form rather than state-space form. Let

$$\mathbf{x} = \begin{bmatrix} e \\ \dot{\hat{\eta}}_c \\ \eta_r \end{bmatrix} \quad (3-7)$$

Then

$$\ddot{\mathbf{x}} + \begin{bmatrix} G_{cc} + D_{cc} + HV_c & 0 & HV_r + G_{cr} + D_{cr} \\ -HV_c & G_{cc} + D_{cc} - \beta_c L & -HV_r \\ -G_{cr}^T + D_{cr}^T & -G_{cr}^T + D_{cr}^T - \beta_r L & G_{rr} + D_{rr} \end{bmatrix} \dot{\mathbf{x}}$$

*Effective damping*

$$+ \underbrace{\begin{bmatrix} \Omega_c^2 + HP_c & 0 & HP_r \\ -HP_c & \Omega_c^2 - \beta_c K & -HP_r \\ 0 & -\beta_r K & \Omega_r^2 \end{bmatrix}}_{\text{Effective stiffness}} x = 0 \quad (3-8)$$

Effective stiffness

Note that only 3 zero-blocks have been created by the observer. These matrices are otherwise not particularly well-structured for further purposes, so we were led to consider the following alternative expression

$$x = \begin{bmatrix} \hat{\eta}_c \\ \eta_c \\ \eta_r \end{bmatrix}$$

We then have the following much more convenient form

$$\ddot{x} + \begin{bmatrix} G_{cc} + D_{cc} - \beta_c L + HV_c & -HV_c & -HV_r \\ -\beta_c L & G_{cc} + D_{cc} & G_{cr} + D_{cr} \\ -\beta_r L & -G_{cr}^T + D_{cr}^T & G_{rr} + D_{rr} \end{bmatrix} \dot{x} + \begin{bmatrix} \Omega_c^2 - \beta_c K + HP_c & -HP_c & -HP_r \\ -\beta_c K & \Omega_c^2 & 0 \\ -\beta_r K & 0 & \Omega_r^2 \end{bmatrix} x = 0 \quad (3-9)$$

or

$$\ddot{x} + \begin{bmatrix} G_{cc} + D_{cc} - \beta_c L + HV_c & -HV \\ -\beta L & G + D \end{bmatrix} \dot{x} + \begin{bmatrix} \Omega_c^2 - \beta_c K + HP_c & -HP \\ -\beta K & \Omega^2 \end{bmatrix} x = 0 \quad (3-10)$$

### 3.2 Symmetrization of Closed-Loop Stiffness Matrices

We note that the closed-loop system can be put into second-order form, but it is not clear whether this could be transformed to an equivalent decoupled system

$$\ddot{\tilde{x}} + [\tilde{G} + \tilde{D}] \dot{\tilde{x}} + \tilde{\Omega}^2 \tilde{x} = 0 \quad (3-11)$$

where

$$\tilde{G} = -\tilde{G}^T, \tilde{D} = \tilde{D}^T, \text{ and } \tilde{\Omega}^2 \text{ is diagonal.}$$

If it could, then a rather simple stability test for second-order systems could be applied. For example [1], [2], when  $\tilde{\Omega}^2$  is positive definite, system (3-11) is asymptotically stable if and only if the following associate system

$$\begin{cases} \ddot{\tilde{z}} + \tilde{G}\dot{\tilde{z}} + \tilde{\Omega}^2 \tilde{z} = 0 \\ y = \tilde{D}\dot{\tilde{z}} \end{cases}$$

is completely observable.

The conversion of (3-10) to (3-11) proceeds in two steps:

Step 1: A symmetrizing transformation,  $S$ , which converts (3-10) so that its last term is symmetric.

Step 2: An orthonormal transformation,  $\Phi$ , which puts the result of Step 1 into modal form.

#### Step 1

Suppose we perform a change of variable  $S$  as follows:

$$Sv = x \quad (S \text{ nonsingular}) \quad (3-12)$$

For simplicity, rewrite system (3-10) in the form

$$\ddot{x} + \bar{F}\dot{x} + \bar{K}x = 0 \quad (3-13)$$

then

$$\ddot{v} + S^{-1}\bar{F}S\dot{v} + S^{-1}\bar{K}Sv = 0 \quad (3-14)$$

If the last term is to be symmetric, there must be an  $S$  such that

$$S^{-1}\bar{K}S = S^T \bar{K}^T S^{-1}T \quad (3-15)$$

$$\text{i.e., } \bar{K} = (SS^T)^{-1} \bar{K}^T (SS^T)^{-1}$$

or equivalently, there must be a nonsingular symmetric transformation  $T$  such that

$$\bar{K}T = T\bar{K}^T \quad (3-16)$$

In other words, such a transformation must be solved from the following matrix equation:

$$\begin{bmatrix} \bar{\Omega}^2 & -HP \\ -\beta K & \Omega^2 \end{bmatrix} \begin{bmatrix} T_{11} & T_{12} \\ T_{12}^T & T_{22} \end{bmatrix} = \begin{bmatrix} T_{11} & T_{12} \\ T_{12}^T & T_{22} \end{bmatrix} \begin{bmatrix} \bar{\Omega}^2 & -K^T \beta^T \\ -P^T H^T & \Omega^2 \end{bmatrix} \quad (3-17)$$

where

$$\bar{\Omega}^2 = \Omega_c^2 - \beta_c K + HP_c$$

To complete Step 1, suppose that such a symmetric nonsingular transformation  $T$  has been obtained. Then there is a nonsingular square root of  $T$ , denoted  $S$ , such that

$$SS^T = T \quad (3-18)$$

This can be found via Cholesky decomposition.

### Step 2

Define

$$\bar{K} = S^{-1}\bar{K}S \quad (3-19)$$

$$\bar{\Delta} = S^{-1}\bar{\Delta}S \quad (3-20)$$

Also define

$$\bar{G} = \frac{1}{2}(\bar{\Delta} - \bar{\Delta}^T) \quad (3-21)$$

$$\bar{D} = \frac{1}{2}(\bar{\Delta} + \bar{\Delta}^T) \quad (3-22)$$

Then there exists an orthogonal transformation  $\phi$  such that

$$\phi^T \bar{K} \phi = \tilde{\lambda}^2 \quad (3-23)$$

Defining

$$\tilde{G} = \phi^T \bar{G} \phi \quad (3-24)$$

$$\tilde{D} = \phi^T \bar{D} \phi \quad (3-25)$$

brings the system into the form (3-11).

Comment 1: If steps 1 and 2 can be carried out, it is then possible to interpret the closed-loop system in terms of modes, i.e., as if it represented a new structure. It was not previously apparent that "closed-loop modes" could be defined in the sense that open-loop ones were.

Comment 2: If any of the steps can be carried through analytically, then explicit stability conditions could be given. This has not yet been accomplished.

Comment 3: This procedure might represent a more simple way to determine closed-loop stability numerically using existing computer programs for high-order systems.

Comment 4: Since the design value of the foregoing results often depend crucially on the ability to obtain analytical expressions involving the gains, several examples were worked in order to obtain a better qualitative feel for how the gains enter the exact analytical expressions for stability. In symmetrization of a two-mode system with control of one critical mode, we carried out step 1 of the symmetrization procedures, Eq. (3-17), assuming  $n_c = n_r = 1$ . The expressions obtained were very complex. It should be apparent, however, that the problem of finding a symmetrizing transformation can be expected to yield interesting stability results.

### 3.3 Closed-Loop Stability Conditions for a Two-Mode Example

The stability problem of system (3-10) can be viewed directly in the frequency domain. In this case, we seek the roots of the polynomial

$$M(s) = \det \begin{bmatrix} s^2 + (G_{cc} + D_{cc} - \beta_c L + HV_c)s + (\omega_c^2 - \beta_c K + HP_c) & -H(Vs + P) \\ -\beta(Ls + K) & s^2 + (G + D)s + \omega^2 \end{bmatrix}$$

Note that the lower right block is just the polynomial of the open-loop system, which is stable by assumption. Thus a stability analysis might be based on the perturbation-theory expression

$$M(s) = \det \left\{ s^2 + (G_{cc} + D_{cc} - \beta_c L + HV_c)s + (\omega_c^2 - \beta_c K + HP_c) - H(Vs + P) [s^2 + (G + D)s + \omega^2]^{-1} \beta(Ls + K) \right\} \cdot \det [s^2 + (G + D)s + \omega^2]$$

An effort has been made to work out  $M(s)$  for a two-mode example, and to apply Routh's criterion so that exact stability conditions might be found for the simplest case of interest. The results follow

$$M(s) = \det \begin{bmatrix} s^2 + (d_{cc} - \beta_c \ell + hv_c)s + (\omega_c^2 - \beta_c k + hp_c) & -h(v_c s + p_c) & -h(v_r s + p_r) \\ -\beta_c (\ell s + k) & s^2 + d_{cc} s + \omega_c^2 & (g_{cr} + d_{cr})s \\ -\beta_r (\ell s + k) & (-g_{cr} + d_{cr})s & s^2 + d_{rr} s + \omega_r^2 \end{bmatrix}$$

where lower-case letters have been used to denote scalar quantities. Note that  $g_{cc} = g_{rr} = 0$  by the requirement that gyroscopic coupling be antisymmetric. Also  $d_{rc} = d_{cr}$  and  $g_{rc} = -g_{cr}$  have been used. Subscript c denotes "critical" and subscript r denotes "residual" as above. Lengthy algebra yields

$$M(s) = \sum_{i=0}^6 M_i s^i$$

where

$$M_6 = 1$$

$$M_5 = -p_c \beta_r + v_c \beta_r + 2d_{cc} + d_{rr}$$

$$M_4 = h(\beta_r v_r - \beta_c v_c) + k(p_c + v_c(d_{cc} + d_{rr})) - \ell \beta_c (d_{cc} + d_{rr})$$

$$-k \beta_c + g_{cr}^2 - d_{cr}^2 + 2d_{cc}d_{rr} + d_{cc}^2 + 2\omega_c^2 + \omega_r^2$$

$$M_3 = h k (\beta_r v_r - \beta_c v_c) + h \ell (\beta_r p_r + d_{cc} \beta_r v_r - \beta_c p_c - d_{rr} \beta_c v_c)$$

$$+ h (d_{cc} p_c + \omega_c^2 v_c + d_{rr} p_c + d_{rr} d_{cc} v_c + \omega_r^2 v_c)$$

$$+ k (-d_{cc} \beta_c - d_{rr} \beta_c) + \ell (-\omega_c^2 \beta_c - d_{rr} d_{cc} \beta_c - \omega_r^2 \beta_c)$$

$$+ 2d_{cc} \omega_c^2 + 2d_{rr} \omega_c^2 + d_{rr} d_{cc}^2 + 2d_{cc} \omega_r^2$$

$$M_2 = h k^2 \beta_c \beta_r p_r + h^2 k \beta_r p_r p_c + h k (\omega_c^2 \beta_r p_r + d_{cc} \beta_r v_r - \beta_c p_c - d_{rr} \beta_c v_c)$$

$$+ h \ell (d_{cc} \beta_r p_r + \omega_c^2 \beta_r v_r - d_{rr} \beta_c p_c - \omega_r^2 \beta_c v_c)$$

$$+ h [p_c (g_{cr}^2 - d_{cr}^2) + p_c (\omega_c^2 + \omega_r^2 + d_{rr} d_{cc}) + d_{rr} \omega_c^2 v_c + d_{cc} \omega_r^2 v_c]$$

$$+ k [-\beta_c (g_{cr}^2 - d_{cr}^2) - \beta_c (\omega_c^2 + \omega_r^2 + d_{rr} d_{cc})]$$

$$+ \ell [-d_{rr} \beta_c^2 - d_{cc} \beta_r^2]$$

$$+ \omega_c^2 (g_{cr}^2 - d_{cr}^2) + \omega_c^2 (\omega_c^2 + \omega_r^2 + d_{rr} d_{cc}) + d_{cc} d_{rr} \omega_c^2$$

$$+ \omega_c^2 \omega_r^2 + d_{cc}^2 \omega_r^2$$

$$M_1 = h k (d_{cc} \beta_r p_r + \omega_c^2 \beta_r v_r - d_{rr} \beta_c p_c - \omega_r^2 \beta_c v_c)$$

$$+ h \ell (\omega_c^2 \beta_r p_r - \omega_r^2 \beta_c p_c)$$

$$\begin{aligned}
& + h(d_{rr}\omega_c^2 p_c + d_{cc}\omega_r^2 p_c + \omega_c^2 \omega_r^2 v_c) \\
& + k(-d_{rr}\omega_c^2 \beta_c - d_{cc}\omega_r^2 \beta_c) - \ell(\omega_r^2 \omega_c^2 \beta_c) \\
& + d_{rr}\omega_c^4 + 2d_{cc}\omega_r^2 \omega_c^2
\end{aligned}$$

$$M_0 = h k (\omega_c^2 \beta_r p_r - \omega_r^2 \beta_c p_c) + h \omega_c^2 \omega_r^2 p_c - k \omega_r^2 \omega_c^2 \beta_c + \omega_r^2 \omega_c^4$$

Forming the Routh array for a general 6th-order polynomial,

$$\begin{array}{cccc}
M_6 & M_4 & M_2 & M_0 \\
M_5 & M_3 & M_1 & 0 \\
N_1 & N_2 & M_0 & 0 \\
O_1 & O_2 & 0 & 0 \\
P_1 & M_0 & 0 & 0 \\
Q_1 & 0 & 0 & 0 \\
M_0 & 0 & 0 & 0
\end{array}$$

where

$$N_1 = (M_5 M_4 - M_6 M_3) / M_5$$

$$N_2 = (M_5 M_2 - M_6 M_1) / M_5$$

$$O_1 = \frac{M_3 (M_5 M_4 - M_6 M_3) - M_5 (M_5 M_2 - M_6 M_1)}{(M_5 M_4 - M_6 M_3)}$$

$$O_2 = \frac{M_1 (M_5 M_4 - M_6 M_3) - M_5^2 M_0}{(M_5 M_4 - M_6 M_3)}$$

$$P_1 = \frac{M_5 M_2 - M_6 M_1}{M_5} - \frac{(M_1 (M_5 M_4 - M_6 M_3) - M_0 M_5^2) (M_5 M_4 - M_6 M_1)}{M_5 [M_3 (M_5 M_4 - M_6 M_3) - M_5 (M_5 M_2 - M_6 M_1)]}$$

$$Q_1 = (P_1 O_2 - M_0 O_1) / P_1$$

The most simple special case assumes

1. No gyroscopic effects  $g_{cr} = 0$
2. No off-diagonal damping,  $d_{cr} = d_{rc} = 0$
3. Velocity sensing only  $p_c = p_r = 0$
4. Feedback only on velocity estimate,  $k = 0$

In this case

$$M_6 = 1$$

$$M_5 = -\beta_c \ell + 2d_{cc} + d_{rr} + v_c h$$

$$M_4 = h\ell(\beta_r v_r - \beta_c v_c) - \ell\beta_c(d_{cc} + d_{rr}) + hv_c(d_{cc} + d_{rr}) + d_{cc}(d_{cc} + d_{rr}) + d_{cc}d_{rr} + 2\omega_c^2 + \omega_r^2$$

$$M_3 = h\ell(d_{cc}\beta_r v_r - d_{rr}\beta_c v_c) + hv_c(\omega_c^2 + \omega_r^2 + d_{rr}d_{cc}) - \ell\beta_c(\omega_c^2 + \omega_r^2 + d_{rr}d_{cc}) + 2(d_{rr} + d_{cc})\omega_c^2 + d_{rr}\omega_c^2 + 2d_{cc}\omega_r^2$$

$$M_2 = h\ell(\omega_c^2\beta_r v_r - \omega_r^2\beta_c v_c) + h(d_{rr}\omega_c^2 v_c + d_{cc}\omega_r^2 v_c) - \ell(d_{rr}\omega_c^2\beta_c + d_{cc}\omega_r^2\beta_c) + \omega_c^2(\omega_c^2 + \omega_r^2 + d_{rr}d_{cc}) + d_{cc}d_{rr}\omega_c^2 + \omega_c^2\omega_r^2 + d_{cc}^2\omega_r^2$$

$$M_1 = h\omega_c^2\omega_r^2 v_c - \ell\omega_r^2\omega_c^2\beta_c + d_{rr}\omega_c^4 + 2d_{cc}\omega_r^2\omega_c^2$$

$$M_0 = \omega_r^2\omega_c^4$$

It is still impractical to work out the entire Routh array analytically, but we note that

$$M_6 = 1 > 0 \text{ (first column must be } > 0 \text{ for stability)}$$

$$M_0 > 0 \text{ (last element of first column is positive)}$$

$$M_5 > 0 \text{ implies } v_c h - \beta_c \ell > - (2d_{cc} + d_{rr})$$

$$\begin{aligned}
N_1 M_5 &= M_5 M_4 - M_6 M_3 \\
&= h^2 \ell v_c (\beta_r v_r - \beta_c v_c) + h^2 v_c^2 (d_{cc} + d_{rr}) \\
&\quad - h \ell^2 \beta_c^2 (\beta_r v_r - \beta_c v_c) + h \ell (-4 \beta_c v_c d_{cc} - 2 \beta_c v_c a_{rr} + \beta_r v_r d_{cc} \\
&\quad + \beta_r v_r d_{rr}) \\
&\quad + h v_c [4 d_{cc} d_{rr} + 3 d_{cc}^2 + d_{rr}^2 + \omega_c^2] \\
&\quad + \ell^2 \beta_c^2 (d_{cc} + d_{rr}) + \ell \beta_c [-4 d_{cc} d_{rr} - 2 d_{cc}^2 - d_{rr}^2 - \omega_c^2] \\
&\quad + [4 d_{cc}^2 d_{rr} + 2 d_{cc} d_{rr}^2 + 2 d_{cc}^3 + 2 d_{cc} \omega_c^2 + 2 d_{cc} \omega_r^2 + \omega_r^2 d_{rr}]
\end{aligned}$$

This shows that the third entry in the first column of the Routh array will be positive under the more restrictive assumptions that

$$h > 0$$

$$\ell < 0$$

$$\beta_c v_c - \beta_r v_r > 0 \text{ (more "control authority" on critical than residual modes)}$$

At this point, our algebraic capacity was exhausted, although it is clear that additional conditions can be derived.

Conclusion: Since in practice  $d_{cc}$ ,  $d_{rr}$  are very small, we have in effect shown that all but three conditions of Routh's test can be satisfied under conditions of a typical example, by choosing  $\ell < 0$ ,  $h > 0$ . It is unlikely that the remaining conditions will allow any less-restrictive condition than this.

#### LIST OF REFERENCES

1. Hughes, P.C., and R.E. Skelton, "Stability, Controllability and Observability of Linear Matrix-Second-Order Systems," presented at the 1979 Joint Automatic Control Conference, Denver, CO, June 1969.
2. Muller, P.C., "Special Problems of Gyrodynamics," Course and Lectures No. 63, International Center for Mechanical Sciences (CISM), Udine, Italy, 1972.

## SECTION 4

### AGGREGATE MODEL DEVELOPMENT

#### 4.0 Abstract

A common practice in obtaining a reduced-order model of a large space structure for designing its vibration controllers is to truncate the vibration modes directly, according to, say, the line-of-sight motions. Such design models do not account for the influences of actuators on the truncated modes nor the influences of the truncated modes on the sensors. The attendant control spillover and observation spillover can cause the vibration controllers to destabilize the structures, even when these controllers have been carefully and satisfactorily designed to ensure the closed-loop stability with respect to the reduced-order design models. The development of aggregate design models was thus intended to provide better reduced-order models of the structures for use in the design of vibration controllers. Vibration modes can be aggregated with respect to actuator and sensor influences by a nonsingular transformation before making any truncation; the truncated portion can then be independent of the actuators and sensors. Such an aggregation transformation in the general form was carefully studied (see Subsection 4.1). A useful set of necessary and sufficient conditions and two separate sets of sufficient conditions for the aggregation transformation to be nonsingular were established; such conditions are useful as a guide in choosing specific values of a diagonal block of free parameters in the aggregation transformation.

The aggregation transformation is not unique. Several interesting ideas of utilizing the uniqueness (i.e., of selecting the specific values of various free parameters in the transformation) for imposing additional properties on the aggregate design models were examined (see Subsection 4.3); some of their potential difficulties in obtaining closed-form analytical results were analyzed.

Vibration modes can be aggregated also with respect to their influences on performance and the influences of disturbances in addition to actuator and sensor influences. For example, the control systems for a large space structure might be designed to minimize the transmission from the disturbance sources to the critical performance variables besides providing the structures with closed-loop stability. By including the influences of the disturbances as a "part" of actuator influences and, similarly, the influences on the performance as a "part" of sensor influences, this "generalized" aggregation problem was able to be recast into the same initial form (see Subsection 4.3), so that the same arguments and the same techniques could be applied and extended directly.

#### 4.1 Aggregation of Vibration Modes with Respect to Actuator and Sensor Influences

A standard approach to model reduction is to truncate the open-loop modal representation directly, by neglecting (generally high-frequency) non-critical natural modes. This generally results in control energy being coupled into the neglected portion in a way which can be destabilizing. Here we explore a different choice of basis. Rather than using the open-loop modes directly, we aggregate them first based on the influence of the actuators and sensors. The advantage is that the coupling with the neglected portion becomes independent of feedback control gains, and is thus much more readily predicted. Furthermore, this choice of basis is also not affected by feedback.

Consider the following usual finite-element modal representation of LSS.

$$\left\{ \begin{array}{l} \ddot{\eta} + \Omega^2 \eta = \Phi^T B_F u \\ y = C_D \Phi \eta + C_V \dot{\Phi} \eta \end{array} \right. \quad (4-1)$$

where  $\eta$  denotes an L-vector of normal coordinates;  $\Omega \equiv \{\omega_1, \dots, \omega_L\}$  and  $\Phi \equiv [\phi_1, \dots, \phi_L]$  are  $L \times L$  matrices;  $\omega_i$  and  $\phi_i$  denote the natural frequency and the natural shape of mode  $i$ , respectively.  $L$  is usually a very large integer.  $\eta = (\eta_1, \dots, \eta_L)$  denotes the corresponding normal coordinates.  $u = (u_1, \dots, u_m)$  denotes the control inputs to  $m$  force actuators, and  $B_F$  the  $L \times m$  influence matrix.  $y = (y_1, \dots, y_\ell)$  denotes the observation outputs from  $\ell_D$  displacement sensors and  $\ell_V$  velocity sensors ( $0 \leq \ell_D \leq L$ ,  $0 \leq \ell_V \leq L$ );  $C_D$  and  $C_V$  denote the corresponding  $\ell \times L$  influence matrices. Superscript T denotes transpose. Normally,  $m < L$  and  $\ell < 2L$ .

A corresponding state-space form is

$$\left\{ \begin{array}{l} \dot{\tilde{x}} = \tilde{A}\tilde{x} + \tilde{B}u \\ y = \tilde{C}\tilde{x} \end{array} \right. \quad (4-2)$$

where

$$\tilde{x} = \begin{bmatrix} \eta \\ \dot{\eta} \end{bmatrix}, \quad \tilde{A} = \begin{bmatrix} 0 & I \\ -\Omega^2 & 0 \end{bmatrix}, \quad \tilde{B} = \begin{bmatrix} 0 \\ \Phi^T B_F \end{bmatrix},$$

$$\tilde{C} = [C_D \Phi \quad C_V \dot{\Phi}]$$

We assume that both  $\tilde{B}$  and  $\tilde{C}$  are of full rank. The rows of matrix  $\tilde{B}$  and the columns of matrix  $\tilde{C}$  can be rearranged such that

$$\tilde{B} = \begin{bmatrix} \tilde{B}_1 \\ \vdots \\ \tilde{B}_2 \end{bmatrix} \quad \tilde{C} = \begin{bmatrix} \tilde{C}_1 & \vdots & \tilde{C}_2 \end{bmatrix} \quad (4-3)$$

with  $\tilde{B}_1$  being an  $n \times m$  matrix of rank  $m$  and  $\tilde{C}_1$  an  $\ell \times n$  matrix of rank  $\ell$  for the smallest integer  $n$ . We assume the corresponding rearrangements have been made on the rows and columns of matrix  $\tilde{A}$ .

Now, to aggregate the state variables of (4-2), namely, the vibration modes of (4-1), with respect to actuator and sensor influences, we aggregate the rows of matrix  $\tilde{B}$  and the columns of  $\tilde{C}$  by a similarity transformation  $T$  such that

$$T\tilde{B} = \begin{bmatrix} B_1 \\ \vdots \\ 0 \end{bmatrix}, \quad \tilde{C}T^{-1} = [C_1 : 0] \quad (4-4)$$

where  $B_1$  is also an  $n \times m$  matrix of rank  $m$  and  $C_1$  also an  $\ell \times n$  matrix of rank  $\ell$ . By defining

$$x = T\tilde{x}, \quad A = T\tilde{A}T^{-1}, \quad B = T\tilde{B}, \quad C = \tilde{C}T^{-1} \quad (4-5)$$

we now have the following special but equivalent representation of the LSS

$$\begin{cases} \dot{x} = Ax + Bu \\ y = Cx \end{cases} \quad (4-6)$$

Partitioning these matrices conformably with (4-4) yields

$$A = \begin{bmatrix} A_{11} & | & A_{12} \\ \hline \vdots & | & \vdots \\ A_{21} & | & A_{22} \end{bmatrix} \quad B = \begin{bmatrix} B_1 \\ \vdots \\ 0 \end{bmatrix} \quad C = [C_1 \quad 0]$$

where  $A_{11}$ , in particular, is an  $n \times n$  matrix. The corresponding state equation can thus be rewritten as

$$\begin{cases} \dot{x}_1 = A_{11}x_1 + A_{12}x_2 + B_1u \\ \dot{x}_2 = A_{21}x_1 + A_{22}x_2 \\ y = C_1x_1 \end{cases} \quad (4-7)$$

Using any such aggregation transformation (and the orthogonal transformation representing the rearrangement of matrices  $\tilde{A}$ ,  $\tilde{B}$ , and  $\tilde{C}$  before aggregation), we have aggregated the vibration modes with respect to the influence of actuators and sensors. Observe, specifically, that the control of (4-7) does not directly affect  $x_2$  nor is the observation directly affected by it.

Neglecting  $x_2$ , we get the following aggregate design model of order only  $n$ :

$$\begin{cases} \dot{x} = A_{11}x + B_1u \\ y = C_1x \end{cases} \quad (4-8)$$

Roughly speaking, such a reduced-order model represents an equivalent dynamics of those linear combinations of natural modes which can be directly measured and controlled. It is not an exact aggregation [1] - [3] of system (4-2) in the sense of Aoki. By proper selection of the aggregation transformation  $T$ , this reduced-model may be made to approximate open-loop performance of system (4-1), much closer than any one obtained by direct truncation of the vibration modes.

Comment 1: In general, it is sufficient to have  $l + m$  rows in the block  $\tilde{B}_1$  and  $l + m$  columns in the block  $\tilde{C}_1$ ; hence  $n \leq l + m$ . Depending on the specific form of matrices  $\tilde{B}$  and  $\tilde{C}$  at hand have, or due to the existence of both velocity and displacement measurements, the blocks  $\tilde{B}_1$  and  $\tilde{C}_1$  need only  $\max\{l, m\}$  rows and columns respectively; hence  $n \leq \max\{l, m\}$ . Note that the possibility of having an aggregate design model (4-8) of order less than  $l + m$  is an improvement over the preliminary results [7].

Comment 2: The rearrangement of matrices  $\tilde{B}$  and  $\tilde{C}$  to have them bear the form described by (4-3) can be carried out using common computational procedures such as Gaussian elimination or Gram-Schmidt orthogonalization on rows of  $B$  and columns of  $C$ . Any prior effort in the placement of actuators (and sensors), or in the synthesis of actuator (and sensor) influences for preventing control spillover to (and observation spillover from) secondary modes, as discussed in [4-6], will facilitate the rearrangement of these matrices, since there will be fewer nonzero rows in  $\tilde{B}$  (and fewer nonzero columns in  $\tilde{C}$ ) to work with. Since the number of actuator-influenced (and sensor-influenced) modes, particularly those which are secondary modes, will be decreased, such spillover prevention efforts will also facilitate the aggregation and reduce the coupling  $A_{12}$  and  $A_{21}$ .

Comment 3: The aggregation of, say, matrix  $\tilde{B}$  as described in (4-4) is equivalent to making proper linear combinations of the rows of  $\tilde{B}$  to produce the specified form. In conjunction with representation (4-7), this can be interpreted as synthesizing the actuator influences so that control inputs will not spill over part  $x_2$  of the aggregated state  $x$ . Compare this interpretation with the idea [4-6] of preventing control spillover to secondary modes by synthesis of actuator influences. To prevent control spillover by synthesis is to make proper linear combinations of columns of matrix  $\tilde{B}$  to achieve a partitioning similar to what is described by (4-4), namely, to determine a transformation  $\Gamma$  such that

$$\tilde{B}\Gamma = \begin{bmatrix} B'_1 \\ 0 \end{bmatrix}$$

It follows from this comparison that the technique developed for computing synthesis transformation  $\Gamma$  can be modified to help compute the aggregation transformation  $T$ . This comment is equally applicable to the aggregation of matrix  $\tilde{C}$  with respect to an aggregation transformation  $S \equiv T^{-1}$ , observation spillover, and synthesis of sensor influences.

Let the transformation be partitioned with respect to (4-3) and (4-4) as follows

$$T = \begin{bmatrix} T_{11} & | & T_{12} \\ \hline \hline T_{21} & | & T_{22} \end{bmatrix}$$

The dimension of the blocks are as follows:

$T_{11}$ ,  $n \times n$ ;  $T_{12}$ ,  $n \times (2L - n)$ ;  $T_{21}$ ,  $(2L - n) \times n$ ;  $T_{22}$ ,  $(2L - n) \times (2L - n)$ .

Then Eq. (4-4) can be written as

$$T_{11}\tilde{B}_1 + T_{12}\tilde{B}_2 = B_1 \quad (4-9)$$

$$T_{21}\tilde{B}_1 + T_{22}\tilde{B}_2 = 0 \quad (4-10)$$

$$C_1 T_{11} = \tilde{C}_1 \quad (4-11)$$

$$C_1 T_{12} = \tilde{C}_2 \quad (4-12)$$

Since  $C_1$  is of the full row rank, its right inverse  $C_1^R$  exists. Therefore, from (4-12), we have

$$T_{12} = C_1^R \tilde{C}_2 \quad (4-13)$$

where

$$C_1^R \equiv C_1^T (C_1 C_1^T)^{-1} + N_{12} \quad (4-14a)$$

and  $N_{12}$  is an arbitrary matrix such that

$$C_1 N_{12} = 0 \quad (4-14b)$$

Similarly,  $\tilde{B}_1$  has its left inverse and, from (4-10), we have

$$T_{21} = -T_{22} \tilde{B}_2 \tilde{B}_1^L \quad (4-15)$$

where

$$\tilde{B}_1^L \equiv (\tilde{B}_1^T \tilde{B}_1)^{-1} \tilde{B}_1^T + N_{21} \quad (4-16a)$$

and  $N_{21}$  is an arbitrary matrix such that

$$N_{21} \tilde{B}_1 = 0 \quad (4-16b)$$

It follows from (4-14) and (4-16) that

$$T = \begin{bmatrix} T_{11} & C_1^R \tilde{C}_2 \\ -T_{22} \tilde{B}_2 \tilde{B}_1^L & T_{22} \end{bmatrix} = \begin{bmatrix} I & 0 \\ 0 & T_{22} \end{bmatrix} \begin{bmatrix} T_{11} & C_1^R \tilde{C}_2 \\ -\tilde{B}_2 \tilde{B}_1^L & I \end{bmatrix}$$

Therefore, the aggregation transformation  $T$  is nonsingular if and only if both  $T_{22}$  and  $(T_{11} + C_1^R \tilde{C}_2 \tilde{B}_2 \tilde{B}_1^L)$  are nonsingular.

Comment 4: The specific value of matrices  $C_1$  and  $B_1$  in (4-4), in general, should be consequences of the aggregation transformation  $T$ . Suppose on the contrary that  $C_1$  has been prescribed before the aggregation. Then, from (4-11)

$$T_{11} = C_1^R \tilde{C}_1$$

Consequently, the matrix sum

$$T_{11} + C_1^R \tilde{C}_2 \tilde{B}_2 \tilde{B}_1^L = C_1^R (\tilde{C}_1 + \tilde{C}_2 \tilde{B}_2 \tilde{B}_1^L)$$

cannot be nonsingular unless for such a very special case that  $n = \ell \geq m$  and  $\tilde{C}_1 + \tilde{C}_2 \tilde{B}_2 \tilde{B}_1^L$  is nonsingular. Therefore, it is better not to prescribe the value of  $C_1$  before aggregation.

Matrix  $B_1$  should not be prescribed, either. Premultiplying (4-9) by  $C_1$  and using (4-11) - (4-12) and (4-3), we have

$$C_1 B_1 = \tilde{C}_1 \tilde{B}_1 + \tilde{C}_2 \tilde{B}_2 \equiv CB \quad (4-17)$$

This relationship in general will not be satisfied if  $B_1$  is assigned a specific value before aggregation.

In the sequel, we assume that both  $T_{11}$  and  $T_{22}$  are nonsingular, and that both  $C_1$  and  $B_1$  are computed after aggregation. Now, from (4-13) and (4-15), we have

$$T = \begin{bmatrix} T_{11} & 0 \\ 0 & T_{22} \end{bmatrix} \begin{bmatrix} I & T_{11}^{-1} C_1^R \tilde{C}_2 \\ -\tilde{B}_2 \tilde{B}_1^L & I \end{bmatrix}$$

Theorem 1: The aggregation matrix  $T$  is nonsingular if and only if the  $n \times n$  matrix  $(I + T_{11}^{-1} C_1^R \tilde{C}_2 \tilde{B}_2 \tilde{B}_1^L)$  or the  $(2L - n) \times (2L - n)$  matrix  $(I + \tilde{B}_2 \tilde{B}_1^L T_{11}^{-1} C_1^R \tilde{C}_2)$  is nonsingular, where

$$C_1 = \tilde{C}_1 T_{11}^{-1} \quad (4-18)$$

Theorem 2: The following are two separate sets of sufficient conditions for the matrix  $T$  to be nonsingular.

$$(a) \quad \tilde{B}_2 = 0 \text{ or } \tilde{C}_2 = 0$$

$$(b) \quad T_{11}^T T_{11} = I, \ell = m, \text{ and } C = E \tilde{B}^T \text{ for some nonsingular matrix } E$$

Comment 5: Condition (a) appears to be trivial, since either the actuator influences or the sensor influences have been aggregated properly. This condition, however, clearly indicates the advantage of using Gram-Schmidt or Gaussian elimination procedure for rearranging the rows of  $\tilde{B}$  and the columns of  $\tilde{C}$ , and the advantage of prior effort made in preventing control and observation spillover by placement or synthesis; see Comment 2.

Comment 6: First part of condition (b) means that  $T_{11}$  is a special kind of non-singular matrix that is orthogonal; the identity matrix obviously is such an orthogonal matrix. The second and third parts mean that there are as many sensors as there are actuators and that the sensor influences as a whole are similar to the actuator influences as a whole. For LSS having only force actuators, this implies that no displacement sensors are considered for aggregation; namely,  $C_D = 0$  in (4-1). The special case in which  $E = kI$  represents the commonly considered case where each force actuator is collocated with a velocity sensor, and vice versa. Notice that vibration modes with such a special case can always be aggregated to achieve the desired representation (4-7).

Comment 7: The expressions (4-13) - (4-16) for  $T_{12}$  and  $T_{21}$  are slightly different from those given in [7]. These slight improvements, however, have made it possible to obtain useful new results, such as Theorems 1 and 2.

#### 4.2 Ideas for Specifying the Nonunique Aggregation Transformation

The similarity transformation  $T$  for accomplishing the aggregation as described by (4-4) is not unique; subject only to some rather minor constraints, submatrices  $T_{11}$ ,  $T_{22}$ ,  $N_{12}$ , and  $N_{21}$  are virtually free parameters. Additional properties may thus be imposed on the aggregate design model (4-8) by specifying these parameters. The following are some interesting ideas we made a quick look at.

##### 4.2.1 Minimization of Coupling Coefficients $A_{12}$ and $A_{21}$

Unlike the reduced-order design model usually obtained from direct truncation of vibration modes, the aggregate design model (4-8) has the desirable property that the coupling between the retained part  $x_1$  and the truncated part  $x_2$  remains unchanged even in the closed loop with feedback control systems. This constancy does not depend on how the control systems are designed, be they designed as LQ regulators and observers, or as dynamic output feedback compensators [7]. Therefore, it would be very desirable if the open-loop coupling coefficients  $A_{12}$  and  $A_{21}$  could be minimized by a suitable choice of the non-unique aggregation transformation.

Partition the aggregated matrix  $A$  defined in (4-5) and the original matrix  $A$  conformably with the similarity transformation  $T$ . Then we have

$$\begin{bmatrix} A_{11} & A_{12} \\ A_{21} & A_{22} \end{bmatrix} \begin{bmatrix} T_{11} & T_{12} \\ T_{21} & T_{22} \end{bmatrix} = \begin{bmatrix} T_{11} & T_{12} \\ T_{21} & T_{22} \end{bmatrix} \begin{bmatrix} \tilde{A}_{11} & \tilde{A}_{12} \\ \tilde{A}_{21} & \tilde{A}_{22} \end{bmatrix}$$

Solving for  $A_{12}$  and  $A_{21}$  yields

$$A_{12} = [T_{11}\tilde{A}_{12} + T_{12}\tilde{A}_{22} - (T_{11}\tilde{A}_{11} + T_{12}\tilde{A}_{21})T_{11}^{-1}T_{12}] (T_{22} - T_{21}T_{11}^{-1}T_{12})^{-1} \quad (4-19)$$

$$A_{21} = [T_{21}\tilde{A}_{11} + T_{22}\tilde{A}_{21} - (T_{21}\tilde{A}_{12} + T_{22}\tilde{A}_{22})T_{22}^{-1}T_{21}] (T_{11} - T_{12}T_{22}^{-1}T_{21})^{-1} \quad (4-20)$$

In terms of  $A_{12}$  and  $A_{21}$ , we have

$$A_{11} = (T_{11}\tilde{A}_{11} + T_{12}\tilde{A}_{21} - A_{12}T_{21})T_{11}^{-1} \quad (4-21)$$

$$A_{22} = (T_{21}\tilde{A}_{22} + T_{22}\tilde{A}_{22} - A_{21}T_{12})T_{22}^{-1} \quad (4-22)$$

Substituting (4-13) and (4-15) in (4-19) and (4-20),

$$A_{12} = T_{11} \left( \tilde{A}_{12} + T_{11}^{-1} C_1^R \tilde{C}_2 - \tilde{A}_{11} T_{11}^{-1} C_1^R \tilde{C}_2 \right. \\ \left. - T_{11}^{-1} C_1^R \tilde{C}_2 \tilde{A}_{21} T_{11}^{-1} C_1^R \tilde{C}_2 \right) \left( I + \tilde{B}_2 \tilde{B}_1^L T_{11}^{-1} C_1^R \tilde{C}_2 \right)^{-1} T_{22}^{-1} \quad (4-23)$$

$$A_{21} = T_{22} \left( -\tilde{B}_2 \tilde{B}_1^L \tilde{A}_{11} + \tilde{A}_{21} - \tilde{B}_2 \tilde{B}_1^L \tilde{A}_{12} \tilde{B}_2 \tilde{B}_1^L \right. \\ \left. + \tilde{A}_{22} \tilde{B}_2 \tilde{B}_1^L \right) \left( I + T_{11}^{-1} C_1^R \tilde{C}_2 \tilde{B}_2 \tilde{B}_1^L \right)^{-1} T_{11}^{-1} \quad (4-24)$$

With the expressions (4-14a) and (4-18), the terms within the parentheses of (4-23) and (4-24) are virtually independent of  $T_{11}$  and  $T_{22}$ . Thus, to minimize  $A_{12}$  is to minimize  $T_{11}$  and maximize  $T_{22}$ , whereas it is the opposite for minimizing  $A_{21}$ . Therefore, the coupling coefficients  $A_{12}$  and  $A_{21}$  cannot be minimized simultaneously by any choice of  $T_{11}$  and  $T_{22}$ .

The only possibility lies in the selection of the null-space matrices  $N_{12}$  and  $N_{21}$  involved respectively in the right inverse  $C_1^R$  and the left inverse  $\tilde{C}_1^L$ . The terms in the first parenthesis of (4-23) can be minimized by a separate choice of  $N_{12}$ , while those of (4-24) can be minimized simultaneously by a separate choice of  $N_{21}$ . The matrix products in the second parenthesis of (4-23) and (4-24) can be maximized simultaneously by a joint choice of  $N_{12}$  and  $N_{21}$ .

The constancy of the terms in the parentheses of both (4-23) and (4-24) can be seen more easily if we consider the class of orthogonal matrices for  $T_{11}$ , namely

$$T_{11}^T T_{11} = I$$

For this class

$$T_{11}^{-1} C_1^R \tilde{C}_2 = \tilde{C}_1^R \tilde{C}_2 \quad (4-25)$$

which is independent of  $T_{11}$ . All the terms within these parentheses are completely independent of  $T_{11}$ !

Nevertheless, the numbers of nonzero columns in  $A_{12}$  and nonzero rows in  $A_{21}$  can be reduced. Yeung Yam of MIT, while expanding the preliminary results in [7], has recently derived a specific choice of the free parameters in  $T$  such that, for the case  $n = l + m$ , only  $n$  columns of  $A_{12}$  and  $n$  rows of  $A_{21}$  are nonzero.

#### 4.2.2 Minimization of Differences in Closed-Loop Transfer Functions

Feedback control systems are to be designed based only on the reduced-order aggregate design model (4-8). The resultant closed-loop transfer functions for the design model alone generally will be different from the resultant ones for the overall system representing the LSS. It would be very desirable if the differences could be minimized by suitably specifying the free parameters of the aggregation transformation.

As in [7], consider fixed-order dynamic compensators of the form

$$\begin{cases} \dot{z} = Fz + Gy \\ u = Hz + Ky + \bar{u} \end{cases} \quad (4-26)$$

where the compensator state,  $z$  has a fixed dimension which is usually much less than  $2L$ ;  $\bar{u}$  denotes the command inputs;  $F$ ,  $G$ ,  $H$ , and  $K$  are design

parameters to be determined based on the reduced-order model (4-8). Substituting (4-26) in (4-8) yields the following closed-loop system of the design model.

$$\left\{ \begin{array}{l} \begin{bmatrix} \dot{z} \\ \dot{x}_1 \end{bmatrix} = \bar{A}_{11} \begin{bmatrix} z \\ x_1 \end{bmatrix} + \begin{bmatrix} 0 \\ B_1 \end{bmatrix} \bar{u} \\ y = [0 \quad C_1] \begin{bmatrix} z \\ x_1 \end{bmatrix} \end{array} \right. \quad (4-27)$$

where

$$\bar{A}_{11} = \begin{bmatrix} F & GC_1 \\ B_1 H & A_{11} + B_1 K C_1 \end{bmatrix} \quad (4-28)$$

The transfer function matrix of the closed loop system (4-27) between  $\bar{u}$  and  $y$  is found to be

$$\begin{aligned} Q(s) &\equiv [0 \quad C_1] (sI - \bar{A}_{11})^{-1} \begin{bmatrix} 0 \\ B_1 \end{bmatrix} \\ &= C_1 \left[ sI - A_{11} - B_1 K C_1 - B_1 H (sI - F)^{-1} \quad GC_1 \right]^{-1} B_1 \end{aligned} \quad (4-29)$$

Now substituting (4-26) in the overall system (4-7) yields the following closed-loop system.

$$\left\{ \begin{array}{l} \begin{bmatrix} \dot{z} \\ \dot{x}_1 \\ \dot{x}_2 \end{bmatrix} = \bar{A} \begin{bmatrix} z \\ x_1 \\ x_2 \end{bmatrix} + \begin{bmatrix} 0 \\ B_1 \\ 0 \end{bmatrix} \bar{u} \\ y = [0 \quad C_1 \quad 0] \begin{bmatrix} z \\ x_1 \\ x_2 \end{bmatrix} \end{array} \right. \quad (4-30)$$

where

$$\bar{A} = \begin{bmatrix} \bar{A}_{11} & \bar{A}_{12} \\ \bar{A}_{21} & \bar{A}_{22} \end{bmatrix} = \begin{bmatrix} F & GC_1 & 0 \\ B_1 H & A_{11} + B_1 K C_1 & A_{12} \\ 0 & A_{21} & A_{22} \end{bmatrix} \quad (4-31)$$

with the same  $\bar{A}_{11}$  as defined by (4-28). The transfer function matrix of the closed loop system (4-30) between  $\bar{u}$  and  $y$  is found to be

$$\bar{Q}(s) = C_1 \left[ sI - A_{11} - B_1 K C_1 - B_1 H (sI - F)^{-1} G C_1 - A_{12} (sI - A_{22})^{-1} A_{21} \right]^{-1} B_1 \quad (4-32)$$

Define the difference by

$$E(s) = \bar{Q}(s) - Q(s) \quad (4-33)$$

Then, one could attempt to choose the parameters  $T_{11}$ ,  $T_{22}$ ,  $N_{12}$ , and  $N_{21}$  such that

$$J = \int_{-\infty}^{\infty} \text{trace} \left[ E(s) E^T(\bar{s}) \right] du \quad (4-34)$$

is minimal, where  $s = \sigma + j\omega$  and  $\bar{s}$  denotes the complex conjugate of  $s$ . To obtain a solution to this minimization problem is impractical, if not impossible, judging from the algebraic complexity involved when the expressions (4-19) - (4-22) for  $A_{ij}$  and (4-13) - (4-16) for  $T_{12}$  and  $T_{21}$  are substituted in (4-29) and (4-32).

Intuitively, the main difference between  $\bar{Q}(s)$  and  $Q(s)$  is the term  $A_{12} (sI - A_{22})^{-1} A_{21}$ . The minimization of this term will also minimize the overall difference as defined by (4-33) or (4-34). See the preceding subsection (Subsection 4.2.1) for discussion on minimizing the coupling coefficients  $A_{12}$  and  $A_{21}$ .

Another intuitive alternative is to maximize the terms within the bracket of (4-29) so that the corresponding terms in (4-32) dominate the term

$$A_{12} (sI - A_{22})^{-1} A_{21}.$$

These two intuitive approaches may be much easier to take than direct minimization of the overall difference defined by (4-34) and any other way using (4-33). The necessary algebra still can be very complicated.

#### 4.2.3 Assurance of Closed-Loop Stability of LSS

Again, feedback controllers are to be designed using only the aggregate design model (4-8), and at least to assure closed loop stability with respect to the design model. It would be desirable if closed loop stability could still be assured when such controllers were implemented on LSS, which contains not only the design model but also the truncated part. Such an assurance is generally impossible for the case of direct truncation of vibration modes. Recall that the coupling  $A_{12}$  and  $A_{21}$  of the aggregate design model are independent of any controllers designed by any method. Thus, if closed-loop stability of the LSS having a controller designed for the aggregate design model using some

model using some method can be guaranteed, then closed-loop stability of the LSS having any such controllers but designed by other methods can also be guaranteed.

Consider again the feedback controllers of the form (4-26). Assume the design parameters  $F$ ,  $G$ ,  $H$ , and  $K$  are computed based on (4-8) so that the closed-loop system (4-27) is stable. The question is whether it is possible to find (and specify) among the nonunique aggregation transformation one such that the closed-loop system (4-30) is also stable. This requires the use of the stability theory for interconnected large scale subsystems; but the development of such stability theory has just begun [8] and no results are directly applicable to (or general enough for) our problem at hand yet. Moreover, with the expressions for  $A_{ij}$ , and  $T_{ij}$  substituted in (4-31), the resultant matrix  $A$  is a very complicated nonlinear matrix function of parameters  $T_{11}$ ,  $T_{22}$ ,  $N_{12}$ , and  $N_{21}$ . Deriving an analytical stability condition for system (4-30) is very difficult, if not impossible, at present. An attempt was made, however, in applying Willems' generalization [9] of Lyapunov theory to system (4-30).

#### 4.3 Aggregation of Vibration Modes also with Respect to Tracking and Disturbance Rejection

In the previous derivations, it was implicitly assumed that the purpose of the fixed-order compensator (4-26) was merely to enhance the stability of the closed-loop system. The aggregation was thus based only on the actuator and sensor influences. Now assume that there are a finite number of disturbance sources on the structure and a finite number of critical response variables (such as LOS motion in  $x$  and  $y$  directions). Then the compensator might be designed for minimizing the transmission from the disturbance sources to the critical response variables for all critical frequencies. This implies that the compensator places particular emphasis on damping out those vibration modes which can influence the critical response variables and can be excited by the disturbance sources. For such a generalized purpose, aggregation of the vibration modes should also include the influences of disturbance sources and critical response variables.

We extend the preceding studies in the following way. Suppose the original representation is now expanded as follows:

$$\left\{ \begin{array}{l} \dot{\tilde{x}} = \tilde{A}\tilde{x} + \tilde{B}u + \tilde{D}v \\ y = \tilde{C}\tilde{x} + \tilde{E}w \\ r = \tilde{M}\tilde{x} + \tilde{N}u \end{array} \right.$$

(4-35)

where

$v$  is a vector of disturbance inputs

$w$  is a vector of observation noises

$r$  is a vector of response (not necessarily measurable)

$u, \hat{x}, y$  are as before.

Now define

$$\hat{B} = [\tilde{B} \tilde{D} 0], \quad \hat{D} = \begin{bmatrix} 0 & 0 & \tilde{E} \\ \tilde{N} & 0 & 0 \end{bmatrix}, \quad \hat{v} = \begin{bmatrix} u \\ v \\ w \end{bmatrix}$$

$$\hat{C} = \begin{bmatrix} \tilde{C} \\ \tilde{M} \end{bmatrix}, \quad \hat{y} = \begin{bmatrix} y \\ r \end{bmatrix}, \quad \hat{A} = \tilde{A}, \quad \hat{x} = \tilde{x}$$

$$\begin{cases} \dot{\hat{x}} = \hat{A}\hat{x} + \hat{B}\hat{u} \\ \dot{\hat{y}} = \hat{C}\hat{x} + \hat{D}\hat{u} \end{cases} \quad (4-36)$$

Now by arguing as before, there is a transformation which brings the representation (4-35) into the form  $(A, B, C, D) = (\hat{A}\hat{T}^{-1}, \hat{B}\hat{T}, \hat{C}\hat{T}^{-1}, D)$ , where

$$A = \begin{bmatrix} A_{11} & A_{12} \\ A_{21} & A_{22} \end{bmatrix}, \quad B = \begin{bmatrix} B_1 \\ 0 \end{bmatrix}, \quad C = [C_1 \quad 0] \quad (4-37)$$

here  $A_{11}$  has the dimension between  $\max \{\dim \hat{u}, \dim \hat{y}\}$  and  $(\dim \hat{u} + \dim \hat{y})$ .

The representation (4-36) is now transformed into a similar form to (4-7). By making the same truncation, we obtain an aggregate design model which is also in a similar form to (4-8).

Now suppose we have a compensator

$$\dot{z} = Fz + Gy$$

$$u = Hz + Ky$$

Then the closed-loop dynamics is given by

$$\begin{bmatrix} \dot{z} \\ \dot{x} \end{bmatrix} = \begin{bmatrix} F & GC^* \\ B^* H & A + B^* K C^* \end{bmatrix} \begin{bmatrix} z \\ x \end{bmatrix} + \begin{bmatrix} 0 & GE \\ D^* & B^* KE \end{bmatrix} \begin{bmatrix} v \\ w \end{bmatrix}$$

$$r = [NH \quad M^* + NKC^*] \begin{bmatrix} z \\ x \end{bmatrix} + [0 \quad NKE] \begin{bmatrix} v \\ w \end{bmatrix}$$

where  $N = \tilde{N}$ ,  $E = \tilde{E}$  (since  $\hat{D} = D$ ), and  $B^*$ ,  $C^*$ ,  $D^*$ ,  $M^*$  are identified by partitioning  $B$  and  $C$ , i.e.,

$$B \equiv \begin{bmatrix} B_1 \\ 0 \end{bmatrix} \equiv \begin{bmatrix} B^* & D^* & 0 \end{bmatrix} \equiv \begin{bmatrix} B_1^* & D_1^* & 0 \\ 0 & 0 & 0 \end{bmatrix}$$

$$C \equiv [C_1 \quad 0] \equiv \begin{bmatrix} C^* \\ M^* \end{bmatrix} \equiv \begin{bmatrix} C_1^* & 0 \\ M_1^* & 0 \end{bmatrix}$$

#### LIST OF REFERENCES

1. Aoki, M., "Control of Large-Scale Dynamic Systems by Aggregation," IEEE Trans. Automat. Contr., Vol. AC-13, pp. 246-253, June 1968.
2. Aoki, M., "Aggregation," in Optimization Methods for Large-Scale Systems ... with Applications, D.A. Wismer, Ed., New York: McGraw-Hill, 1971.
3. Sandell, N.R., Jr., P. Varaiya, M. Athans, and M.G. Safonov, "Survey of Decentralized Control Methods for Large Scale System," IEEE Trans. Automat. Contr., Vol. AC-23, pp. 108-128, April 1978.
4. Lin, J.G., "Reduction of Control and Observation Spillover in Vibration Control of Large Flexible Space Structures," Paper No. 79-1763, AIAA Guidance and Control Conference, August 1979.
5. "Actively Controlled Structures Theory - Final Report," C. S. Draper Laboratory Report No. R-1338, December 1979, Section 2.

6. Lin, J.G., "Three Steps to Alleviate Control and Observation Spillover Problems of Large Space Structures," to be presented at 19th IEEE Conference on Decision and Control, Albuquerque, NM, December 1980.
7. Johnson, T.L. and Lin, J.G., "An Aggregation Method for Active Control of Large Space Structures," Proceedings of 18th IEEE Conference on Decision and Control, December 1979, pp. 1-3.
8. Special Issue on Large-Scale Systems and Decentralized Control, IEEE Trans. Automatic Control, Vol. AC-23, No. 2, pp. 105-371, April 1978.
9. Willems, J.C., "Stability of Large Scale Interconnected Systems," Directions in Large-Scale Systems: Many-Person Optimization and Decentralized Control, Y.C. Ho and S.K. Mitter, Eds., New York: Plenum, 1976, pp. 401-410.

## SECTION 5

### PARETO-OPTIMAL CONTROL

#### 5.0 Abstract

Canavin's "modal-dashpot" concept and Aubrun's "low-authority control" theory were two off-the-shelf examples used to illustrate the multiple-objective optimization problems underlying the design of vibration controllers for large space structures (see Subsection 5.1). Canavin used pseudo-inverses to compute the output feedback gains required for augmenting a certain level of damping to primary modes (or, specifically, critical modes); the computed gains were of disarmingly high values. A careful examination showed that such a high-gain problem need not exist because there were free parameters that could be adjusted to minimize the magnitude of the required gains. It also showed that the desire for large possible achievable damping and for small possible required gains could easily be formulated as a two-objective optimization problem and solved directly and efficiently by multiple-objective methods without computing the pseudo inverses and the appropriate values for the free parameters. In Aubrun's theory, the feedback gains were to minimize a cost functional that was the sum of two disparate design objectives: the magnitude of the errors between predicted and desired closed-loop damping, and the magnitude of feedback gains. The tradeoff between the closed-loop damping errors and the feedback gains, and the variation of the former versus the latter, could be systematically and efficiently made by formulating the underlying two-objective optimization problem and then applying a multiple-objective optimization method.

The applicability and application of two multiple-objective optimization methods were demonstrated by Pareto-optimal designs of modal dashpots for the 12-mode Draper model (see Subsection 5.2). Not only a sequence of the two-objective Pareto optimal designs but also the maximum damping achievable for each level of feedback gains were computed systematically. Insights into the movement of the closed-loop poles as the feedback gains increase their magnitude were easy to obtain from the resulting root loci. Systematic evaluation for robustness of the resulting sequence of designs to parameter variations and to spillover became easy. The variations of the sensitivity (i.e., of the robustness) were also obtained.

### 5.1 Applicability of Multiple-Objective Optimization Methods to the Design of Vibration Controllers

The design of a control system normally has more than one performance objective to achieve: e.g., large modal damping, low control response, little small feedback gains, small errors or overshoots, fast response, little spillover. As a standard practice, a designer usually combines the multiple objectives into one single performance index using some rather arbitrary weights. The designer, usually not satisfied with the resultant control systems, then repeatedly, aimlessly, and sometimes endlessly, changes the weighting coefficients to obtain new designs. Such frustration is not uncommon in the design of "modern control systems" using the linear-quadratic regulator theory; the weighting matrices Q and R frequently are changed over and over again. Experience with artificial single-objective optimization used on multiple-objective design problems has often left the designer dissatisfied with the lack of information (or systematic information) on the available tradeoffs between his multiple objectives and his "multiple-objective optimal" designs. Realistically, incompatible objectives cannot be unified; important multiple objectives should be addressed directly and their trade-off be made efficiently and systematically.

Pareto optimality is a practical notion of "multiple-objective" optimality that is useful to control systems designers faced with multiple disparate performance objectives. Stated simply, a design is Pareto optimal if none of the multiple objectives can be further improved without degrading any other. Multiple-objective optimization by the method of proper equality constraints (PEC) or the method of proper inequality constraints (PIC) help the designers obtain both Pareto optimal designs of control systems and efficient tradeoffs of the multiple objectives directly and systematically.

Consider the following two different approaches to the design of vibration controllers for large space structures: Canavin's "modal-dashpot" concept [1-4] and Aubrun's "low authority control" theory [5,6]. Let us point out their underlying multiple-objective design problems and briefly demonstrate the applicability of the above-mentioned multiple-objective methods [7-10].

Assume that large space structures are represented in modal coordinates as follows:

$$\ddot{\eta} + \Omega^2 \eta = \Phi^T B_F u \quad (5-1)$$

$$y = C_V \dot{\Phi} \eta \quad (5-2)$$

where  $\Omega = \text{diag } \{\omega_1, \dots, \omega_L\}$ , and  $\Phi = [\phi_1, \dots, \phi_L]$  are  $L \times L$  matrices:  $\omega_i$  and  $\phi_i$  denote respectively the natural frequency and shape of the  $i$ th normal mode of vibration.  $\eta = (\eta_1, \dots, \eta_L)$  denotes the corresponding normal coordinates.  $u = (u_1, \dots, u_m)$  denotes the control inputs to  $m$  force actuators, and  $B_F$  denotes the  $L \times m$  influence matrix.  $y = (y_1, \dots, y_\ell)$  denotes the observation outputs from  $\ell$  velocity sensors:  $C_V$  denotes the corresponding  $\ell \times L$  influence matrix. Superscript T denotes transpose.

In general, a very large number of vibration modes are included in this model. Let  $\{\omega_{pi}, \phi_{pi}\}$ ,  $i = 1, \dots, p$ , denote a selected subset for suppression; we call them primary modes for a self-explanatory reason. Completely neglecting all nonprimary modes yields the following truncated form

$$\ddot{\eta}_p + \Omega_p^2 \eta_p = \Phi_p^T B_F u \quad (5-3)$$

$$y = C_V \Phi_p \dot{\eta}_p \quad (5-4)$$

where  $\Omega_p$  and  $\Phi_p$  are similarly defined in terms of the  $p$  primary modes, and  $\eta_p = (\eta_{p1}, \dots, \eta_{pp})$  denotes the corresponding normal coordinates. Vibration control systems are then designed for this model as if it had exactly modeled the LSS in question.

Both Canavin's and Aubrun's approaches are for designing constant-gain velocity-output feedback control in the form

$$u = -G_V y \quad (5-5)$$

Substituting (5-5) in (5-3) and (5-4) yields the following closed-loop system dynamics

$$\ddot{\eta}_p + \Phi_p^T B_F G_V C_V \Phi_p \dot{\eta}_p + \Omega_p^2 \eta_p = 0 \quad (5-6)$$

Consider Canavin's modal-dashpot concept first. In order that each primary mode may be damped independently and arbitrarily, the feedback gain matrix  $G_V$  is computed using pseudo-inverses as follows:

$$G_V = (\Phi_p^T B_F)^T \left[ \Phi_p^T B_F (\Phi_p^T B_F)^T \right]^{-1} (2Z_p \Omega_p) \left[ (C_V \Phi_p)^T C_V \Phi_p \right]^{-1} (C_V \Phi_p)^T \quad (5-7)$$

where  $Z_p$  denotes a diagonal matrix of desired damping ratios  $\zeta_i$  for the  $p$  primary modes. It is assumed that  $\ell \geq p$  and  $m \geq p$ . Each actuator was assumed to be collocated with a velocity sensor in his numerical example [1,2]. For 10% damping for each primary mode, the computation using (5-7) resulted in a gain matrix of shockingly large values. He felt that "modal dashpots may be of limited utility due to the high gains produced by this approach" [1,2].

Such a high-gain problem actually need not exist. For exactly the same purpose of independently and arbitrarily damping the primary modes, the gain matrix  $G_V$  can be computed using a right inverse of  $\Phi_P^T B_F$  and a left inverse of  $C_V \Phi_P$ , instead, as follows:

$$G_V = (\Phi_P^T B_F)^R (2Z_p \Omega_p) (C_V \Phi_P)^L \quad (5-8)$$

where

$$(\Phi_P^T B_F)^R \equiv (\Phi_P^T B_F)^T \left[ \Phi_P^T B_F (\Phi_P^T B_F)^T \right]^{-1} + N_F \quad (5-9)$$

$$(C_V \Phi_P)^L \equiv \left[ (C_V \Phi_P)^T C_V \Phi_P \right]^{-1} (C_V \Phi_P)^T + N_V \quad (5-10)$$

with  $N_F$  and  $N_V$  being arbitrary null-space matrices such that

$$\Phi_P^T B_F N_F = 0 \quad (5-11)$$

$$N_V C_V \Phi_P = 0 \quad (5-12)$$

(See Section 6.2, particularly Comments 7 and 8, concerning a generalization and an extension of the modal dashpot concept.) The similarity and the difference between (5-7) and (5-8) are obvious. Whenever the rank of  $\Phi_P^T B_F$  is less than the number  $m$  of actuators, matrix  $N_F$  need not be zero. Similarly, whenever the rank of  $C_V \Phi_P$  is less than the number  $\ell$  of sensors, matrix  $N_V$  need not be zero, either. Nonzero  $N_F$  and  $N_V$  serve as free parameters and can be used to reduce the magnitude of gain matrix  $G_V$ . The undesirable consequence of neglecting these adjustable free parameters is thus clear.

Now that we have recognized the existence and advantage of free parameters  $N_F$  and  $N_V$ , an obvious question is how to choose their values to minimize the magnitude of the required feedback gains while using the feedback gains to augment as much damping to the primary modes as possible.

The underlying two performance objectives now become evident, and are formulated as a bi-objective optimization problem as follows. Note that in the interest of improving model fidelity, we also retain in the control design model some other important modes which we call secondary modes and denote by subscript S. Active damping of secondary modes is not required, but prevention of control spillover to and observation spillover from them is desired. Both primary and secondary modes are altogether referred to as modeled modes and denoted by subscript M. Therefore, the bi-objective modal-dashpot design problem is to find the feedback gains  $g_{ij}$  and the damping ratios  $\zeta_i$  that maximize

$$J_1 = \sum_{i=1}^P w_i \zeta_{pi} \quad (5-13)$$

and minimize

$$J_2 = \sum_{i=1}^m \sum_{j=1}^l g_{ij}^2 \quad (5-14)$$

subject to

$$\Phi_M^T B_F G_V C_V \Phi_M = 2Z_M \Omega_M \quad (5-15)$$

$$\zeta_i \geq \zeta_{Pmin} \text{ for primary modes} \quad (5-16)$$

$$\zeta_i \geq \zeta_{Smin} \text{ for secondary modes} \quad (5-17)$$

where weighting factors  $w_i$  are useful for expressing desired mode movement (see Subsection 5.2). Observe that no computation of the pseudo-inverses, the right or the left inverses, or the free parameters is required. They are all embedded in the equality constraint (5-16) of closed-loop modal decoupling. The method of proper equality constraints (PEC) is to set the first objective to a parametric level, i.e.,

$$\sum_{i=1}^P w_i \zeta_{pi} = \alpha \quad (5-18)$$

whereas the method of proper inequality constraints (PIC) is to bound the first objective by a parametric level, i.e.,

$$\sum_{i=1}^P w_i \zeta_{pi} \leq \alpha \quad (5-19)$$

Whether the method of PEC or PIC is used, the bi-objective problem (5-13) - (5-17) is all converted to a parametric single-objective quadratic programming problem of the following standard form: minimize

$$J = \mathbf{x}^T \mathbf{Q} \mathbf{x} \quad (5-20)$$

subject to

$$\mathbf{A} \mathbf{x} \geq \mathbf{b}$$

$$\mathbf{x} \geq \mathbf{0}$$

Many algorithms and computer programs have been developed for solving the quadratic programming problem (5-20); see, for example, References [11-15]. For each selected value of the parameter  $\alpha$ , the resulting quadratic programming problem is solved for the single-objective optimal solutions. Using the test for Pareto optimality as given in References [7-10], the Pareto optimal values of feedback gain  $g_{ij}$  and damping ratios  $\zeta_i$  are obtained systematically in the increasing order of  $\alpha$ . The resulting minimized values of the objective  $J_2$  (i.e., the magnitude of gain matrix  $G_V$ ), plotted versus parameter  $\alpha$ , will help the designer make optimal tradeoffs efficiently and systematically between achievable damping and minimum required gains. See Subsection 5.2 or Refs. [16-17] for more details.

It is worth mentioning that the free parameters  $N_F$  and  $N_V$  are implicitly used to minimize the magnitude of required feedback gains and to decouple secondary modes from primary modes in the closed loop. Such was not possible with Canavin's origin modal-dashpot concept. On the other hand, there is no question at all about the applicability of multiple-objective optimization methods to design of modal dashpots.

Now, consider Aubrun's low-authority-control (LAC) theory. According to Aubrun [5,6], for sufficiently "small" feedback gains  $g_{ij}$ , the closed-loop damping of mode  $i$  is predicted using the following formula [5,6]:

$$d\lambda_i \approx 2\zeta_i \omega_i \approx \phi_i^T B_F G_V C_V \phi_i \quad (5-21)$$

using the open-loop frequency  $\omega_i$  and mode shape  $\phi_i$ . To compute the gains  $g_{ij}$ , let  $(d\lambda_i)_P$  denote the predicted closed-loop damping given by the above formula, and let  $(d\lambda_i)_D$  denote the desired closed-loop damping imposed by the LAC controller design. Then the gains  $g_{ij}$  are chosen so as to minimize the quadratic cost functional

$$J(G_V) = \sum_i w_i \left[ (d\lambda_i)_D - (d\lambda_i)_P \right]^2 + \sum_{i,j} g_{ij}^2 \quad (5-22)$$

in which the modal weights  $w_i$  help specify pole locations and the term  $\sum_{i,j} g_{ij}^2$  improve robustness of the controller [6]. It is not difficult to see from (5-22) that two disparate objectives, one concerning damping and the other concerning gains, are "unified". The underlying bi-objective optimization problem is to minimize

$$J_1 = \sum_i w_i \left[ (d\lambda_i)_D - (d\lambda_i)_P \right]^2 \quad (5-23)$$

and minimize

$$J_2 = \sum_{i,j} g_{ij}^2 \quad (5-23)$$

Pareto optimal solutions of this problem by the method of PEC or PIC will provide a curve of  $J_2$  versus  $J_1$  for systematically making efficient tradeoff between achievable damping errors and the corresponding feedback gains required. The first objective,  $J_1$ , is converted to a parametric equality constraint if the method of PEC is used, while it is converted to a parametric inequality constraint if the method of PIC is used instead. All converts the bi-objective problem to a simplest form of nonlinear programming problem, where the single objective function and the parametric constraint are quadratic. Many nonlinear programming algorithms and computer programs already developed [14,15] can be used in solving the resultant constrained optimization problem. Applicability of the multiple-objective optimization methods is, again, not a problem at all.

Comment 1: Both underlying bi-objective design problems (5-13) - (5-17) and (5-23) - (5-24), have the minimization of feedback gains as an objective; such is a very practical engineering objective in addition to the design objective on damping.

Comment 2: The closed-loop damping expressed by formula (5-21) may not be valid since the closed-loop modes may not remain decoupled with the same open-loop frequencies, even with respect to the reduced design model. Only when the gains  $g_{ij}$  are extremely small will the closed-loop modes be virtually uncoupled. On the other hand, the desired independence can be explicitly imposed, such as (5-15); the resultant Pareto optimal designs then will certainly ensure that the open-loop modes remained decoupled at least in the closed loop of the design model.

Comment 3: The minimization of feedback gains, such as expressed by (5-14) or (5-24), does not actually provide robustness of the controllers designed. It will reduce control and observation spillover, however, because the residual modes will be less excited and less observed.

## 5.2 Application to Draper Tetrahedral Model of LSS

The 12-mode Draper tetrahedral model of LSS was used as an example [16,17]. Pareto optimal designs of modal dashpots and the tradeoff curve were sequentially generated by a bi-objective optimization program developed. In search of more or less uniform movement of the primary modes under efficient tradeoffs of damping and gain objectives, we found the form of inverse-sum-of-squared-influence (ISSI) for the weighting factors  $w_i$  in (5-13) more satisfactory than others.

Each of the resulting designs was then examined for its robustness to model parameter variation and spillover (resulting from modal truncation). For all designs with velocity sensors collocated with force actuators, robustness of stability to parameter variation and to spillover was clearly demonstrated. The damping performance is relatively insensitive to parameter variation and to spillover; however, the sensitivity rapidly increases as the desired level of critical-mode damping increases. In other words, modal dashpots can theoretically be designed to provide any desired level of damping to the critical vibration modes. In practice, however, only low designed levels of modal damping can be closely achieved due to this sensitivity to parameter variation and spillover.

For those designs where the sensors and actuators were not all collocated, stability and damping performance are also relatively insensitive to parameter variation. However, spillover causes all designs to destabilize the originally stable structure; at least half of the resultant closed-loop poles have positive real parts. Destabilization by modal dashpots, which are also referred to as robust controllers, has not been demonstrated before. Consequently, collocation of sensors with actuators is essential to the robustness of modal dashpots when used as vibration dampers for realistic large space structures.

## LIST OF REFERENCES

1. "Passive and Active Suppression of Vibration Response in Precision Structures, State-of-the-Art Assessment," Technical Report R-1138, Vol. 2, Technical Analysis, The Charles Stark Draper Laboratory, Inc., Cambridge, Mass., 28 February 1978.
2. Canavin, J.R., "The Control of Spacecraft Vibrations Using Multivariable Output Feedback," Paper 78-1419, AIAA/AAS Conference, Los Angeles, CA, August 1978.
3. Elliott, L.E., Mingori, D.L., and Iwens, R.P., "Performance of Robust Output Feedback Controller for Flexible Spacecraft," Proceedings of Second Symposium on Dynamics and Control of Large Flexible Spacecraft, Blacksburg, Virginia, June 1979, pp. 409-420.

4. Lin, Y.H. and Lin, J.G., "An Improved Output Feedback Control of Flexible Large Space Structures," to be presented at 19th IEEE Conference on Decision and Control, Albuquerque, NM, December 1980.
5. Aubrun, J.N., "Theory of the Control of Structures by Low Authority Controllers," Paper No. 78-1689, AIAA Conference on Large Space Platforms: Future Needs and Capabilities, Los Angeles, CA, Sept. 1978.
6. Aubrun, J.N., Gupta, N.K., Lyons, M.G., and Margulies, G., "Large Space Structures Control: An Integrated Approach," Paper No. 79-1764, AIAA Guidance and Control Conference, Boulder, CO, August 1979.
7. Lin, J.G., "Multiple-Objective Problems: Pareto-Optimal Solutions by Method of Proper Equality Constraints," IEEE Trans. Automatic Control, Vol. AC-21, No. 5, pp. 641-650, October 1976.
8. Lin, J.G., "Proper Equality Constraints and Maximization of Index Vectors," J. Optimization Theory and Applications, Vol. 20, No. 2, pp. 215-244, October 1976.
9. Lin, J.G., "Proper Inequality Constraints and Maximization of Index Vectors," J. Optimization Theory and Applications, Vol. 21, No. 4, pp. 505-521, April 1977.
10. Lin, J.G., "Multiple-Objective Optimization by Multiplier Method of Proper Equality Constraints - Part 1: Theory," IEEE Trans. Automatic Control, Vol. 24, No. 4, pp. 567-573, August 1979.
11. Wolfe, P., "The Simplex Method for Quadratic Programming," Econometrica, Vol. 27, pp. 382-398, 1959.
12. Lemke, C.E., "Bimatrix Equilibrium Points and Mathematical Programming," Management Science, Vol. 11, No. 7, pp. 681-689, May 1965.
13. Ravindran, A., "Algorithm 431, A Computer Routine for Quadratic and Linear Programming Problems," CACM, Vol. 15, No. 9, pp. 818-820, September 1972.
14. Kuester, J.L. and Mize, J.H., Optimization Techniques with Fortran, McGraw-Hill, New York, 1973.
15. Himmelblau, D.M., Applied Nonlinear Programming, McGraw-Hill, New York, 1972.
16. Preston, R.B. and Lin, J.G., "Pareto Optimal Vibration Damping of Large Space Structures with Modal Dashpots," Proceedings of 1980 Joint Automatic Control Conference, August 1980, Paper FP1-C.
17. Preston, R.B. and Lin, J.G., "An Application of Pareto Optimization Methods to Vibration Damping of Large Space Structures," to be presented at 19th IEEE Conference on Decision and Control, Albuquerque, NM, December 1980.

## SECTION 6

### GENERAL REQUIREMENTS FOR STABILIZATION

#### 6.0 Abstract

Feedback from velocity sensor outputs can augment damping and feedback from displacement sensor outputs can augment stiffness to large space structures. The design of the feedback gains are normally based only on modeled modes; the existence of unmodeled modes is completely ignored. Due to the attendant control and observation spillover, even stability of the closed-loop system having feedback controllers thus designed may not be ensured, let alone the additional damping and stiffness desired. Useful general conditions in various useful forms were recently established (see Subsection 6.1) for guaranteeing closed-loop asymptotic stability. Such conditions are useful as a guide to the design of closed-loop stabilizing feedback gains. Large space structures considered were not limited to those having only stable elastic modes; rigid-body modes and unstable modes were not excluded. For those special structures having only stable elastic modes and rigid-body modes, useful simple conditions were also established. The conditions for robustness to parameter variation and to modal truncation were also established.

Canavin's modal-dashpot concept was generalized and extended (see Subsection 6.2). The similar concept of "modal springs" was therefore proposed. The general formulas for computing the feedback gains of generalized modal dashpots and modal springs were derived. These formulas contain various adjustable free parameters. The closed-loop asymptotic stability assurance and the robustness to parameter variation and to modal truncation of modal dashpots and modal springs were established, thus at least providing a theoretic foundation for Canavin's original concept. Although no analytic proofs for the closed-loop stability assurance and robustness of modal dashpots were given by Canavin when he proposed the intuitive concept, a numerical demonstration was made with a typical example of large space structures.

Control spillover to and observation spillover from secondary modes can be prevented before the beginning of the controller design process by proper placement of actuators and sensors or by proper synthesis of actuator and sensor influences. A general-purpose computer program is being developed for synthesizing actuator influences so that control spillover to secondary modes can be prevented and the desired control influences on primary modes can be obtained simultaneously. A recent theoretical analysis has led to the conclusion that such a computer program can be used to synthesize sensor influences by duality and even to determine the proper location of actuators and sensors (see Subsection 6.3).

### 6.1 General Conditions for Closed-Loop Stabilization by Output Feedback Control

Consider the active control of a generic large space structure (LSS) which may contain rigid-body modes, unstable and stable elastic modes. As usual, let the modal equations generated by a finite-element computer program (such as NASTRAN) be

$$\ddot{\eta} + \Delta \dot{\eta} + \Sigma \eta = \dot{\varphi}^T f \quad (6-1)$$

where  $\eta$  denotes the  $L$  (normal) modal coordinates and  $\dot{\varphi}$  the natural mode shapes;  $f$  denotes the  $m$  generalized forces;  $\Delta$  and  $\Sigma$  are diagonal matrices denoting, respectively, the modal damping and the modal stiffness coefficients. In general, the diagonal elements of  $\Delta$  and  $\Sigma$  may be positive, zero, or even negative, and can be extremely small if not zero. Note that if  $q$  denotes the generalized physical coordinates, then

$$q = \dot{\varphi} \eta \quad (6-2)$$

Consider specifically the case of constant-gain output feedback control, namely, if  $y_V$  velocity measurements and  $y_D$  displacement measurements are fed back to  $m$  force actuators with constant gains as follows

$$f = B_F u \quad (6-3)$$

$$u = -G_V y_V - G_D y_D \quad (6-4)$$

$$y_V = C_V \dot{q} \quad (6-5a)$$

$$y_D = C_D q \quad (6-5b)$$

In other words

$$f = -B_F G_V C_V \dot{q} - B_F G_D C_D q \quad (6-6)$$

Substituting (6-6) in (6-1) yields

$$\ddot{\eta} + \left( \dot{\varphi}^T \Delta \dot{\varphi} + \dot{\varphi}^T \Sigma \dot{\varphi} \right) \dot{\eta} + \left( \dot{\varphi}^T B_F G_D C_D \dot{\varphi} \right) q = 0 \quad (6-7)$$

where

$$D_A \equiv B_F^T G_V C_V \quad (6-8a)$$

$$K_A \equiv B_F^T G_D C_D \quad (6-8b)$$

denote the additional damping and stiffness matrices respectively. The design of gain matrices  $G_V$  and  $G_D$  should make both the augmented damping matrix  $(\Delta + \Phi^T D_A \Phi)$  and the augmented stiffness matrix  $(\Sigma + \Phi^T K_A \Phi)$  symmetric and positive definite, in addition to achieving certain design objectives (e.g., increasing the damping of critical modes to desired levels). The reason is simple, since it is well known that a closed-loop system as described by (6-7) is asymptotically stable if both matrices  $(\Delta + \Phi^T D_A \Phi)$  and  $(\Sigma + \Phi^T K_A \Phi)$  are symmetric and positive definite, and closed-loop stability is a basic requirement.

Note, however, that the matrices  $\Delta$  and  $\Sigma$  are not positive definite unless all their diagonal elements are positive. Also note that both matrices  $D_A$  and  $K_A$  are singular, since there are more modes represented by (6-1) than there are actuators or sensors placed on the structure (i.e.,  $L > \lambda_V$ ,  $L < \lambda_D$ ). Moreover, the design of gains  $G_V$  and  $G_D$ , in general, can be based only on a reduced-order model of the structure; in other words, only a truncated version of (6-1) can be used. Therefore, the asymptotic stability of the closed-loop system (6-7) does not follow automatically with an arbitrary design of  $G_V$  and  $G_D$ .

Let subscript M denote the part of (6-1) that is included in the reduced-order model for control system design and subscript U the unmodeled (i.e., truncated) part. Then Eqs. (6-1) - (6-5) can be rewritten as follows

$$\ddot{\eta}_M + \Delta_M \dot{\eta}_M + \Sigma_M \eta_M = \Phi_M^T B_F u \quad (6-9a)$$

$$\ddot{\eta}_U + \Delta_U \dot{\eta}_U + \Sigma_U \eta_U = \Phi_U^T B_F u \quad (6-9b)$$

$$u = -G_V y_V - G_D y_D \quad (6-10)$$

$$y_V = C_V \Phi_M \dot{\eta}_M + C_V \Phi_U \dot{\eta}_U \quad (6-11a)$$

$$y_D = C_D \Phi_M \eta_M + C_D \Phi_U \eta_U \quad (6-11b)$$

The design of gains  $G_V$  and  $G_D$  ignores the existence of the unmodeled part completely, and is to make only the modeled part achieve desired damping and

stiffness objectives. Due to control spillover to and observation spillover from the unmodeled part, as can be seen from Eq. (6-9b) and (6-11), the overall closed-loop system (6-7) may not achieve the damping and stiffness objectives. In particular, the symmetry and positive definiteness of the overall matrices  $(\Delta + \Phi^T D_A \Phi)$  and  $(\Sigma + \Phi^T K_A \Phi)$  do not follow automatically from only making their modeled parts,  $(\Delta_M + \Phi_M^T D_A \Phi_M)$  and  $(\Sigma_M + \Phi_M^T K_A \Phi_M)$ , symmetric and positive definite. We have recently obtained the following general conditions (Theorems 1 through 5) for guaranteeing the symmetry and positive definiteness of such overall matrices and hence for guaranteeing the asymptotic stability of closed-loop system (6-7). Such conditions are also useful as a guide in the design of gain matrices  $G_V$  and  $G_D$ . A useful special case is discussed in Subsection 6.2.

Theorem 1: Assume that  $D_A$  is symmetric and  $(\Delta_M + \Phi_M^T D_A \Phi_M)$  is positive definite. Then, for  $(\Delta + \Phi^T D_A \Phi)$  to be positive definite, it is necessary and sufficient that

$$\Delta_1 \equiv \Delta_U + \Phi_U^T D_A \Phi_U - \Phi_U^T D_A \Phi_M (\Delta_M + \Phi_M^T D_A \Phi_M)^{-1} \Phi_M^T D_A \Phi_U \quad (6-12)$$

is positive definite.

Theorem 2: Assume that  $K_A$  is symmetric and  $(\Sigma_M + \Phi_M^T K_A \Phi_M)$  is positive definite. Then, for  $(\Sigma + \Phi^T K_A \Phi)$  to be positive definite, it is necessary and sufficient that

$$\Sigma_1 \equiv \Sigma_U + \Phi_U^T K_A \Phi_U - \Phi_U^T K_A \Phi_M (\Sigma_M + \Phi_M^T K_A \Phi_M)^{-1} \Phi_M^T K_A \Phi_U \quad (6-13)$$

is positive definite.

Comment 1: For closed-loop asymptotic stability of the overall system, it is not enough just to guarantee the positive definiteness of the modeled parts  $(\Delta_M + \Phi_M^T D_A \Phi_M)$  and  $(\Sigma_M + \Phi_M^T K_A \Phi_M)$ . According to Theorems 1 and 2, the matrices  $\Delta_1$  and  $\Sigma_1$  defined by (6-12) and (6-13), respectively must be made positive definite as well in the design of  $G_V$  and  $G_D$ . This explains why current approaches to the design of LSS controllers (e.g., direct applications of state-of-the-art control techniques only to the modeled part without any consideration of the unmodeled part) cannot guarantee closed-loop asymptotic stability.

Comment 2: It is convenient as well as intuitively desirable to be able to find a design of, say,  $G_V$  such that the additional damping matrix for the modeled part is diagonal. For example, using the pseudo-inverses of  $\Phi_M^T B_F$  and  $C_V^T M$  with a diagonal matrix will make  $\Phi_M^T D_A \Phi_M$  diagonal. Notice, however that those  $G_V$  designed using such pseudo-inverses will make only  $\Phi_M^T D_A \Phi_M$  symmetric; to

make the whole matrix  $\Phi^T D_A \Phi$  symmetric requires that each velocity sensor be collocated with a force actuator such that  $C_V = k_V B_F^T$  for some nonzero constant  $k_V$ . Note, however, that collocation is not assumed in either Theorem 1 or 2.

Comment 3: These theorems are applicable to the general case of large space structures that contain not only stable elastic modes but also rigid-body modes and unstable modes. To provide a better insight into the requirements in stabilization of general large space structures, refine the partitioning of matrices  $\Delta$  and  $\Sigma$  as follows. Denote the group by subscript G if their diagonal elements of  $\Delta$  are greater than zero, and by double subscript LE, if otherwise. Similarly, denote the group by  $G'$  if their diagonal elements of  $\Sigma$  are greater than zero, and by  $L'E'$ , if otherwise. Then we get the following similar general conditions

Theorem 3: Assume that  $D_A$  is symmetric and  $(\Delta_{LE} + \Phi_{LE}^T D_A \Phi_{LE})$  is positive definite. Then, for  $(\Delta + \Phi^T D_A \Phi)$  to be positive definite, it is necessary and sufficient that

$$\Delta_2 \equiv \Delta_G + \Phi_G^T D_A \Phi_G - \Phi_{G'A}^T \Phi_{LE} (\Delta_{LE} + \Phi_{LE}^T D_A \Phi_{LE})^{-1} \Phi_{LE}^T D_A \Phi_G \quad (6-14)$$

is positive definite.

Theorem 4: Assume that  $K_A$  is symmetric and  $(\Sigma_{L'E'} + \Phi_{L'E'}^T K_A \Phi_{L'E'})$  is positive definite. Then, for  $(\Sigma + \Phi^T K_A \Phi)$  to be positive definite, it is necessary and sufficient that

$$\Sigma_2 \equiv \Sigma_{G'} + \Phi_{G'}^T K_A \Phi_{G'} - \Phi_{G'A}^T K_A \Phi_{L'E'} (\Sigma_{L'E'} + \Phi_{L'E'}^T K_A \Phi_{L'E'})^{-1} \Phi_{L'E'}^T K_A \Phi_{G'} \quad (6-15)$$

is positive definite.

Comment 4: The unstable or undamped modes, having either nonpositive modal damping or nonpositive modal stiffness, naturally should be included in the model for designing gain matrices  $G_V$  and  $G_D$ , and at least both

$(\Delta_{LE} + \Phi_{LE}^T B_F G_V C_V \Phi_{LE})$  and  $(\Sigma_{L'E'} + \Phi_{L'E'}^T B_F G_D C_D \Phi_{L'E'})$  should be made positive definite. Theorems 3 and 4, however, show that this is not sufficient unless both  $\Delta_2$  and  $\Sigma_2$ , as defined by (6-14) and (6-15), are guaranteed to be positive definite. In general, flexible structures having small positive modal damping (i.e., small diagonal elements of  $\Delta_G$ ), and lower natural vibration frequencies (i.e., small diagonal elements of  $\Sigma_{G'}$ ), will be difficult in providing such guarantees.

Consider the following common special cases: only rigid-body modes, and elastic modes, undamped and lightly damped, are present. In the above partitioning, the groups denoted by LE and  $L'E'$  now correspond to only zero.

diagonal elements of  $\Delta$  and  $\Sigma$ , respectively. Denoting these groups now by  $E$  and  $E'$ , we get the following two very useful consequences of Theorems 3 and 4, concerning closed-loop stability and its robustness.

Theorem 5: Assume that each unmodeled elastic mode has some positive damping, no matter how small it is. Then the closed-loop overall system (6-7) is asymptotically stable, i.e., both  $(\Delta + \Phi^T D_A \Phi)$  and  $(\Sigma + \Phi^T K_A \Phi)$  are symmetric and positive definite if

- (a)  $D_A$  and  $K_A$  are symmetric and at least positive semidefinite, and
- (b)  $\Phi^T D_A \Phi$  and  $\Phi^T K_A \Phi$  are positive definite.

Comment 5: This theorem implies that the closed-loop asymptotic stability is robust to modal truncation, so long as conditions (a) and (b) are satisfied and all the unmodeled (i.e., the truncated) modes have some positive damping, finite or infinitesimal. First, unmodeled modes do not appear in conditions (a) and (b) at all, control spillover and observation spillover thus have no effect on closed-loop asymptotic stability so long as the assumption and conditions of Theorem 5 satisfied. Second, closed-loop asymptotic stability does not depend on how many damped elastic modes are included in the design model nor on which of them are, since neither conditions (a) nor (b) depend on any damped elastic mode.

Theorem 6: Suppose the gain matrices  $G_V$  and  $G_D$  have been designed to satisfy conditions (a) and (b) of Theorem 5. Let there be parameter variations (or errors) in the mass matrix, the stiffness matrix, the natural frequencies, or the mode shapes of the structure concerned. Assume that

- (i) the number of rigid-body modes and that of undamped modes remains unchanged, and
- (ii)  $\bar{\Phi}_E = \Phi_E C_E$ ,  $\bar{\Phi}_{E'} = \Phi_{E'} C_{E'}$ ,

Where the overbars denote the presence of parameter variations (errors);  $C_E$  and  $C_{E'}$  are nonsingular matrices. Then the closed-loop overall system remains asymptotically stable.

Comment 6: Theorem 6 implies that closed-loop asymptotic stability is robust to changes in the shape of any damped elastic modes, modeled or not.

The following subsection (Subsection 6.2) continues the discussion of this special case with a specific design of gain matrices  $G_V$  and  $G_D$  that can provide not only the closed-loop asymptotic stability but also its robustness to modal truncation and parameter variation. Before concluding this subsection, we remark that the controllability and observability of all the rigid-body modes, all the unstable modes (with either negative modal damping or negative modal stiffness coefficients), and all the critical elastic modes, are assumed. The actuators and sensors should therefore be properly placed or their existent influences be properly synthesized, according to the techniques and conditions previously derived; see Refs. 1-3; Subsections 6.3 and 6.4.

## 6.2 Closed-Loop Stabilization with "Modal Dashpots" and "Modal Springs"

A special output feedback control design technique is presented in this section for integrated control of elastic and rigid-body modes, for increasing both the damping and frequency of selected modes, and for providing closed-loop asymptotic stability and its robustness to modal truncation and to parameter variation. This technique represents an improvement over previous work [4-8] concerning output feedback control of LSS or control of rigid-body modes, and is an advancement along Canavin's modal-dashpot design philosophy [4].

Consider again the common special case of large space structures: rigid-body modes, undamped and lightly damped elastic modes may all be present. Assume that the rigid-body modes are not to be ignored as was in [4] but to be controlled along with the undamped elastic modes and those lightly damped elastic modes which are critical to the damping performance of the LSS. These modes constitute the primary modes. Assume that the design model is formed by these primary modes. Therefore, all other modes are unmodeled modes and all are assumed to have some positive damping, despite how small they are. Using the same partitioning as described at the end of the foregoing subsection, we have the following direct consequences of Theorem 5.

Theorem 7: Denote the number of modeled (i.e., the primary) modes by  $p$ . Assume that there are at least as many force actuators as there are modeled modes (i.e.,  $m \geq p$ ), and that each force actuator is collocated with a velocity sensor and a displacement sensor, (i.e.,  $C_V = k_V B_F^T$ ,  $C_D = k_D B_F^T$ , for some non-zero constants  $k_V$  and  $k_D$ ). Assume further that all modeled modes are completely controllable. Then the closed-loop system is asymptotically stable if the gain matrices  $G_V$  and  $G_D$  are computed as follows

$$G_V = \left( \Phi_M^T B_F \right)^R \Delta_M^* \left( C_V \Phi_M \right)^L \quad (6-16)$$

$$G_D = \left( \Phi_M^T B_F \right)^R \Sigma_M^* \left( C_D \Phi_M \right)^L \quad (6-17)$$

$$\left( \Phi_M^T B_F \right)^R \equiv \left( \Phi_M^T B_F \right)^T \left[ \Phi_M^T B_F \left( \Phi_M^T B_F \right)^T \right]^{-1} + N_F \quad (6-18a)$$

$$\left( C_V \Phi_M \right)^L \equiv \left[ \left( C_V \Phi_M \right)^T C_V \Phi_M \right]^{-1} \left( C_V \Phi_M \right)^T + N_V \quad (6-19a)$$

$$\left( C_D \Phi_M \right)^L \equiv \left[ \left( C_D \Phi_M \right)^T C_D \Phi_M \right]^{-1} \left( C_D \Phi_M \right)^T + N_D \quad (6-20a)$$

where  $\Delta_M^*$  and  $\Sigma_M^*$  denote two arbitrary positive definite  $p \times p$  matrices desired as the additional damping and stiffness for the modeled modes;  $N_F$ ,  $N_V$ , and  $N_D$  are any null-space matrices such that

$$\Phi_M^T B_F N_F = 0 \quad (6-18b)$$

$$k_V N_V = N_F^T \quad (6-19b)$$

$$k_D N_D = N_F^T \quad (6-20b)$$

Comment 7: It is technically convenient, though not necessary, to consider  $\Delta_M^*$  and  $\Sigma_M^*$  as diagonal matrices. Canavin [4] originally called the resulting modally decoupled velocity output feedback controllers "modal dashpots", in which the rigid-body modes were ignored, no displacement feedback was considered, both  $N_F$  and  $N_V$  were zero, and  $\Delta_M^*$  was diagonal. Here, we extend the concept in two ways. First, any velocity feedback controllers designed according to (6-16), (6-18) and (6-19) are called (generalized) modal dashpots, so long as  $\Delta_M^*$  is diagonal. Second, any displacement feedback controllers designed according to (6-17), (6-18) and (6-20) are similarly called "modal springs", so long as the matrix  $\Sigma_M^*$  is diagonal. It should be noted that these terms (including the one initiated by Canavin) and, particularly, the implied modal independence in the closed loop make sense only with respect to the design model. In the presence of unmodeled modes, the modeled modes may not maintain their designed independence due to control and observation spillover.

Comment 8: Since the gain matrices  $C_V$  and  $C_D$  given by (6-16) - (6-20) represent a special form that satisfies conditions (a) and (b) of Theorem 5, the assertions on robustness of closed-loop asymptotic stability to modal truncation and to parameter variation remain valid; see Comments 5 and 6, and Theorem 6.

Comment 9: Stability and robustness results for the special subcase [9] in which there are no undamped elastic modes, matrices  $N_F$ ,  $N_V$ , and  $N_D$  in the design equations (6-18)-(6-20) are all zero, matrices  $\Delta_M^*$  and  $\Sigma_M^*$  in design equations (6-16)-(6-17) are all diagonal, and matrix  $C_E$  in Theorem 6 is diagonal were obtained jointly with Dr. Y.H. Lin of the Jet Propulsion Laboratory, California Institute of Technology (who was formerly with the C.S. Draper Laboratory). Various numerical demonstrations were also made, using a 10-meter free-free beam.

### 6.3 Prevention of Control and Observation Spillover by Synthesis of Actuator and Sensor Influences

Theorem 5 implies that for LSS having no unstable modes whatsoever and no undamped unmodeled modes, control and observation spillover will not cause closed-loop instability so far as output feedback control is concerned. The design of the output feedback controllers can be based entirely on the modeled modes which include all rigid-body modes, all undamped elastic modes, as well as critical elastic modes. Nevertheless, the closed-loop performance of the vibration controllers (e.g., the damping and frequency shifting of primary modes) will be degraded if control spillover and observation spillover exist. Theorems 4 and 5 imply that control and observation spillover problems may make it difficult to guarantee closed-loop stability of LSS having some unstable modes, unless the control spillover matrices  $\Phi_G^T B_F$  and  $\Phi_{G'}^T B_F$ , observation-spillover matrices  $C_V \Phi_G$  and  $C_D \Phi_{G'}$ , are all of small magnitude. It is now a standard understanding that control spillover and observation spillover will cause closed-loop instability for LSS using state-feedback controllers with state estimators.

Control spillover to and observation spillover from secondary modes can be prevented by proper placement of actuators and sensors on the structures and by proper synthesis of actuator and sensor influences [10-12]. We have recently concluded that the technique proposed in [10-12] for synthesizing actuator influences can be extended not only to the synthesis of sensor influences (because of duality) but also to the placement of actuators and sensors. The formulas derived [10-12] for proper placement of actuators (and sensors) can be recasted into similar mathematical forms for proper synthesis of actuator (sensor) influences. A general-purpose computer program is being developed for synthesizing actuator influences so that control spillover to secondary modes is prevented and, moreover, desired control influences on primary modes is obtained.

For preventing control spillover to secondary modes by synthesis of actuator influences, the control spillover matrix  $\Phi_S^T B_F$  is to be transformed using column operations  $Q$  and row operations  $P$  such that

$$\begin{bmatrix} W_{11} & W_{12} \\ W_{21} & W_{22} \end{bmatrix} = P(\Phi_S^T B_F)Q \quad (6-21)$$

with  $W_{11}$  being nonsingular and having the same rank as  $\Phi_S^T B_F$ . Such transformation (using  $Q$  and  $P$ ) can be accomplished by Gaussian elimination, Gram-Schmidt orthogonalization, or singular-value decomposition. Preferably,  $W_{12}$  is made to be zero. Then the synthesizer  $\Gamma$  for prevention of control spillover to secondary modes, i.e., as a solution of

$$\Phi_S^T B_F \hat{\Gamma} = 0 \quad (6-22)$$

is given by

$$\hat{\Gamma} = \left( Q_1 W_{11}^{-1} W_{12} + Q_2 \right) \hat{\Gamma} \quad (6-23)$$

where  $Q = [Q_1, Q_2]$ . The matrix  $\hat{\Gamma}$  represents free parameters and can be adjusted for achieving desired control influences on primary modes. Let  $\tilde{B}$  denote a desired control-influence matrix for the primary modes. Then  $\hat{\Gamma}$  is to be solved from the following equations

$$\left( -V_1 W_{11}^{-1} W_{12} + V_2 \right) \hat{\Gamma} = \tilde{B} \quad (6-24)$$

where

$$[V_1, V_2] = \Phi_P^T B_F [Q_1, Q_2] \quad (6-25)$$

The program under development is first to carry out the transformation (6-21) using Gaussian elimination, so that  $W_{12} = 0$ . The transformation (6-25) of actuator influence matrix  $\Phi_P^T B_F$  on primary modes is carried out simultaneously, since the same operations  $Q$  are used. This program is then to compute  $\hat{\Gamma}$  from (6-24). A desired synthesizer  $\Gamma$  is thus obtained from (6-23). Notice that  $W_{12}$  in both (6-23) and (6-24) is zero. A very simple and specific version was developed for application to the Draper tetrahedral model of LSS. Modification, generalization, and addition are underway.

For preventing control spillover to secondary modes by placement of actuators the corresponding formulas for determining the proper actuator-influence matrix  $B_F$  are as follows

$$[W_1, W_2] = \Phi_S^T Q \quad (6-26)$$

with  $W_1$  being nonsingular and having the rank of  $\Phi_S^T$ , which is equal to the number of secondary modes.  $B_F$  is to be a solution of

$$\Phi_S^T B_F = 0 \quad (6-27)$$

and is given by

$$B_F = \left( -Q_1 W_1^{-1} W_2 + Q_2 \right) \hat{B} \quad (6-28)$$

where  $Q = [Q_1, Q_2]$  and  $\hat{B}$  represents free parameters. Let  $\tilde{B}$  denote a desired control-influence matrix for the primary modes. Then  $\tilde{B}$  is to be solved from

$$\left( -V_1 W_1^{-1} W_2 + V_2 \right) \hat{B} = \tilde{B} \quad (6-29)$$

where

$$\begin{bmatrix} V_1, V_2 \end{bmatrix} = \Phi_P^T [Q_1, Q_2] \quad (6-30)$$

The one-to-one mathematical similarity between (6-26) - (6-30) and (6-21) - (6-25) is obvious.

To place actuators to prevent control spillover to all nonprimary modes, if possible, is to find a matrix  $B$  such that the composite matrix  $M_P \tilde{B}$  is realizable as actuator influences, where  $M$  denotes the mass (inertia) matrix and the orthogonality of mode shapes is used. The influences of a real actuator on LSS are zero at some modes, and nonzero at others. So, the realization of the above ideal actuator influences by placement is to find  $\tilde{B}$  such that "control spillover" to some modes is prevented while desired control influences at some other modes are obtained. The applicability and usefulness of the above-mentioned general-purpose computer program initially only for synthesis of actuator influences is obvious.

#### LIST OF REFERENCES

1. Lin, J.G., Lin, Y.H., Hegg, D.R., Johnson, T.L., and Keat, J.E., "Actively Controlled Structures Theory - Interim Technical Report, Volume 1: Theory of Design Methods," C.S. Draper Laboratory Report No. R-1249, April 1979, Appendix B.
2. Lin, J.G., "Reduction of Control and Observation Spillover in Vibration Control of Large Space Structures," Paper No. 79-1763, AIAA Guidance and Control Conference, August 1979.
3. Strunce, R.R., Hegg, D.R., Lin, J.G., and Henderson, T.C., "Actively Controlled Structures Theory - Final Report," C.S. Draper Laboratory Report No. R-1338, December 1979, Section 2.
4. Canavin, J.R., "The Control of Spacecraft Vibrations Using Multivariable Output Feedback," Paper 78-1419 AIAA/AAS Conference, Los Angeles, CA, August 1978.
5. Balas, M.J., "Direct Velocity Feedback Control of LSS," J. Guidance and Control, March-April 1979, pp. 252-253.
6. Lin, J.G., Hegg, D.R., Lin, Y.H., and Keat, J.E., "Output Feedback Control of Large Space Structures: An Investigation of Four Design Methods," Proceedings of Second Symposium on Dynamics and Control of Large Flexible Spacecraft, Blacksburg, Virginia, June 1979, pp. 1-18.
7. Elliott, L.E., Mingori, D.L., and Iwens, R.P., "Performance of Robust Output Feedback Controller for Flexible Spacecraft," Proceedings of Second Symposium on Dynamics and Control of Large Flexible Spacecraft, Blacksburg, Virginia, June 1979, pp. 409-420.
8. Meirovitch, L. and Oz, H., "Computational Aspects of the Control of Large Flexible Structures," Proceedings of 18th IEEE Conference on Decision and Control, Fort Lauderdale, Florida, December 1979, pp. 220-229.
9. Lin, Y.H., and Lin, J.G., "An Improved Output Feedback Control of Flexible Large Space Structures," to be presented at the 19th IEEE Conference on Decision and Control, Albuquerque, NM, December 1980.
10. Lin, J.G., "Reduction of Control and Observation Spillover in Vibration Control of Large Flexible Space Structures," Paper No. 79-1763, AIAA Guidance and Control Conference, August 1979.
11. "Actively Controlled Structures Theory - Final Report," C.S. Draper Laboratory Report No. R-1338, December 1979, Section 2.
12. Lin, J.G., "Three Steps to Alleviate Control and Observation Spillover Problems of Large Space Structures," to be presented at 19th IEEE Conference on Decision and Control, Albuquerque, NM, Dec. 1980.

SECTION 7  
STOCHASTIC OUTPUT FEEDBACK CONTROL

7.1 Introduction

The minimum variance fixed form output feedback compensator has been recently proposed [1,2] as a possible solution to the problem of designing reduced order controllers for plants of large dimension. The zero order limit of this compensator, the stochastic output feedback controller [3], is of particular interest because it is the easiest such compensator to implement and simultaneously results in the simplest design problem. The price of this simplicity is that this compensator generally achieves poorer performance than optimal compensators of higher order. As a result, the stochastic output feedback controller should prove useful in assessing complexity/performance tradeoffs in the design of simple compensators for complex plants.

Like the reduced order compensators considered earlier by Levine, Athans and Johnson [4,5,6], however, even in the zero order limit the minimum variance fixed form output feedback compensator gains and cost are difficult to compute, especially for plants of large dimension. Consequently, upper and lower bounds on the optimal constant gain cost that are relatively easy to compute have been developed and are described in the following sections. Specifically, Section 7.2 presents a more detailed discussion of the stochastic output feedback controller and its relation to several other compensator formulations such as the minimum order dual observer based compensator [1,7] and the Levine-Athans-Johnson reduced order compensator [4,5,6]. Section 7.3 derives an easily computed lower bound on the optimal stochastic output feedback controller cost while Section 7.4 derives three easily computed upper bounds on the cost. Finally, Section 7.5 discusses the principal results of the previous sections.

7.2 Minimum Various Fixed Form Output Feedback Compensator

Consider a plant of the form

$$\dot{\underline{x}}(t) = A\underline{x}(t) + B\underline{u}(t) + \underline{v}(t) \quad (7-1)$$

with observations

$$\underline{y}(t) = C\underline{x}(t) + \underline{w}(t) \quad (7-2)$$

Here  $\underline{x}(t) \in \mathbb{R}^n$  is the plant state vector,  $\underline{u}(t) \in \mathbb{R}^m$  is the control input vector,  $\underline{y}(t) \in \mathbb{R}^p$  is the observation vector and  $A, B, C$  are constant matrices of dimension  $n \times n$ ,  $n \times m$  and  $p \times n$ , respectively. The vectors  $\underline{v}(t) \in \mathbb{R}^n$  and  $\underline{w}(t) \in \mathbb{R}^p$  are white noise processes representing plant driving noise and

observation noise, respectively. These are independent stationary zero-mean processes with covariances

$$E\{\underline{v}(t) \underline{v}'(\tau)\} = V\delta(t - \tau)$$

and

$$E\{\underline{w}(t) \underline{w}'(\tau)\} = W\delta(t - \tau) \quad (7-3)$$

As defined in [1,2], the minimum variance fixed form output feedback compensator is of the form

$$\underline{u}(t) = H\underline{z}(t) + M\underline{y}(t) \quad (7-4)$$

where  $\underline{z}(t) \in R^q$  is the compensator state vector whose dynamics are described by

$$\dot{\underline{z}}(t) = F\underline{z}(t) + G\underline{y}(t) \quad (7-5)$$

Here  $F$ ,  $G$ ,  $H$  and  $M$  are constant matrices of dimension  $q \times q$ ,  $q \times p$ ,  $m \times q$  and  $m \times p$ , respectively. If mean-square stabilizing compensators of this form exist for given dynamic order  $q$ , the optimal compensator is defined as the one that minimizes the asymptotic state covariance weighted by the  $n \times n$  matrix  $Q$  of design parameters with respect to the matrices  $F$ ,  $G$ ,  $H$ , and  $M$ , i.e.,

$$J = \lim_{t \rightarrow \infty} E\{\underline{x}'(t) Q \underline{x}(t)\} \quad (7-6)$$

Necessary conditions for the optimality of this compensator are presented in [1,2] for compensators of arbitrary dynamic order  $q$ . Two cases of particular interest are the stochastic output feedback compensator (SOFC), corresponding to  $q = 0$ , and the minimum order dual observer based compensator (MODOBC), corresponding to  $q = n - m$ .

For the SOFC problem, the necessary conditions reduce to

$$(A + BMC)X + X(A + BMC)' + V + BMWM'B' = 0 \quad (7-7)$$

$$M = -(B'PB)^{-1}B'PXC'W^{-1} \quad (7-8)$$

$$P(A + BMC) + (A + BMC)'P + Q = 0 \quad (7-9)$$

assuming the required inverse exists. The  $n \times n$  matrix  $X$  represents the asymptotic state covariance matrix so the cost may be expressed as

$$J = \text{tr}[QX] \quad (7-10)$$

As in the case of the compensators considered in [4,5,6] it is to be expected that the cost functional will exhibit local minimum [8] so that equations (7-7), (7-8) and (7-9) will not possess a unique solution.

Specific necessary conditions can also be developed for the MODOBC problem [1]. Here the process is more difficult, but the solution can be shown to be unique [7] implying the conditions are also sufficient for optimality. These equations are derived by first transforming the problem into standard controllable form and then applying the necessary conditions for the minimum variance fixed form output feedback compensator. Determination of the optimal MODOBC cost then reduces to the solution of a single  $n \times n$  Riccati equation while determination of the gains requires the solution of an additional  $(n - m) \times (n - m)$  Riccati equation. This compensator is of general interest because it is of sufficient dynamic order to allow arbitrary placement of the closed loop poles [7] and is of specific interest here because the optimal MODOBC cost represents a lower bound on the optimal SOFC cost. (This follows from the fact that any compensator of order zero is a degenerate case of a compensator of order  $n - m$ , assuming  $n \geq m$ ).

Before proceeding with derivations of other bounds on the optimal SOFC cost, it is useful to put this reduced order compensator problem in perspective relative to two other reduced order formulations. First, note that no explicit control penalty is included in the cost functional considered here. As noted in [1], no such direct penalty is required because as the compensator gains increase, so does the contribution of the observation noise to the state covariance. In particular, lack of an explicit control penalty does not result in a singular problem in this case as it does in the standard linear regulator problem. If an explicit control penalty is included in the cost, the minimum variance compensator formulation of Martin and Bryson [9,10] is obtained. Specifically, the cost functional considered in [9,10] is

$$J = \lim_{t \rightarrow \infty} E\{\underline{x}'(t) Q_1 \underline{x}(t) + \underline{u}'(t) Q_2 \underline{u}(t)\} \quad (7-11)$$

providing the designer greater freedom to control the magnitude of the compensator gains at the expense of specifying additional design parameters. The principal disadvantage of this compensator is that it becomes ill-posed in the constant gain limit since the cost becomes infinite if the control is allowed to contain direct feedthrough from a plant output contaminated by white noise. Furthermore, since the SOFC problem considered here does not penalize the control, the resulting optimal cost represents the best performance achievable with any constant gain compensator. Also, since the optimal gains are finite, they provide a physically useful indication of the difficulty of achieving such performance.

The other reduced order compensator formulation with which the present formulation should be compared is the Levine-Athans-Johnson formulation [4,5,6]. The compensator structure considered in this case is the same, but the plant driving noise and observation noise are replaced by initial state uncertainties and the cost is the same as that for the linear regulator

problem. Consequently, the resulting optimal compensator depends on the initial state statistics which may be more difficult to specify than observation and driving noise statistics. Also, at least partially as a result of the greater number of design parameters involved, the necessary conditions for this compensator are more difficult to solve than the SOFC necessary conditions.

### 7.3 A Lower Bound on the Optimal SOFC Cost

As noted in the last section, the optimal MODOBC cost is a lower bound on the optimal SOFC cost. However, it is possible to derive a more easily computed lower bound by noting that the necessary conditions can be solved in the special case where  $B$  is a nonsingular  $n \times n$  matrix. This approach also has the advantage of providing additional insight into the nature of the SOFC problem and, in fact, motivates the upper bounds developed in the next section. Specifically, if  $B^{-1}$  exists and  $P^{-1}$  exists, determination of the optimal SOFC gain reduces to the solution of

$$M_o = -B^{-1} X_o C' W^{-1} \quad (7-12)$$

$$AX_o + X_o A' + V - X_o C' W^{-1} C X_o = 0 \quad (7-13)$$

Note that in this case, the optimal gain  $M_o$  is independent of the cost weighting matrix  $Q$  provided only that it is sufficiently well-behaved for the solution of equation (7-9) to be positive definite. This would appear to imply that the effect of the optimal gain  $M_o$  is to minimize all of the asymptotic state covariances independently.

An even more significant observation is that the asymptotic state covariance  $X_o$  is independent of  $B$  itself and only depends on the existence of  $B^{-1}$ . Because of this, for any given matrix  $Q$  the same optimal cost  $J_o$  is achieved by applying the optimal gain  $M_o$  (which does depend on  $B$ ), around any open loop plant described by the same  $A$  and  $C$  matrices and subject to the same disturbances  $V$  and  $W$ , provided only that  $B^{-1}$  exists. In addition, if  $J_B(M)$  represents the cost associated with applying the gain  $M$  around the open loop system  $(A, B, C, V, W)$ , then for any  $\tilde{B}$  and  $\hat{B}$

$$\tilde{B}M = \hat{B}M \Rightarrow J_{\tilde{B}}(\tilde{M}) = J_{\hat{B}}(\hat{M}) \quad (7-14)$$

provided  $A, C, V, W$  and  $Q$  are the same in both cases. Now suppose  $\hat{M}^*$  is the optimal SOFC gain for the plant  $(A, \hat{B}, C, V, W)$  and that  $\hat{B}$  is not necessarily invertible, but that  $\tilde{B}$  is. Thus, we can define an "equivalent gain"  $\tilde{M}^*$  for

the plant  $(A, \tilde{B}, C, V, W)$  by

$$\tilde{M}^+ = \tilde{B}^{-1} \hat{M}^* \quad (7-15)$$

so that

$$\tilde{B}\tilde{M}^+ = \hat{M}^* \Rightarrow J_{\tilde{B}}(\tilde{M}^+) = J_{\hat{B}}(\hat{M}^*) \quad (7-16)$$

However, since  $\tilde{B}^{-1}$  exists, the optimal gain  $\hat{M}^*$  associated with  $(A, \tilde{B}, C, V, W)$  can be computed from (7-12) with the optimal cost computed from (7-13) as

$$J_o = \text{tr}[QX_o] \quad (7-17)$$

Clearly, then, we must have

$$J_o \leq J_{\tilde{B}}(\tilde{M}^+) = J_{\hat{B}}(\hat{M}^*) \quad (7-18)$$

so that  $J_o$  represents a lower bound on the optimal SOFC cost for the plant  $(A, B, C, V, W)$  for any actuator influence matrix  $B$ .

Note that if  $B^{-1}$  does not exist, the computation of the lower bound cost  $J_o$  is easier than the computation of the MODOBC cost since it is not necessary to first transform the plant into standard controllable form. If  $B^{-1}$  does exist, it follows that  $m = n$  so the MODOBC problem and the SOFC problem are identical. In this case, the problem is effectively in standard controllable form (i.e., the required transformation is  $\underline{z}(t) = B^{-1}\underline{x}(t)$ , so no additional work is necessary. Finally, note that the covariance equation (7-13) is the same algebraic Riccati equation that is used to compute the Kalman filter gains required to estimate the state of the open loop plant. Consequently, many theoretical and numerical results are available pertaining to its solution. For example, it is known [11] that if the open loop plant is stabilizable and detectable with respect to the noise sources, there exists a unique positive semidefinite solution  $X_o$  that is positive definite if and only if the system is completely controllable from the plant driving noise.

#### 7.4 Suboptimal SOFC Compensators

The simplifications of the optimal SOFC problem resulting when  $B^{-1}$  exists suggest that it may be profitable to cast the problem in terms of a generalized inverse [12,13] of  $B$  when  $B^{-1}$  does not exist. To do this, note

that the gain expression may be written as

$$M = -B^T X C' W^{-1} \quad (7-19)$$

where the generalized inverse  $B^+$  is given by

$$B^+ = (B' P B)^{-1} B' P \quad (7-20)$$

and is in fact a weighted least squares inverse [13] of  $B$ . That is, defining  $S$  as the positive definite square root of  $P$  (assuming  $P$  is positive definite), i.e.,

$$S' S = P, \quad S > 0 \quad (7-21)$$

the vector  $\underline{x}_0 = B^+ \underline{y}$  is the minimum  $S$ -norm approximate solution of the inconsistent equation  $B\underline{x} = \underline{y}$ . Consequently, an alternate way of viewing the optimal SOFC design problem is as that of minimizing the error

$$e = \|\underline{B}\underline{u} + X C' W^{-1} \underline{y}\|_S = \|S \underline{B}\underline{u} + S X C' W^{-1} \underline{y}\| \quad (7-22)$$

subject to the constraints

$$\underline{u} = M \underline{y} \quad (7-23)$$

$$(A + BMC)X + X(A + BMC)' + V + BMWM'B' = 0 \quad (7-24)$$

$$P(A + BMC) + (A + BMC)'P + Q = 0 \quad (7-25)$$

where  $S' S = P$ . Physically, equation (7-23) just specifies the form of the control law, equation (7-24) defines  $X$  as the closed loop state covariance and equation (7-25) relates the norm  $\|\cdot\|_S$  to the cost weighting matrix  $Q$ . Note also that if  $B^{-1}$  exists, it is immediately apparent that the minimum error  $e = 0$  is achievable independent of the norm  $\|\cdot\|_S$ . This formulation of the problem thus makes immediately clear the independence of the optimal gains from the design parameters noted in Section 7.3 when  $B$  is non-singular.

This formulation of the optimal SOFC design problem also suggests several suboptimal control problems that may be useful in obtaining either upper bounds on the optimal SOFC cost or initial gain estimates for iteratively computing the optimal SOFC gains. For example, since the principal difficulty in computing the optimal gains is the coupling between

equations (7-24) and (7-25), one possible approach would be to assume a least squares weighting  $\hat{S}$  and minimize the error defined in equation (7-22) subject to constraints (7-23) and (7-24). Defining  $\hat{P} = \hat{S}'\hat{S}$ , the solution to this problem is

$$M_1 = -(B'\hat{P}B)^{-1}B'\hat{P}X_1C'W^{-1} \quad (7-26)$$

where the closed loop covariance  $X_1$  satisfies the equation

$$AX_1 + X_1A' + V - X_1C'W^{-1}CX_1 = -(I - B(B'\hat{P}B)^{-1}B'\hat{P})X_1C'W^{-1}CX_1(I - \hat{P}B(B'\hat{P}B)^{-1}B') \quad (7-27)$$

A particularly convenient choice of weighting matrix  $\hat{S}$  would be the  $n \times n$  identity matrix, reducing the problem to a standard least squares minimization.

Another possible approach to decoupling equations (7-24) and (7-25) would be to assume a value  $X$  for the closed loop state covariance and minimize the error defined in equation (7-22) subject to constraints (7-23) and (7-25). The solution to this problem is

$$M_2 = -(B'P_2B)^{-1}B'P_2\hat{X}C'W^{-1} \quad (7-28)$$

where  $P_2$  satisfies the equation

$$P_2A + A'P_2 + Q - P_2B(B'P_2B)^{-1}B'P_2\hat{X}C'W^{-1}C - C'W^{-1}C\hat{X}P_2B(B'P_2B)^{-1}B'P_2 = 0 \quad (7-29)$$

with the least squares weighting matrix  $S_2$  defined as the positive definite square root of  $P_2$ . A particularly convenient choice of covariance matrix would be the lower bound covariance  $X_0$  defined by equation (7-13) since the suboptimal solution then becomes exact when  $B$  is nonsingular.

Finally, a third suboptimal SOFC problem results if both the least squares weighting matrix  $S$  and the closed loop covariance matrix  $X$  are fixed. In particular, assuming  $S = \hat{S}$  and  $X = \hat{X}$ , the suboptimal gain  $M_3$  is given by

$$M_3 = -(B'\hat{P}B)^{-1}B'\hat{P}\hat{X}C'W^{-1} \quad (7-30)$$

where  $\hat{P} = \hat{S}'\hat{S}$  as before. Note that if  $\hat{S}$  is taken as the  $n \times n$  identity matrix this approach is very similar to Kosut's minimum norm suboptimal compensator for the Levine-Athans-Johnson reduced order compensator [14].

### 7.5 Conclusions

Motivated primarily by the exact solution of the optimal SOFC problem when the actuator influence matrix  $B$  is nonsingular, bounds have been derived for the optimal SOFC cost for plants with singular  $B$  matrices. These bounds satisfy the inequality

$$\min (J_0, J_-) \leq \max (J_0, J_-) \leq J \leq J_+ \leq J_{++} \leq J_{+++} \quad (7-31)$$

where  $J_-$  is the optimal MODOBC cost for the plant  $(A, B, C, V, W)$ ,  $J_0$  is the optimal SOFC cost for the same plant but with a nonsingular  $B$  matrix,  $J$  is the optimal SOFC cost and  $J_+, J_{++}, J_{+++}$  are the costs associated with the suboptimal gains  $M_1, M_2$ , and  $M_3$  ranked in order of increasing cost. It should be noted that if  $B$  is nonsingular, it follows immediately that  $J_0 = J_- = J = J_1$  and that if  $\hat{X}$  is taken as the solution  $X_0$  of equation (7-13) in computing  $M_2$  and  $M_3$ ,  $J_2$  and  $J_3$  are also equal to the optimal cost.

In terms of computational difficulty, the cost  $J_0$  is clearly the easiest to evaluate, requiring the solution of a single Riccati equation. If the plant is in standard controllable form, the optimal MODOBC cost  $J_-$  is equally easy to compute, but if it is not (as is normally the case), the evaluation of  $J_-$  can be considerably more difficult. Of the upper bounds, the cost  $J_3$  is the easiest to evaluate, requiring the solution of a single Riccati equation if  $\hat{X}$  is available. Evaluation of  $J_1$  is somewhat more difficult since it requires the solution of equation (7-27) which is not a standard Riccati equation. Similarly, the cost  $J_2$  should be still more difficult to evaluate because of the more complex nonlinearity of equation (7-29). Note, however, that all of these bounds on the optimal SOFC cost are more easily evaluated, assuming they exist, than the optimal cost itself, since they involve the solution of uncoupled equations.

In terms of applications, three possibilities are apparent. First, the lower bound  $J_0$  and the upper bound  $J_3$  should be useful in preliminary evaluation of optimal SOFC performance for particular applications. This would be particularly convenient if the lower bound covariance  $X_0$  were used in the computation of the suboptimal cost  $J_3$ . Secondly, an examination of the suboptimal compensators  $M_1$  and  $M_2$  suggests a possible computational algorithm for evaluating the optimal SOFC gains  $M$ . Specifically, if reasonably efficient algorithms could be developed for solving

equations (7-27) and (7-29), it might be reasonable to approach the problem by first fixing either  $\hat{P}$  or  $\hat{X}$ , solving the appropriate equation to obtain  $X$  or  $P$ , respectively, and using these to derive updated values of  $\hat{P}$  or  $\hat{X}$  from the other equation. Finally, any of the suboptimal gains  $M_1$ ,  $M_2$  or  $M_3$

could be used as a starting estimate for any iterative calculation of the optimal SOFC gains, as has been done with Kosut's suboptimal compensator in evaluating the Levine-Athans-Johnson reduced order compensator gains [15]. Because of its relative ease of evaluation,  $M_3$  appears to be a particularly attractive candidate for this application.

#### LIST OF REFERENCES

1. Johnson, T.L., "Optimization of Low Order Compensators for Infinite Dimensional Systems", Proceedings of the 9th IFIP Symposium on Optimization Techniques, Warsaw, Poland, September 1979.
2. Johnson, T.L., "Minimum-Variance Fixed-Form Compensation of Linear Systems", Proceedings of the 17th Conference on Decision and Control, January 1979, San Diego, California.
3. Interim Technical Report: Actively Controlled Structures Theory, Vol. 1, C. S. Draper Laboratory Technical Report R-1249, April 1979.
4. Levine, W.S. and Athans, M., "On the Determination of the Optimal Constant Output Feedback Gains for Linear Multivariable Systems", IEEE Trans. Auto. Control, 15, 1, 1970, pp. 44-48.
5. Johnson, T.L. and Athans, M., "On the Design of Optimal Constrained Dynamic Compensators for Linear Constant Systems", IEEE Trans. Auto. Control, 15, 6, 1970, pp. 658-660.
6. Levine, W.S., Johnson, T.L. and Athans, M., "Optimal Limited State Variable Feedback Controllers for Linear Systems", IEEE Trans. Auto. Control, 16, 6, 1971, pp. 788-793.
7. Blanvillain, P.J. and Johnson, T.L., "Specific-Optimal Control with a Dual Minimal-Order Observer-Based Compensator", Int. J. Control, 28, 1978, pp. 277-294.
8. Choi, S.S. and Sirisena, J.R., "Computation of Optimal Output Feedback Gains for Linear Multivariable Systems", IEEE Trans. Automatic Control, Vol. AC-23, p. 760, August 1978.
9. Martin, G.D. and Bryson, A.E., Jr., "Attitude Control of a Flexible Spacecraft", AIAA Guidance and Control Conference, August 1978, Palo Alto, California.

10. Martin, G.D., "On the Control of Flexible Mechanical Systems", Stanford University Department Aero/Astro, Report No. 511, May 1978.
11. Kwakernaak, H. and Sivan, R., Linear Optimal Control Systems, Wiley-Interscience, New York, 1972.
12. Ben-Israel, A. and Greville, T.N.E., Generalized Inverses, Theory and Applications, Wiley, New York 1974.
13. Strang, G., Linear Algebra and Its Applications, Academic Press, New York, 1976.
14. Kosut, R.L., "Suboptimal Control of Linear Time-Invariant Systems Subject to Control Structure Constraints", IEEE Trans. Automatic Control, Vol. AC-15, pp. 557-563, October 1970.
15. Petkovski, D.J.B. and Rakic, M., "On the Calculation of Optimum Feedback Gains for Output-Constrained Regulators", IEEE Trans. Automatic Control, Vol. AC-15, pp. 557-563, October 1970.

## SECTION 8

### CALCULATION OF OPTICAL LINE-OF-SIGHT

#### 8.1 Introduction

For the ACOSS test problem #2 we need a line-of-sight model giving the law of displacement of the image of a target when the structure deforms. The purpose of the model is to give line-of-sight changes of the same order of magnitude as those produced by current DARPA large wide-angle optical systems.

We assume that the mirror surfaces are simply displaced and maintain their nominal shape. We also neglect any effect of light redistribution in the image.

The structural model given is shown in Figures 8-1 and 8-2. It was assumed that the base optical design would be close to an existing DARPA design. The mirror shapes are off axis sections of rotationally symmetric surfaces which are coaxial. As we want only a first order model and neglect the influence of light distribution in the image of a point, the asphericity of each mirror was disregarded.

#### 8.2 Results

The line-of-sight change is the sum of the changes due to the displacement of each of the components of the optical system taken individually. For a given mirror or focal plane displacement, the location of the intermediate and/or final images are calculated using the well-known (see Ref. 1) first order optics equations

$$\frac{1}{d_1} = \frac{1}{d_0} + \frac{2}{r} \quad (8-1)$$

$$m = \frac{d_1}{d_0} \quad (8-2)$$

relating the distance  $d_1$  between the image and the mirror, the distance  $d_0$  between the object and the mirror (both distances being taken along the optical axis), the radius of curvature  $r$  of the mirror and the magnification  $m$ . The equations (8-1) and (8-2) utilize the vertex of the mirror as origin; therefore, when a mirror is displaced, the results are given in relation to the displaced positions, and this is taken into consideration in the transfer to the next mirror.

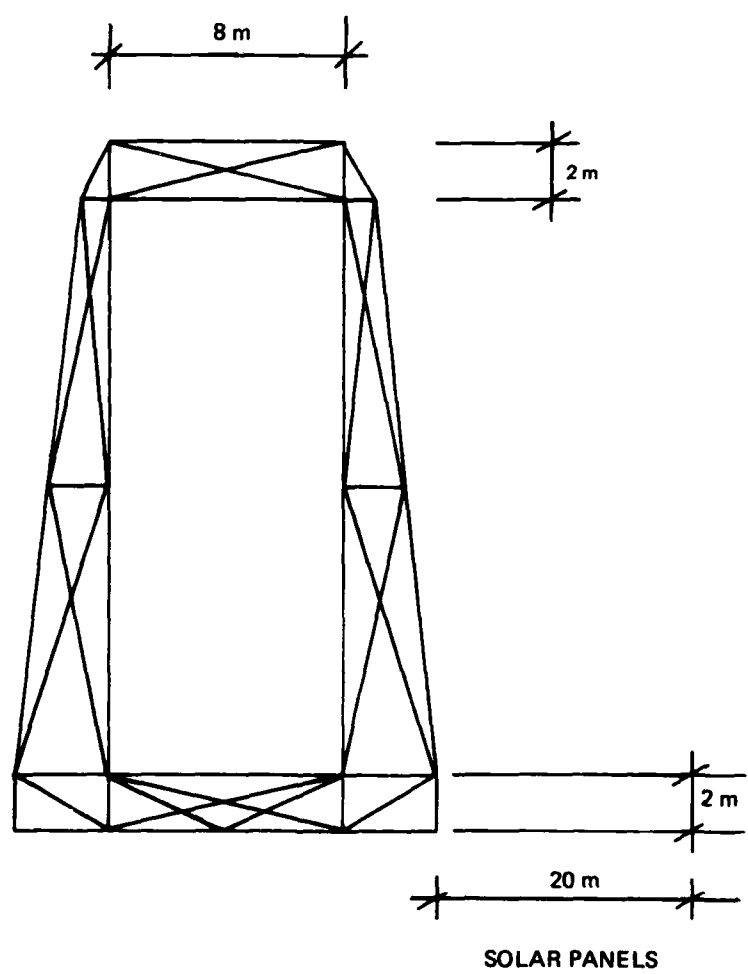


Figure 8-1.

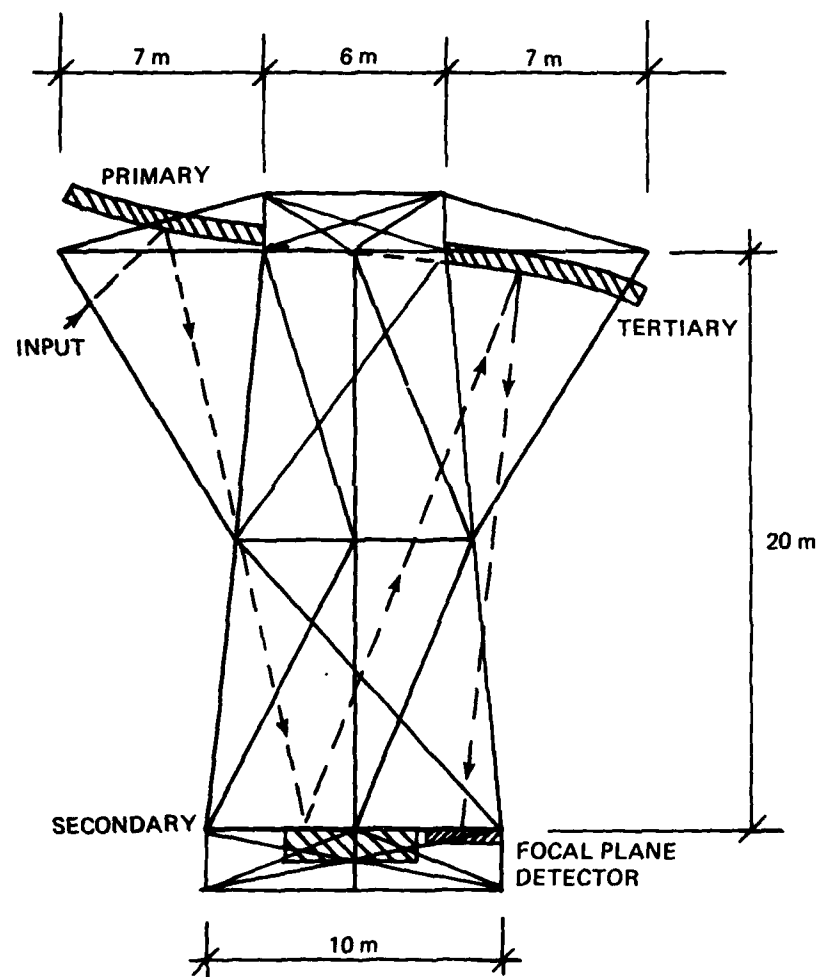


Figure 8-2.

Using the paraxial optics equations (8-1) and (8-2), expressions relating optical element movements and the resultant longitudinal defocus  $z_F$  and transverse defocus  $(x_F, y_F)$  are given for the three-mirror ACOSS system. Translations of the mirrors are represented by the displacements of the vertices, and rotations are defined for each mirror with the pivot point located at its own vertex (on the optical axis). Movements of the focal surface are also considered;  $x_I$  and  $y_I$  are the coordinates of the image point, and the pivot point for rotation is again at the intersection of the focal plane with the optical axis (see Figure 8-3). Line-of-sight (LOS) error is determined by the transverse defocus  $(x_F, y_F)$ .

The pertinent variables are defined as follows:

$R_p$  = radius of curvature of the primary

$R_t$  = radius of curvature of the tertiary

$t_1$  = axial distance between the primary and the secondary

$t_2$  = axial distance between the secondary and the tertiary

We will use the letter  $\alpha$  as a running index which stands for the letter  $p$  for primary,  $s$  for secondary,  $t$  for tertiary and  $F$  for focal plane,  $x_{i\alpha}$  will represent the displacement of the element  $\alpha$  along the  $i$ th axis (see Figure 8-3) and  $\theta_{i\alpha}$  will represent the counter-clockwise rotation of the element  $\alpha$  about the  $i$ th axis (looking towards the origin). With these notations the defocus components  $(x_F, y_F, z_F)$  will be given by

$$x_F = \left[ -x_{1p} + x_{1t} - R_p \theta_{2p} + 2\theta_{2s} \left( \frac{R_p}{2} + t_1 \right) - 2\theta_{2t} T \right] \frac{R_t}{2T - R_t} + x_{1t} - x_{1F} + \theta_{3F} y_I \quad (8-3)$$

$$y_F = \left[ -x_{2p} + x_t + R_p \theta_{1p} - 2\theta_{1s} \left( \frac{R_p}{2} + t_1 \right) + 2\theta_{1t} T \right] \frac{R_t}{2T - R_t} + x_{2t} - x_{2F} - \theta_{3F} x_I \quad (8-4)$$

$$z_F = (x_{3p} - 2x_{3s} + x_{3t}) \frac{R_t^2}{[R_p - R_t + 2(t_1 + t_2)]^2} + x_{3t} - x_{3F} - y_I \theta_{1F} + x_I \theta_{2F} \quad (8-5)$$

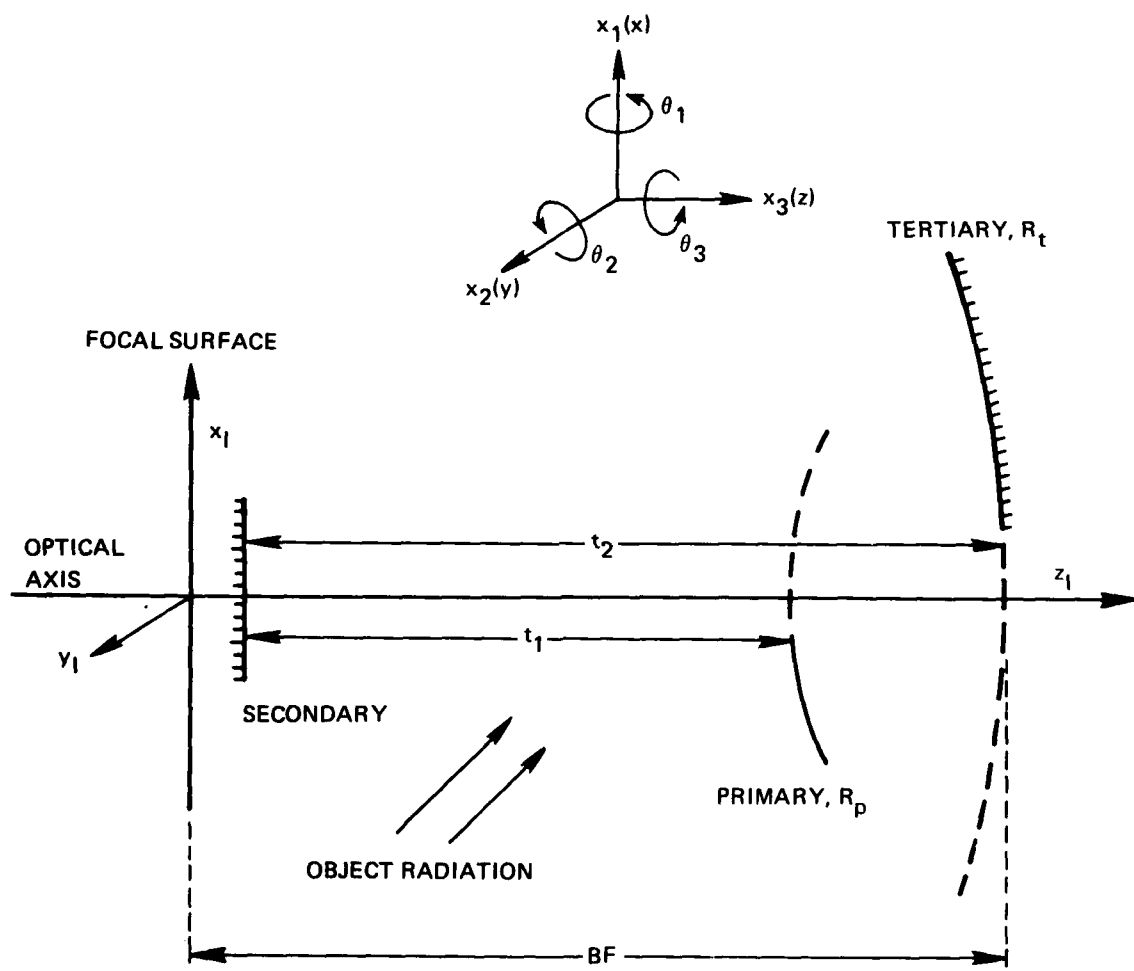


Figure 8-3. Three-mirror system.

where

$$T = \frac{R_p}{2} + t_1 + t_2 \quad (8-6)$$

The LOS error is given by

$$\vec{\theta}_{LOS} = \left( \frac{y_F}{f}, \frac{x_F}{f} \right) \quad (8-7)$$

where  $f$  is the focal length of the system and is expressed as

$$f = \frac{R_t R_p}{2(2T - R_t)} \quad (8-8)$$

The magnitude of the LOS error is given by

$$|\vec{\theta}_{LOS}| = \frac{1}{f} \left( x_F^2 + y_F^2 \right)^{1/2} \quad (8-9)$$

The location of the image plane is a function of the parameters of the three-mirror optical system. The distance  $BF$  between the tertiary mirror and the image plane (see Figure 8-3) is given by

$$BF = \frac{R_t T}{2T - R_t} \quad (8-10)$$

and for all cases the focal surface must be placed at this location, or, alternately the radius of curvature of the tertiary should be calculated using

$$R_t = \frac{2T \cdot BF}{T + BF} \quad (8-11)$$

so that the final image coincides with the focal plane.

In the above expressions, all radii of curvature and axial distances should have positive values.

It should also be reiterated that all rotations of the individual elements are defined with the pivot points on the optical axis. The justification for this definition lies in the fact that all three elements of the optical system are coaxial, i.e., the centers of curvature of these elements lie along a common axis.

As a final note, the  $(x_F, y_F, z_F)$  expressions were derived with first-order paraxial optics. As a consequence of this approximation, the angle of incidence of the object radiation and all displacements and rotations of the individual elements must be small. If this condition is not met, not only will higher order terms become appreciable, but the focal length and consequently the backfocus BF will change and aberrations of the optical system will no longer be negligible. Therefore those equations cannot be realistically used in an open attitude control loop.

### 8.3 Application to the Test Case #2

For the test case #2 corresponding to the structural model given on Figures 8-1 and 8-2, the primary and tertiary mirror vertices are coincident, and the focal plane and tertiary mirror (flat) are coplanar.

The numerical values of the basic variables which have been used are:

$$R_p = 53.9$$

$$t_1 = t_2 = 20$$

$$BF = 20$$

$T$ ,  $R_t$  and  $f$  are calculated using Equations (8-6), (8-11), and (8-8).

### LIST OF REFERENCES

1. Military Standardization Handbook MIL-HDBK-141.

## SECTION 9

### DRAPER MODEL #2

#### 9.1 Introduction

In order to assess the performance, sensitivity, and hardware requirements of the various active structural control methods which are being developed, a universal system model is required. This section contains a complete description of Draper Model #2 which is a simple but realistic evaluation model. The design of this system was driven by the desire to incorporate certain attributes into the overall system characteristics. The desired features were

- structural design based on realistic sizes and weights
- a simple unclassified optical system with associated performance measures and tolerances
- a set of disturbances typical of equipment vibration and attitude control (slew).

The resulting model is described in detail in Section 9.2 along with the resulting mode shapes and natural frequencies of the system. Section 9.4 contains a description of the line of sight (LOS) performance measure including theory and implementation. The tolerances on the optical system and a set of disturbances are given in Section 9.5. A perturbed model which can be used to evaluate the sensitivity of the control system is given in Section 9.6.

#### 9.2 Structural Design

The example problem is shown in Figure 9-1. It consists of a flexible optical support structure and an isolated equipment section which contains the solar panels.

##### 9.2.1 Optical Support Structure

The optical support structure consists of the upper mirror support truss, lower mirror support truss, and the metering truss which maintains mirror separation. The finite element model is shown in Figure 9-2. It contains 35 node points and 117 beam elements. The structure is configured as a truss, but it is assumed that all joints allow a full moment connection. Thus, both bending and axial stiffness are included in the model for all structural members. All members are assumed to be graphite epoxy hollow tubes. The sizes and section properties are given in Table 9-1. The mass of this subsystem including the structural mass, mirrors, and equipment has been lumped at 18 node points as shown in Figure 9-3. The total mass of the optical support structure is 5084 kg.

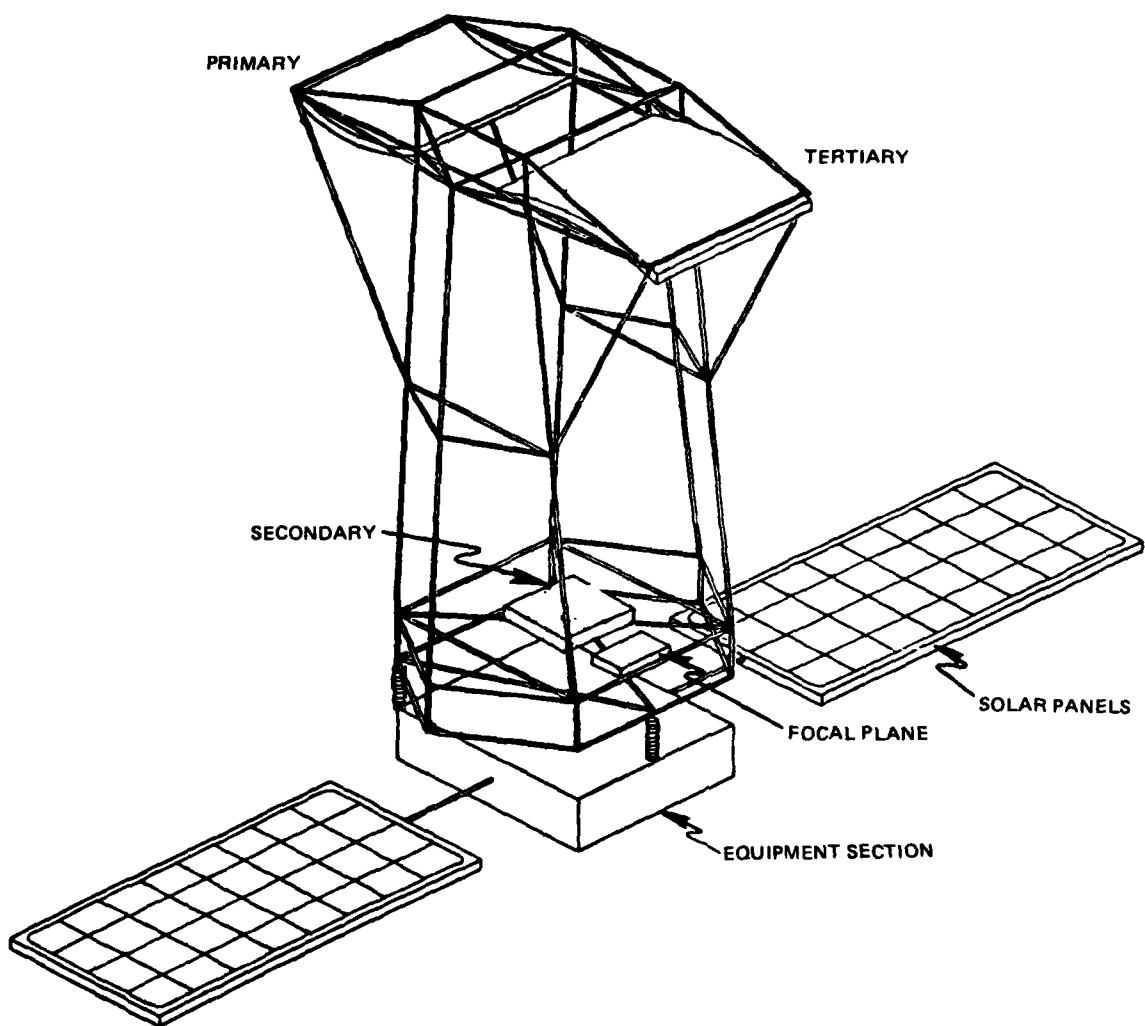


Figure 9-1. Draper model No. 2.

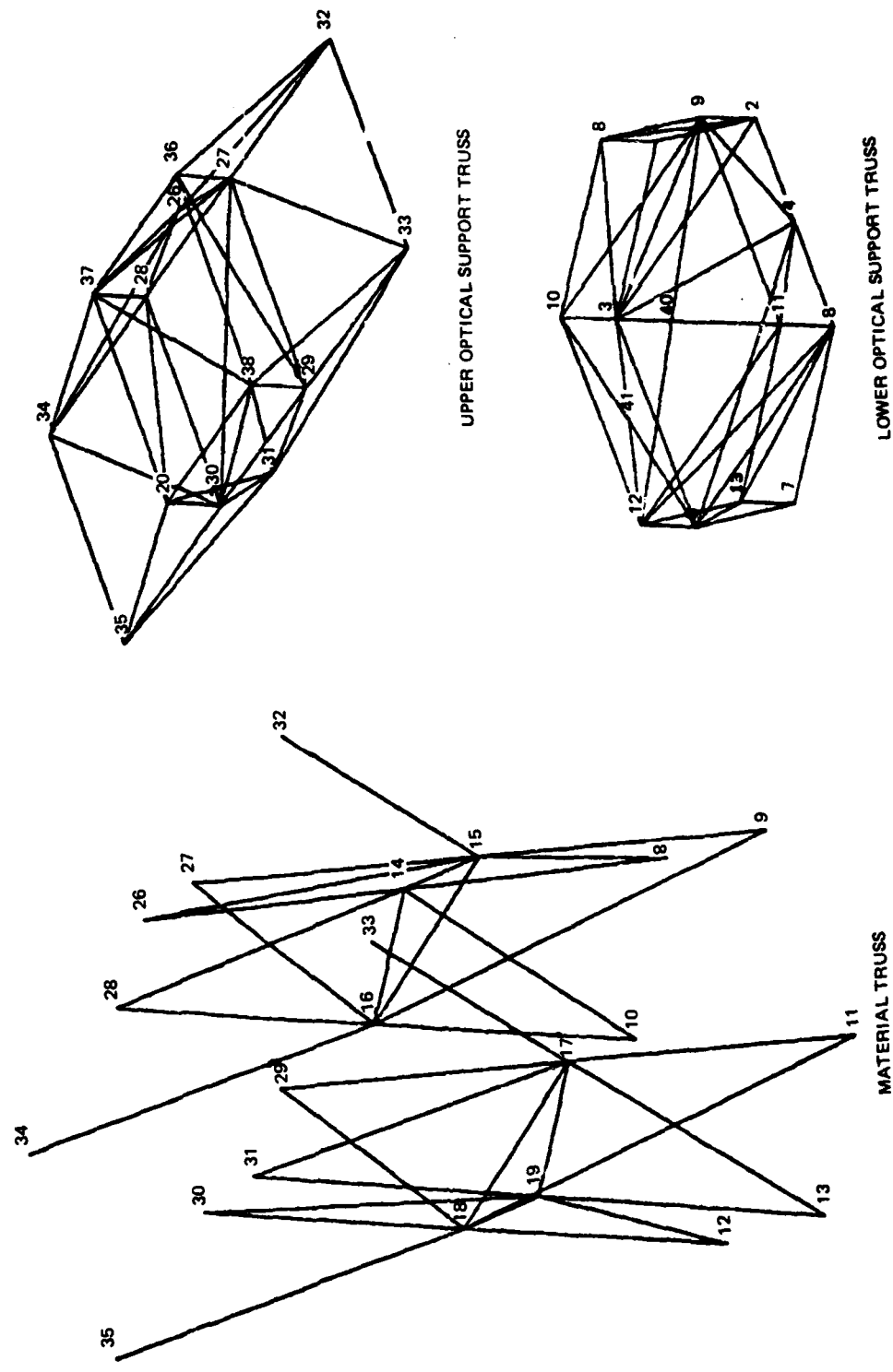


Figure 9-2. Draper model No. 2—Finite element model.

PRECISION STRUCTURE

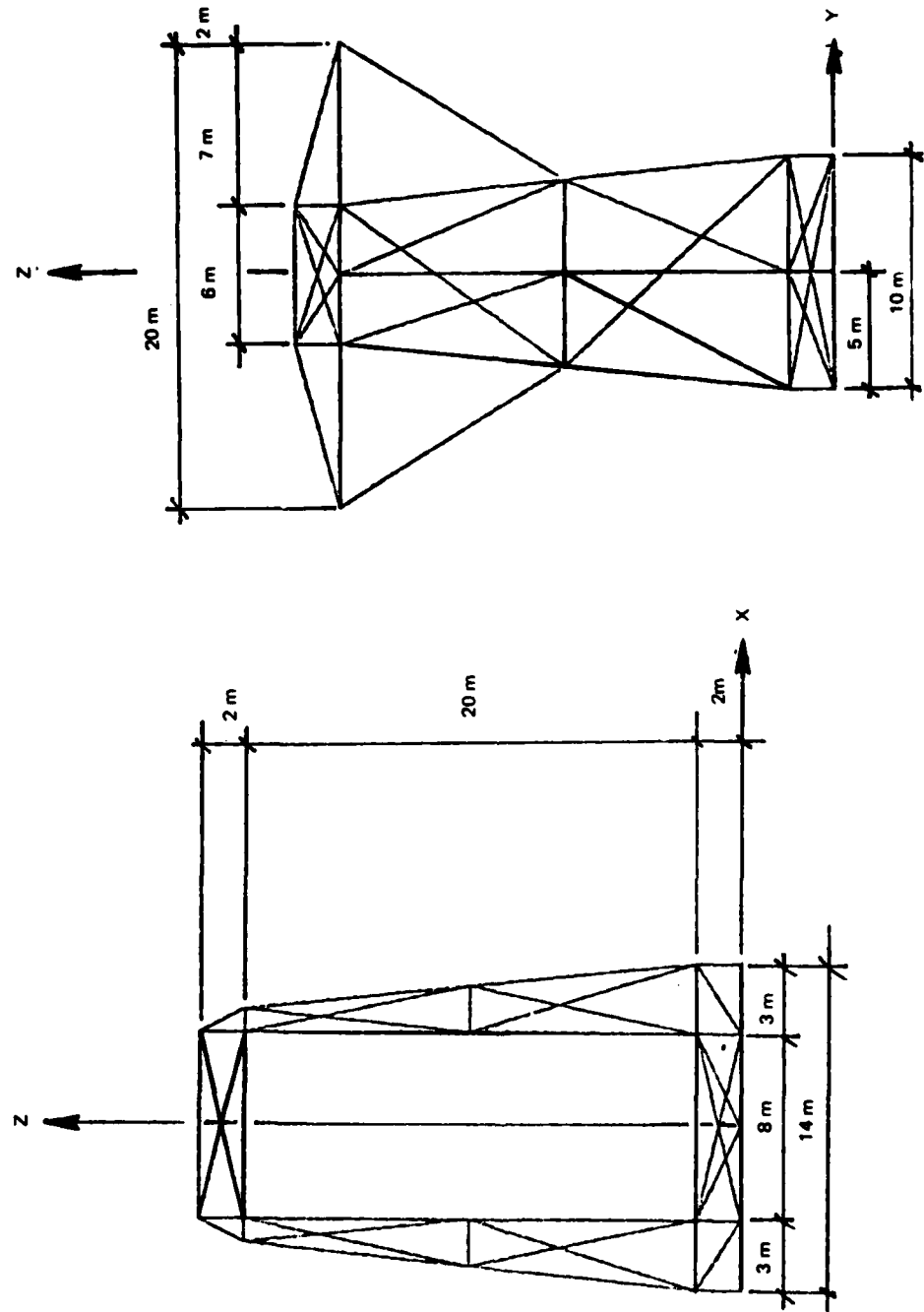


Figure 9-2 (Cont.)

Table 9-1.

## MEMBER PROPERTIES

20 cm dia. x .1 cm Round Tube		20 cm dia x .05 cm Round Tube		20 cm dia x .05 cm Round Tube	
TYPE 200		TYPE 300		TYPE 500	
A = 6.250 x $10^{-4}$ m <sup>2</sup>		A = 3.133 x $10^{-4}$ m <sup>2</sup>		A = 9.407 x $10^{-4}$ m <sup>2</sup>	
I = 3.075 x $10^{-6}$ m <sup>4</sup>		I = 1.559 x $10^{-6}$ m <sup>4</sup>		I = 1.874 x $10^{-5}$ m <sup>4</sup>	
J = 6.189 x $10^{-6}$ m <sup>4</sup>		J = 3.118 x $10^{-6}$ m <sup>4</sup>		J = 3.749 x $10^{-5}$ m <sup>4</sup>	
25 cm dia x .05 cm Round Tube		40 cm dia x .075 cm Round Tube			
TYPE 400		TYPE 500			
A = 3.919 x $10^{-4}$ m <sup>2</sup>		A = 9.407 x $10^{-4}$ m <sup>2</sup>		A = 9.407 x $10^{-4}$ m <sup>2</sup>	
I = 3.0496 x $10^{-6}$ m <sup>4</sup>		I = 1.874 x $10^{-5}$ m <sup>4</sup>		I = 1.874 x $10^{-5}$ m <sup>4</sup>	
J = 6.099 x $10^{-6}$ m <sup>4</sup>		J = 3.749 x $10^{-5}$ m <sup>4</sup>		J = 3.749 x $10^{-5}$ m <sup>4</sup>	

EQUIPMENT SECTION & SOLAR PANELS

Table 9-1. (Cont.)

NODE	X	Y	Z
42	0.0	5.0	0.0
43	-2.0	0.0	0.0
44	0.0	0.0	0.0
45	2.0	0.0	0.0
46	-4.0	-5.0	0.0
47	4.0	-5.0	0.0
48	-26.0	0.0	0.0
49	-21.0	0.0	0.0
50	-16.0	0.0	0.0
51	-11.0	0.0	0.0
52	-6.0	0.0	0.0
53	5.0	0.0	0.0
54	11.0	0.0	0.0
55	16.0	0.0	0.0
56	21.0	0.0	0.0
57	26.0	0.0	0.0

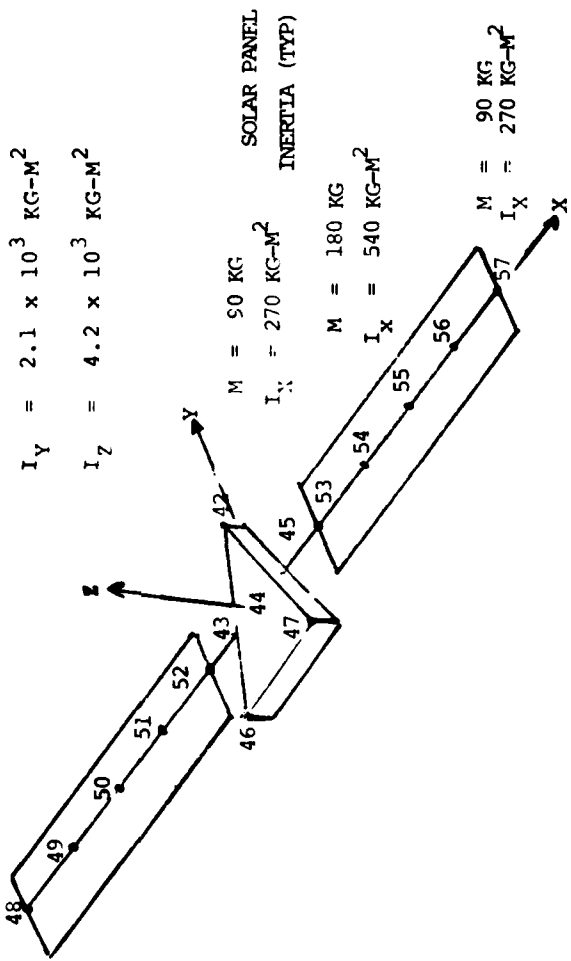
EQUIPMENT SECTION INERTIA

$$M = 3500 \text{ KG}$$

$$I_X = 2.1 \times 10^3 \text{ KG-M}^2$$

$$I_Y = 2.1 \times 10^3 \text{ KG-M}^2$$

$$I_Z = 4.2 \times 10^3 \text{ KG-M}^2$$



EQUIPMENT SECTION - MEMBER CONNECTIVITIES

NODES 42-47 RIGID PLATE

Table 9-1. (Cont.)

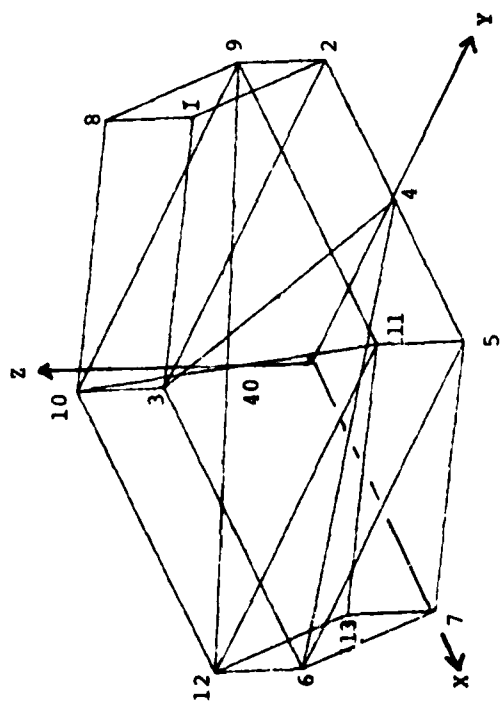
SOLAR PANELS - MEMBER CONNECTIVITIES

MEMBER #	NODE A	NODE B	PROP #
131	48	49	500
132	49	50	
133	50	51	
134	51	52	
135	52	43	
136	45	53	
137	53	54	
138	54	55	
139	55	56	
140	56	57	

LOWER SUPPORT TRUSS - NODE LOCATIONS

Table 9-1. (Cont.)

NODE	X	Y	Z	MASS (KG)
1	-7.0	0.0	0.0	
2	-4.0	5.0	0.0	
3	-4.0	-5.0	0.0	
4	0.0	5.0	0.0	
5	4.0	5.0	0.0	
6	4.0	-5.0	0.0	
7	7.0	0.0	0.0	
8	-7.0	0.0	2.0	
9	-4.0	5.0	2.0	500.0
10	-4.0	-5.0	2.0	500.0
11	4.0	5.0	2.0	500.0
12	4.0	-5.0	2.0	500.0
13	7.0	0.0	2.0	
40	0.0	0.0	2.0	
41	0.0	-5.0	1.0	



DIAGONAL MEMBERS OMITTED FOR CLARITY

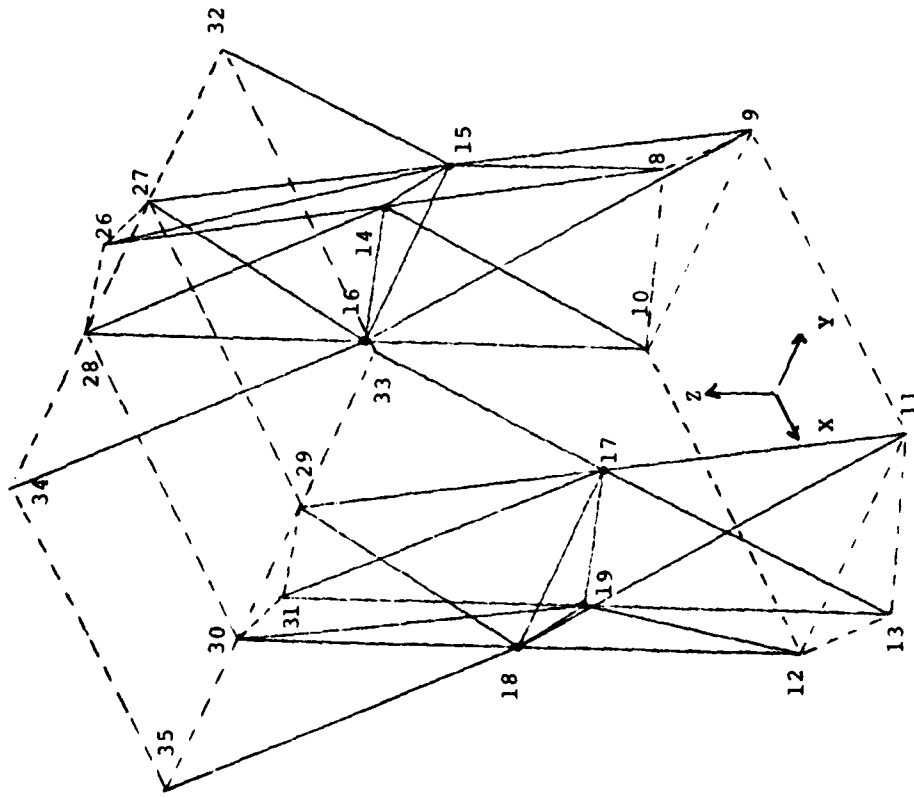
## LOWER SUPPORT TRUSS - MEMBER CONNECTIVITIES

Table 9-1. (Cont.)

MEMBER #	NODE A	NODE B	PROP #	MEMBER #	NODE A	NODE B	PROP #
1	1	2	200	21	4	9	200
2	1	3	1	22	4	11	
3	2	3		23	5	12	
4	2	4		24	5	13	
5	3	4		25	6	13	
6	4	5		26	12	41	
7	4	6		27	6	41	
8	3	6		28	10	41	
9	5	6		29	3	41	
10	5	7		30	8	9	
11	6	7		21	8	10	
12	1	8		32	9	10	
13	2	9		33	9	40	
14	3	10		34	10	40	
15	5	11		35	11	40	
16	6	12		36	12	40	
17	7	13		37	9	11	
18	3	8		38	10	12	
19	2	8		39	11	12	
20	3	9		40	11	13	
				41	12	13	

METERING TRUSS - NODE LOCATIONS

Table 9-1. (Cont.)



NODE	X	Y	Z	MASS (KG)
14	-6.0	0.0	12.0	8.0
15	-4.0	4.0		17.0
16	-4.0	-4.0		17.0
17	4.0	4.0		17.0
18	4.0	-4.0		17.0
19	6.0	0.0		8.0

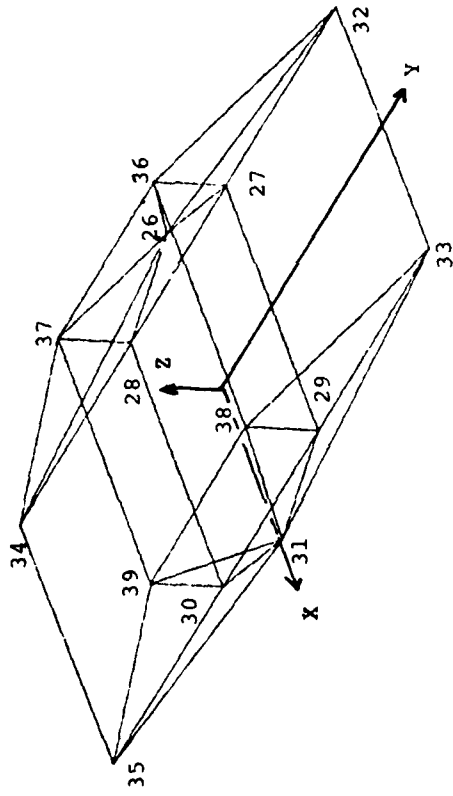
METERING TRUSS - MEMBER CONNECTIVITIES

Table 9-1. (Cont.)

MEMBER #	NODE A	NODE B	PROP #	MEMBER #	NODE A	NODE B	PROP #
42	14	15	300	86	13	17	400
43	14	16		87	14	26	
44	16	15		88	14	28	
45	17	18		89	16	28	
46	17	19		90	16	27	
47	18	19		91	15	27	
76	8	14	400	92	15	26	
77	10	14		93	17	29	
78	10	16		94	18	29	
79	16	9		95	18	30	
80	9	15		96	19	30	
81	11	17		97	19	31	
181	8	15		98	17	31	
82	11	18		99	15	32	
83	12	18		100	16	34	
84	12	19		101	17	33	
85	13	19		102	18	35	

Table 9-1. (Cont.)  
UPPER SUPPORT TRUSS - NODE LOCATIONS

NODE	X	Y	Z	MASS (KG)
26	-5.0	0.0	22.0	
27	-4.0	3.0		375.0
28	-4.0	-3.0		375.0
29	4.0	3.0		375.0
30	4.0	-3.0		375.0
31	5.0	0.0		
32	-4.0	10.0		500.0
33	4.0	10.0		500.0
34	-4.0	-10.0		250.0
35	4.0	-10.0		250.0
36	-4.0	3.0	24.0	
37	-4.0	-3.0		
38	4.0	3.0		
39	4.0	-3.0		



DIAGONAL MEMBERS OMITTED FOR CLARITY

Table 9-1. (Cont.)  
 UPPER SUPPORT TRUSS - MEMBER CONNECTIVITIES

MEMBER #	NODE A	NODE B	PROP #	MEMBER #	NODE A	NODE B	PROP #
54	26	27	300	111	26	32	400
55	26	28		112	27	32	
56	27	28		113	27	33	
57	29	30		114	29	33	
58	29	31		115	31	33	
59	30	31		116	32	33	
60	27	29		117	26	34	
61	27	30		118	28	34	
62	28	30		119	30	34	
63	27	36		120	30	35	
64	28	37		121	31	35	
65	30	39		122	34	35	
66	29	38		123	32	36	
67	29	36		124	33	38	
68	27	37		125	34	37	
69	28	39		126	35	39	
70	30	38		127	26	37	
71	36	37		128	26	36	
72	37	39		129	31	39	
73	39	38		130	31	38	
74	36	38					
75	37	38					

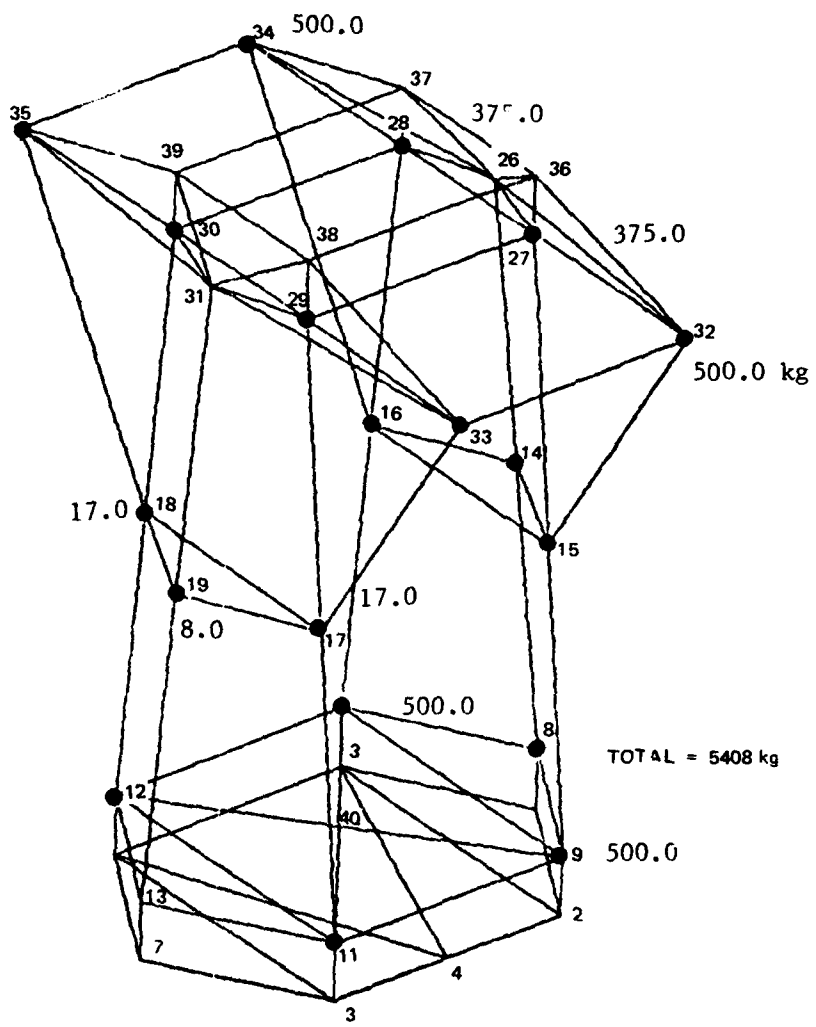


Figure 9-3. Optical support structure—mass distribution.

### 9.2.2 Equipment Section

The equipment section consists of a central rigid body and two symmetric solar panels. The support structure for the solar panels is a hollow graphite epoxy tube. The structural properties of the solar panels are not included in the model. The inertia properties are lumped at 6 node points on the support structure. Details of the finite element model and the inertia properties of the equipment section are given below in Figure 9-4.

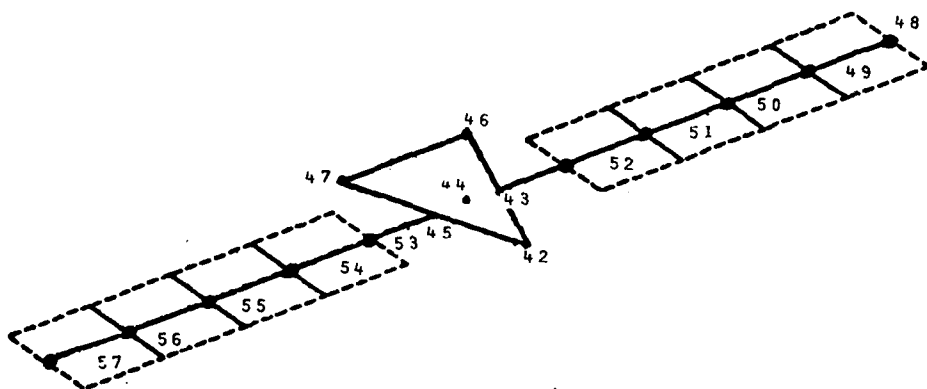


Figure 9-4.

#### Rigid Body Properties

##### Node 44

$$\begin{aligned}m &= 3500 \text{ kg} \\I_{xx} &= 2100 \text{ kg-m}^2 \\I_{yy} &= 2100 \text{ kg-m}^2 \\I_{zz} &= 4200 \text{ kg-m}^2\end{aligned}$$

#### Solar Panel Properties

##### Nodes 48, 52, 53, 57

$$\begin{aligned}m &= 90 \text{ kg} \\I_{xx} &= 270 \text{ kg-m}^2\end{aligned}$$

##### Node 50, 55

$$\begin{aligned}m &= 180 \text{ kg} \\I_{xx} &= 540 \text{ kg-m}^2\end{aligned}$$

### 9.2.3 Isolation System

The optical support structure and the equipment section are connected by a passive isolator at three points acting in all three translational directions. The isolator is designed to reduce the amount of force transmitted from the equipment section to the optics. This is accomplished by designing an isolator with the natural frequency much lower than expected disturbance frequency. In addition, the isolator frequency should be lower than the optical structure bending frequency. A passive isolator consists of a spring and a viscous dashpot in parallel as shown in Figure 9-5.

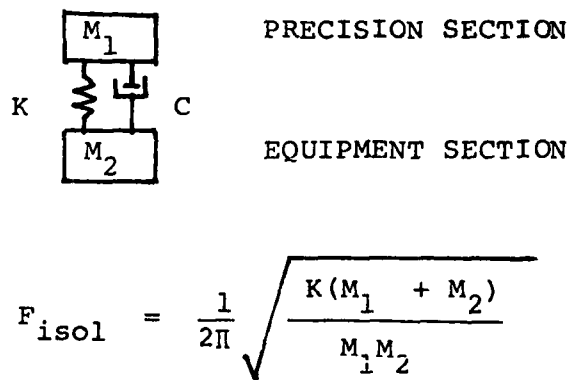


Figure 9-5.

If the isolator frequency is lower than the lowest natural frequencies of the two sections, they can be modelled by their inertia properties only. For this system, the isolator was sized to have a frequency of 0.5 Hz. The dashpot size has been specified as it is assumed to be part of the overall control design. The spring constants are given in Table 9-2.

### 9.3 Structural Analysis

A modal analysis was performed using the NASTRAN finite element program. The input deck is listed in Table 9-3. This model contains 84 dynamic degrees of freedom, thus 84 frequencies and mode shapes were extracted. Table 9-4 gives a list of frequencies and descriptions of the first fifty mode shapes.

### 9.4 System Performance

The performance of this system is measured by the ability of maintain line-of-sight (LOS) rotation (jitter) and defocus within specified tolerances. These quantities can be computed using simple linear equations with the movement of the mirrors as inputs. The motion of the mirrors is a function of the movement of the support points. This section presents the equations necessary to compute LOS error from support point displacements.

ISOLATOR SPRING CONNECTIVITIES

TABLE 9-2

SPRING A	NODE A	DOF	NODE B	DOF
1	4	1	42	1
2	4	2	42	2
3	4	3	42	3
4	3	1	46	1
5	3	2	46	2
6	3	3	46	3
7	6	1	47	1
8	6	2	47	2
9	6	3	47	3

$K = 5790 \text{ N/m}$

Table 9-3. JUNE 6. 1980 NASTRAN 6/ 7/79 PAGE 1  
NASTRAN EXPRTTIVE CONTROL N E C K F C H O

IN DRAPER \* MODEL  
CHPNT YFS  
SOL 25  
DTAG 21.35  
CPNL

ECHO OF FIRST CARD IN CHECKPOINT DICTIONARY TO BE PUNCHED OUT FOR THIS PROBLEM

RESTART DRAPER \* MODEL \* 6/ 6/80. 54914.

Table 9-3\* (cont.)

Table 9-3. (Cont.)

DATAFILE MODEL ? JUN1F 6. 1980 NASTRAN 6/ 7/79 PAGE 2

RAISE CONTROL DECK ECHO.

CARD COUNT	
1	TITLE = DRAPFL MDOFL ?
2	DISP = ALL
3	METHOD = 600
4	WGIN RILK
	TOTAL COUNT= 237

\*\*\* USE INFORMATION MESSAGE 207. QULK DATA NOT SORTED XSOR WILL RE-ORDER DECK.



Table 9-3. (Cont.) JUNE 6, 1980 NASTRAN 6/7/79 PAGE

		S O R T E D   R U L K   D A T A   E C H O									
CARD	COUNT	1	2	3	4	5	6	7	8	9	10
51-	CB10	56	309	27	28						
52-	CB1Q	57	306	29	30						
53-	CB1Q	58	306	29	31						
54-	CB1Q	59	300	30	31						
55-	CB1Q	60	300	27	29						
56-	CB1Q	61	300	27	30						
57-	CB1Q	62	306	28	30						
58-	CB1Q	63	306	27	36						
59-	CB1Q	64	306	28	37						
60-	CB1Q	65	300	30	39						
61-	CB1Q	66	300	29	38						
62-	CB1Q	67	300	29	36						
63-	CB1Q	68	300	27	37						
64-	CB1Q	69	300	28	39						
65-	CB1Q	70	300	30	38						
66-	CB1Q	71	300	26	37						
67-	CB1Q	72	300	37	39						
68-	CB1Q	73	300	39	38						
69-	CB1Q	74	300	36	38						
70-	CB1Q	75	300	37	34						
71-	CB1Q	76	400	8	14						
72-	CB1Q	77	400	10	14						
73-	CB1Q	78	400	10	16						
74-	CB1Q	79	400	16	9						
75-	CB1Q	80	400	9	15						
76-	CB1Q	81	400	11	17						
77-	CB1Q	82	400	11	14						
78-	CB1Q	83	400	12	18						
79-	CB1Q	84	400	12	19						
80-	CB1Q	85	400	13	19						
81-	CB1Q	86	400	13	19						
82-	CB1Q	87	400	13	17						
83-	CB1Q	88	400	14	26						
84-	CB1Q	89	400	14	24						
85-	CB1Q	90	400	16	28						
86-	CB1Q	91	400	16	27						
87-	CB1Q	92	400	15	26						
88-	CB1Q	93	400	17	29						
89-	CB1Q	94	400	18	29						
90-	CB1Q	95	400	18	30						
91-	CB1Q	96	400	19	30						
92-	CB1Q	97	400	19	31						
93-	CB1Q	98	400	17	31						
94-	CB1Q	99	400	15	32						
95-	CB1Q	100	400	15	34						
96-	CB1Q	101	400	17	33						
97-	CB1Q	102	400	14	35						
98-	CB1Q	111	400	26	32						
99-	CB1Q	112	400	27	32						
100-	CB1Q	113	400	27	33						

Table 9-3. (Cont.) JUNE 6, 1970 NASTRAN 6/779 PAGE 5

CARD		SORTED BULK DATA ECHO																
COUNT		2	..	3	..	4	..	5	..	6	..	7	..	8	..	9	..	10
101-	CHAR	114	400	29	33	31	33	33	33	32	34	34	34	34	34	34	34	34
102-	CHAR	115	400	31	33	32	33	33	33	32	34	34	34	34	34	34	34	34
103-	CHAR	116	400	31	33	32	33	33	33	32	34	34	34	34	34	34	34	34
104-	CHAR	117	400	31	33	32	33	33	33	32	34	34	34	34	34	34	34	34
105-	CHAR	118	400	31	33	32	33	33	33	32	34	34	34	34	34	34	34	34
106-	CHAR	119	400	31	33	32	33	33	33	32	34	34	34	34	34	34	34	34
107-	CHAR	120	400	31	33	32	33	33	33	32	34	34	34	34	34	34	34	34
108-	CHAR	121	400	31	33	32	33	33	33	32	34	34	34	34	34	34	34	34
109-	CHAR	122	400	31	33	32	33	33	33	32	34	34	34	34	34	34	34	34
110-	CHAR	123	400	31	33	32	33	33	33	32	34	34	34	34	34	34	34	34
111-	CHAR	124	400	31	33	32	33	33	33	32	34	34	34	34	34	34	34	34
112-	CHAR	125	400	31	33	32	33	33	33	32	34	34	34	34	34	34	34	34
113-	CHAR	126	400	31	33	32	33	33	33	32	34	34	34	34	34	34	34	34
114-	CHAR	127	300	26	37	30	36	36	36	35	36	36	36	36	36	36	36	36
115-	CHAR	128	300	26	37	30	36	36	36	35	36	36	36	36	36	36	36	36
116-	CHAR	129	300	26	37	30	36	36	36	35	36	36	36	36	36	36	36	36
117-	CHAR	130	300	26	37	30	36	36	36	35	36	36	36	36	36	36	36	36
118-	CHAR	131	500	48	49	50	50	50	50	50	50	50	50	50	50	50	50	50
119-	CHAR	132	500	48	49	50	50	50	50	50	50	50	50	50	50	50	50	50
120-	CHAR	133	500	48	49	50	50	50	50	50	50	50	50	50	50	50	50	50
121-	CHAR	134	500	51	52	50	51	52	50	51	52	50	51	52	50	51	52	50
122-	CHAR	135	500	52	43	50	51	52	50	51	52	50	51	52	50	51	52	50
123-	CHAR	136	500	45	53	50	51	52	50	51	52	50	51	52	50	51	52	50
124-	CHAR	137	500	53	54	50	51	52	50	51	52	50	51	52	50	51	52	50
125-	CHAR	138	500	54	55	50	51	52	50	51	52	50	51	52	50	51	52	50
126-	CHAR	139	500	55	56	50	51	52	50	51	52	50	51	52	50	51	52	50
127-	CHAR	140	500	56	57	50	51	52	50	51	52	50	51	52	50	51	52	50
128-	CHAR	181	400	8	15	1	1	1	1	1	1	1	1	1	1	1	1	1
129-	CEIAS2	142	5.79E3	4	4	4	4	4	4	4	4	4	4	4	4	4	4	4
130-	CEIAS2	143	5.79E3	4	4	4	4	4	4	4	4	4	4	4	4	4	4	4
131-	CEIAS2	144	5.79E3	4	4	4	4	4	4	4	4	4	4	4	4	4	4	4
132-	CEIAS2	145	5.79E3	3	3	3	3	3	3	3	3	3	3	3	3	3	3	3
133-	CEIAS2	146	5.79E3	3	3	3	3	3	3	3	3	3	3	3	3	3	3	3
134-	CEIAS2	147	5.79E3	3	3	3	3	3	3	3	3	3	3	3	3	3	3	3
135-	CEIAS2	148	5.79E3	6	6	6	6	6	6	6	6	6	6	6	6	6	6	6
136-	CEIAS2	149	5.79E3	6	6	6	6	6	6	6	6	6	6	6	6	6	6	6
137-	CEIAS2	150	5.79E3	6	6	6	6	6	6	6	6	6	6	6	6	6	6	6
138-	COIN2	501	27	27	27	27	27	27	27	27	27	27	27	27	27	27	27	27
139-	COIN2	502	28	28	28	28	28	28	28	28	28	28	28	28	28	28	28	28
140-	COIN2	503	29	29	29	29	29	29	29	29	29	29	29	29	29	29	29	29
141-	COIN2	504	30	30	30	30	30	30	30	30	30	30	30	30	30	30	30	30
142-	COIN2	505	32	32	32	32	32	32	32	32	32	32	32	32	32	32	32	32
143-	COIN2	506	33	33	33	33	33	33	33	33	33	33	33	33	33	33	33	33
144-	COIN2	507	34	34	34	34	34	34	34	34	34	34	34	34	34	34	34	34
145-	COIN2	508	35	35	35	35	35	35	35	35	35	35	35	35	35	35	35	35
146-	COIN2	509	36	36	36	36	36	36	36	36	36	36	36	36	36	36	36	36
147-	COIN2	510	10	10	10	10	10	10	10	10	10	10	10	10	10	10	10	10
148-	COIN2	511	11	11	11	11	11	11	11	11	11	11	11	11	11	11	11	11
149-	COIN2	512	12	12	12	12	12	12	12	12	12	12	12	12	12	12	12	12
150-	COIN2	520	14	14	14	14	14	14	14	14	14	14	14	14	14	14	14	14

Table 9-3. (Cont.) JUNE 6, 1980 NASTRAN 6/ 1/79 PAGE

S O R T E D   R U L K   D A T A   E C H O										
CARD	1	2	3 ..	4 ..	5 ..	6 ..	7 ..	8 ..	9 ..	10 ..
COUNT	• 521	15				17.0				
151-	C0NM2	522	16			17.0				
152-	C0NM2	523	17			17.0				
153-	C0NM2	524	18			17.0				
154-	C0NM2	525	19			6.0				
155-	C0NM2	526	44			35n0.				
156-	C0NM2	527	2.10F3				4.20E3			
157-	• 544									
158-	C0NM2	548	4H			90.0				
159-	• 548	270.0								
160-	C0NM2	550	50			180.0				
161-	• 550	540.0								
162-	C0NM2	552	52			90.0				
163-	• 552	270.0								
164-	C0NM2	553	53			90.0				
165-	• 553	270.0								
166-	C0NM2	555	55			180.0				
167-	• 555	540.0								
168-	C0NM2	557	57			90.0				
169-	• 557	270.0								
170-	FIGR	600	61V							
171-	• 1n									
172-	GRTD	1								
173-	GRTD	2								
174-	GRTD	3								
175-	GRTD	4								
176-	GRTD	5								
177-	GRTD	6								
178-	GRTD	7								
179-	GRTD	8								
180-	GRTD	9								
181-	GRTD	10								
182-	GRTD	11								
183-	GRTD	12								
184-	GRTD	13								
185-	GRTD	14								
186-	GRTD	15								
187-	GRTD	16								
188-	GRTD	17								
189-	GRTD	18								
190-	GRTD	19								
191-	GRTD	20								
192-	GRTD	21								
193-	GRTD	22								
194-	GRTD	23								
195-	GRTD	24								
196-	GRTD	25								
197-	GRTD	26								
198-	GRTD	27								
199-	GRTD	28								
200-	GRTD	29								
		30								
		31								
		32								
		33								
		34								
		35								

Table 9-3. (Cont.)

846

STEAM 4/ 7/70

JUN 6 1980

(cont.)

Table 9-

S O R T E D   Q U I L K   D A T A   E C C 4 0										
1	2	3	4	5	6	7	8	9	10	11
CARD COUNT	201-	36	74.0	36.0	24.0					
	202-	GRTD	17	44.0	33.0					
	203-	GRTD	38	44.0	24.0					
	204-	GRTD	39	44.0	33.0					
	205-	GRTD	40	44.0	24.0					
	206-	GRTD	41	44.0	33.0					
	207-	GRTD	42	44.0	24.0					
	208-	GRTD	43	72.0	0.0					
	209-	GRTD	44	0.0	0.0					
	210-	GRTD	45	2.0	0.0					
	211-	GRTD	46	-4.0	-5.0					
	212-	GRTD	47	4.0	-5.0					
	213-	GRTD	48	-26.0	0.0					
	214-	GRTD	49	-26.00	0.0					
	215-	GRTD	50	-16.0	0.0					
	216-	GRTD	51	-11.0	0.0					
	217-	GRTD	52	-6.0	0.0					
	218-	GRTD	53	6.0	0.0					
	219-	GRTD	54	11.0	0.0					
	220-	GRTD	55	16.0	0.0					
	221-	GRTD	56	21.0	0.0					
	222-	GRTD	57	26.0	0.0					
	223-	MATI	100	1.24E+11	3					
	224-	OMTTI	56	48	50	52	55	57		
	225-	OMTTI	456	9	10	11	12	14	15	
	226-	OMTTI	456	17	18	19	27	28	29	30
	227-	OMTTI	456	32	THRU	35				
	228-	OMTTI	123456	1	THRU	8				
	229-	OMTTI	123456	13	36	THRU	31	49	51	54
	230-	OMTTI	123456	36	THRU	41				
	231-	GRDPNT	0							
	232-	PHAR	200	100	6.250E+43.195E+63.095E+66.1195E+6					
	233-	PHAR	300	100	3.133E+41.509E+61.509E+63.118E+6					
	234-	PHAR	400	100	3.919E+43.049E+63.049E+66.099E+6					
	235-	PHAR	500	100	9.607E+41.974E+51.974E+53.949E+5					
	236-	RFB2	44						45	46
		RFB2	141						43	42

TOTAL COUNT = 236

Table 9-4. Frequencies and mode shapes.

	Freq. (Hz)	Description	Freq. (Hz)	Description
1-6	0.0	rigid body	17	1.72 torsion
7	.145	Isolator Y-rotation	18	1.82 2 <sup>nd</sup> S.P. X-Z plane
8	.263	Isolator Z-rotation	19	1.82 2 <sup>nd</sup> S.P. X-Y plane
9	.317	1 <sup>st</sup> S.P. X-Z plane	20	1.89 1 <sup>st</sup> S.P. torsion asym
10	.333	1 <sup>st</sup> S.P. X-Y plane	21	2.36 1 <sup>st</sup> bending
11	.443	Isolator Z-trans	22	2.99 1 <sup>st</sup> S.P. torsion syn
12	.577	Isolator Y-trans	23	3.18 3 <sup>rd</sup> S.P. X-Y plane
13	.581	Isolator X-trans	24	3.39 3 <sup>rd</sup> S.P. X-Z plane
14	1.22	2 <sup>nd</sup> S.P. X-Z plane	25	5.16 2 <sup>nd</sup> S.P. torsion
15	1.30	2 <sup>nd</sup> S.P. X-Y plane	26	5.26 2 <sup>nd</sup> S.P. torsion
16	1.35	Isolator X-rotation	27	7.87 3 <sup>rd</sup> S.P. torsion

Table 9-4. Frequencies and mode shapes. (Cont.)

	FREQ (HZ)	DESCRIPTION	FREQ (HZ)	DESCRIPTION
28	8.11	LEG TORSION	39	15.65
29	8.36	3rd S.P. TORSION	40	16.07
30	8.57	LEG TORSION	41	16.52
31	8.81	3rd S.P. X-Y PLANE	42	16.75
32	8.81	3rd S.P. X-Z PLANE	43	17.16
33	11.35	4th S.P. X-Y PLANE	44	17.83
34	11.50	LEG BENDING	45	19.07
35	12.73	LEG BENDING	46	23.77
36	13.58	4th S.P. X-Z PLANE	47	24.41
37	13.71	LEG BENDING	48	25.91
38	14.16	LEG & LOWER TRUSS BENDING	49	26.36
			50	26.43
				S.P. AXIAL

#### 9.4.1 LOS Error Algorithm

The equations (9-2), (9-3), and (9-4), relating optical surface motion and the resultant LOS rotations about the X and Y axes below with notations and orientation consistent with the structural analysis. The movement of each mirror is defined to be the displacements and rotations in the global X, Y, Z directions at a point on the sphere (primary, tertiary) or plane (focal plane) which intersects the optical (global Z) axis. The LOS rotation and defocus are given by

$$\text{LOSX} = Y/F \quad \text{LOSY} = X/F \quad \text{Defocus} = Z \quad (9-1)$$

where

$$F = 8.051$$

$$X = A_1 [-X_p + X_t - R \cdot \theta Y_p + A_2 \cdot \theta Y_s - 2T \cdot \theta Y_t] + X_t - X_f \quad (9-2)$$

$$Y = A_1 [-Y_p + Y_t + R \cdot \theta X_p - A_2 \cdot \theta X_s + 2T \cdot \theta X_t] + Y_t - Y_f \quad (9-3)$$

$$Z = A_3 [Z_p - 2Z_s + Z_t] + Z_t - Z_f \quad (9-4)$$

where

$$A_1 = 0.2987$$

$$A_2 = 93.90$$

$$A_3 = 0.0892$$

$$R = 53.9$$

$$T = 66.95$$

The terms  $X_i$ ,  $Y_i$ ,  $Z_i$ ,  $\theta X_i$ ,  $\theta Y_i$ ,  $\theta Z_i$  refer to the translations and rotations in the global X, Y, and Z directions of the primary (p) and secondary (s), tertiary (t), and focal plane (f).

#### 9.4.2 LOS Error Algorithm Implementation

The motion of each mirror is based on the displacements of the support points and its position relative to the optical axis. It is assumed that the mirrors are kinematically mounted in order to decouple their dynamic motion from the structure. A typical kinematic mount is shown in Figure 9-6.

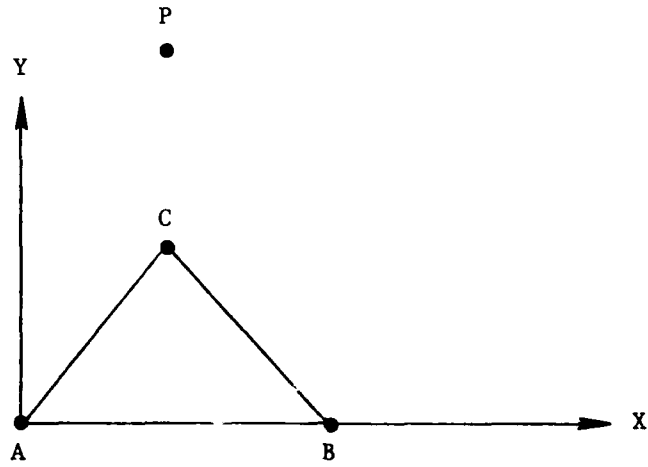


Figure 9-6. Kinematic Mount

Point A is supported in X, Y, and Z directions, Point B in the Y and Z directions, and Point C in the Z direction. Using small displacement theory, the displacement and rotation of any point P can be found.

$$\Delta x_P = \Delta x_A + z_P \Delta \theta_Y - y_P \Delta \theta_Z \quad (9-5)$$

$$\Delta y_P = \Delta y_A - z_P \Delta \theta_X - x_P \Delta \theta_Z \quad (9-6)$$

$$\Delta z_P = \Delta z_A + y_P \Delta \theta_X - x_P \Delta \theta_Y \quad (9-7)$$

where

$$\Delta \theta_X = (\Delta x_C - \Delta z_A + x_C (\Delta z_A - \Delta z_B) / x_B) / y_C \quad (9-8)$$

$$\Delta \theta_Y = (\Delta z_A - \Delta z_B) / x_B \quad (9-9)$$

$$\Delta \theta_Z = (\Delta y_B - \Delta y_A) / x_B \quad (9-10)$$

The locations of the support points and point P for each surface in this system are shown in Figure 9-7 and are summarized in Table 9-5.

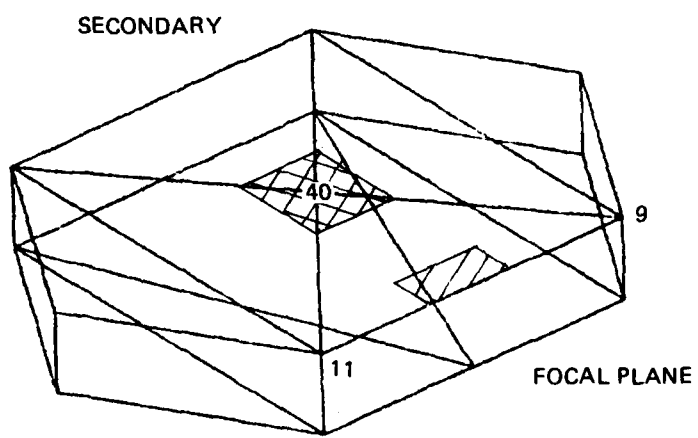
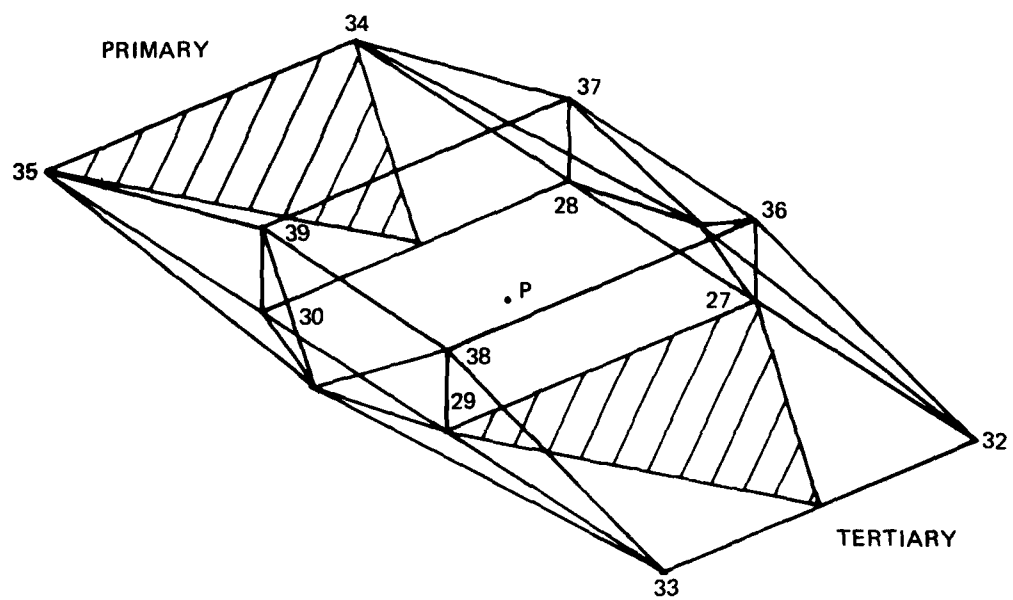


Figure 9-7.

Surface	Node A	Node B	Node C	$x_p$	$y_p$	$z_p$
Primary	34	35	30-28	4.0	10.0	0.0
Secondary	40	-	-	-	-	-
Tertiary	27	29	33-32	4.0	-3.0	0.0
F.P.	11	9	40	-4.0	-5.0	0.0

Table 9-5

It should be noted that since node C of the primary and tertiary is not located at a structural node point, the displacement can be found by interpolating between the two nodes given in the table. Also, all six degrees of freedom of the secondary correspond to the six degrees of freedom at node 40. The location of point P is in the local coordinate system of each mirror which are all parallel to the global coordinate system. Using equations (9-5) - (9-10) and the information in Table 9-5, a displacement transformation matrix (DTM) which relates the motion of each mirror to the displacements of the support points in the global coordinate system.

If modal analysis is employed to compute the displacements, the LOS error and defocus for each modal vector can be computed beforehand and the total errors found by modal superposition.

$$\begin{Bmatrix} LOSX \\ LOSY \\ z \end{Bmatrix} = [\phi_{LOS}] \{\eta\} \quad (9-11)$$

where  $[\phi_{LOS}]$  is a matrix which relates LOS error and defocus to modal amplitude. It is computed by first computing the mirror motions due to each mode shape using the DTM and then applying equations (9-1) through (9-3). For Draper model #2  $[\phi_{LOS}^T]$  is given in Table 9-6 for modes 1 - 50. It was calculated using mode shapes which were normalized to unit generalized mass.

### 9.5 Parameter Variations

In order to assess the sensitivity of the control system to changes in the natural frequencies and mode shapes, a set of perturbed frequencies and mode shapes can be used. This perturbed model can be obtained by either varying the frequencies and mode shapes directly or by changing selected

Table 9-6.

MODE ****	LOSX ****	LOSY ****	DEFOCUS *****	LOSMAG *****	FREQ ****
1	0.2705D-04	0.3778D-03	0.9313D-09	0.3787D-03	0.0001
2	-.1580D-04	0.8426D-06	-.1863D-07	0.1582D-04	0.0001
3	0.4927D-03	-.3133D-04	-.9604D-09	0.4937D-03	0.0001
4	0.1166D-03	0.1155D-03	0.4366D-10	0.1641D-03	0.0001
5	-.3502D-04	-.8110D-03	-.2721D-08	0.8117D-03	0.0001
6	-.7835D-03	0.4676D-04	0.6985D-09	0.7849D-03	0.0001
7	-.2641D-06	0.3263D-03	-.4904D-07	0.3263D-03	0.1455
8	0.3489D-06	-.2141D-03	-.1099D-05	0.2141D-03	0.2632
9	-.1505D-05	-.3452D-06	-.5238D-05	0.1544D-05	0.3173
10	-.2293D-03	0.4407D-06	-.1467D-06	0.2293D-03	0.3329
11	0.6041D-05	0.1066D-05	0.1559D-04	0.6135D-05	0.4432
12	0.7359D-03	-.6768D-05	0.1906D-05	0.7360D-03	0.5779
13	0.2330D-05	0.8731D-03	-.4276D-06	0.8731D-03	0.5814
14	-.1027D-05	-.2362D-03	-.4831D-07	0.2362D-03	1.2238
15	0.3759D-05	-.1519D-03	-.7763D-05	0.1519D-03	1.3002
16	-.1539D-03	-.1413D-05	0.9364D-05	0.1589D-03	1.3475
17	0.2738D-04	-.2777D-02	-.4955D-04	0.2777D-02	1.7209
18	0.2590D-05	-.4976D-06	0.2634D-05	0.2637D-05	1.8187
19	0.1151D-04	-.2364D-05	-.5493D-06	0.1175D-04	1.8187
20	-.3597D-13	-.3518D-14	0.3030D-14	0.3615D-13	1.8892
21	0.2237D-04	0.1376D-01	0.9028D-05	0.1376D-01	2.3635
22	0.1345D-03	0.2724D-05	-.1509D-04	0.1346D-03	2.9895
23	-.4355D-05	-.2602D-03	0.2500D-05	0.2602D-03	3.1759
24	0.5573D-06	-.4536D-03	-.4258D-06	0.4536D-03	3.3873
25	-.1814D-13	-.4398D-15	0.2601D-14	0.1815D-13	5.1617
26	-.3395D-04	-.7013D-06	0.4747D-05	0.3396D-04	5.2603
27	0.1038D-14	0.7264D-16	-.9614D-16	0.1040D-14	7.8769
28	-.4275D-03	-.1701D-02	-.1950D-03	0.1753D-02	8.1168
29	0.2916D-03	0.4775D-06	-.3638D-05	0.2916D-03	8.3600
30	0.1668D-01	-.1103D-04	0.1072D-02	0.1868D-01	8.5706
31	-.3822D-04	-.2919D-06	-.3755D-05	0.3822D-04	8.8135
32	-.4494D-04	0.7780D-07	0.9546D-06	0.4494D-04	8.8135
33	0.3762D-05	0.6995D-05	-.5240D-06	0.9750D-05	11.3462
34	-.1225D-02	0.1870D-02	0.3982D-03	0.2236D-02	11.4978
35	0.1098D-01	-.5662D-03	-.1593D-01	0.1099D-01	12.7258
36	0.2097D-04	0.7475D-03	-.6865D-04	0.7478D-03	13.5832
37	-.7143D-03	-.1011D-01	0.1142D-02	0.1014D-01	13.7141
38	0.3953D-02	0.5935D-02	-.1084D-02	0.7131D-02	14.1604
39	-.1414D-01	0.3213D-02	-.4966D-02	0.1451D-01	15.6523
40	0.1907D-02	0.1044D-01	-.2294D-03	0.1062D-01	16.0724
41	-.6760D-02	-.2220D-02	0.1413D-01	0.7134D-02	16.5248
42	0.3853D-02	-.9540D-03	-.1375D-01	0.3969D-02	16.7453
43	0.1132D-03	-.6405D-02	-.1739D-02	0.8406D-02	17.1555
44	0.3244D-02	-.1168D-02	0.7174D-02	0.3448D-02	17.8283
45	-.6439D-03	-.1446D-01	-.1545D-02	0.1447D-01	19.0713
46	-.2266D-01	0.1669D-01	0.5217D-01	0.2814D-01	23.7716
47	0.9058D-02	0.3711D-01	-.2293D-01	0.3820D-01	24.4140
48	0.2688D-03	0.1205D-01	-.3317D-02	0.1206D-01	25.4081
49	-.1444D-01	-.1042D-01	0.2362D-02	0.1781D-01	26.3625
50	0.9416D-14	-.6257D-14	-.1485D-14	0.1131D-13	26.4292

physical parameters which will cause a variation in the modal characteristics. Since the effects of modelling and manufacturing errors are of primary concern, the latter method was chosen. Two sets of physical parameter variations are presented here. Modal analyses including the modal LOS error were conducted using NASTRAN. The resulting natural frequencies and mode shapes are given and compared with the original system.

Two sets of parameter variations are summarized in Table 9-7. The changes are confined to the optical support structure and involve mass distribution changes on the upper optical support truss and stiffness changes in the metering truss. These parameters were chosen based on their impact on LOS error in several critical modes. The amount of variation is driven by the desire to vary the natural frequency by 10%.

Dynamic analyses were conducted on both perturbed models using NASTRAN. The resulting natural frequencies are given in Table 9-8 along with those of the original model. The modal LOS errors about the X and Y axes and the overall magnitude are given for all three cases in Table 9-9. The results show that both sets of parameter variations had more impact on the higher frequency modes because the upper support truss and the metering truss contain a higher percentage of the total energy in these modes than in the lower modes.

The perturbed models presented here are, of course, two point designs from an infinite number of possible parameter variations. In order to fully evaluate the stability limits of a particular control system design, it may be necessary to evaluate several perturbed models. Another type of variation which must also be considered are the changes in amplitude and frequency of the system disturbances.

## 9.6 System Disturbances and Tolerances

### 9.6.1 Description

The disturbance model consists of two sinusoidal forces which are applied to a point on the optical support structure and a point on the equipment section. The location, direction magnitude and frequency are given in Figure 9-8. These forces simulate on-board vibrating equipment. It is assumed that both forces will act simultaneously.

The tolerances for system line of sight error and defocus are

$$\text{LOS} = 1.0 \times 10^{-6} \text{ radians}$$

$$\text{Defocus} = .50 \times 10^{-3} \text{ meters}$$

Table 9-7.

• Mass changes

Node	Original Mass	Case #2 - 2A	Case #4 - 4A
27	375.0	350.0	375.0
28	375.0	350.0	350.0
29	375.0	350.0	350.0
30	375.0	350.0	350.0
32	500.0	500.0	550.0
33	500.0	550.0	450.0
34	250.0	300.0	300.0
35	250.0	250.0	200.0

• Stiffness changes

Memb.	NA	NB	Section Property #	
			Case 2A	Case 4A
76	8	14	1	1
80	9	15	1	1
81	11	17	1	1
85	13	19	1	2
99	15	32	1	2
101	17	33	1	2

• Section Properties

#1 - 25cm dia.  $\times$  0.10 cm round tube      #2 - 25cm dia.  $\times$  0.025 cm round tube

$$A = 7.823 \times 10^{-4} \text{ m}^2$$

$$I = 6.063 \times 10^{-6} \text{ m}^4$$

$$J = 1.213 \times 10^{-5} \text{ m}^4$$

$$A = 1.962 \times 10^{-4} \text{ m}^2$$

$$I = 1.529 \times 10^{-6} \text{ m}^4$$

$$J = 3.059 \times 10^{-6} \text{ m}^4$$

Table 9-8

Mode	Original	Case #2	Case #4
1-6	0.0	0.0	0.0
7	.1455	.1455	.1455
8	.2632	.2616	.2632
9	.3173	.3172	.3173
10	.3329	.3328	.3329
11	.4432	.4432	.4432
12	.5779	.5764	.5778
13	.5814	.5815	.5815
14	1.224	1.224	1.224
15	1.300	1.301	1.299
16	1.348	1.348	1.348
17	1.721	1.764	1.699
18	1.819	1.819	1.819
19	1.819	1.819	1.819
20	1.889	1.889	1.889
21	2.363	2.430	2.339
22	2.990	2.990	2.989
23	3.176	3.176	3.176
24	3.387	3.387	3.387
25	5.162	5.162	5.162
26	5.260	5.260	5.260
27	7.877	7.877	6.798
28	8.117	8.360	7.877
29	8.360	8.567	8.360
30	8.571	8.813	8.813
31	8.813	8.813	8.813
32	8.813	9.522	9.246
33	11.346	11.346	11.346
34	11.498	11.575	11.469
35	12.726	12.882	12.492
36	13.583	13.583	13.046
37	13.714	13.872	13.583
38	14.160	14.278	13.634
39	15.652	16.323	14.212
40	16.072	16.945	15.262
41	16.525	17.077	15.693
42	16.745	17.266	15.884
43	17.155	19.321	16.724
44	17.828	20.064	17.897
45	19.071	20.994	20.035
46	23.772	25.071	23.819
47	24.419	25.204	24.671
48	25.909	25.952	25.482
49	26.363	26.429	26.201
50	26.429	27.322	26.429

**Original Model**

**Case No. 2**

**Case No. 4**

**Table 9-9.**

TYPE	FREQ	LOSS		LOSS		LOSS		LOSS		LOSS	
		LOSS	LOSS	LOSS	LOSS	LOSS	LOSS	LOSS	LOSS	LOSS	LOSS
1	0.27050-04	0.37720-03	0.37720-03	-49270-03	0.29900-13	0.40300-03	-30000-05	-11700-12	2.30000-01		
2	0.17530-04	0.35530-04	0.35530-04	49270-03	0.11660-12	0.48400-03	60000-05	11200-12	0.46300-01		
3	0.46270-03	0.11200-04	0.11200-04	0.45570-03	0.11660-12	0.48400-03	60000-05	11200-12	0.46300-01		
4	0.11660-03	0.11570-04	0.11570-04	0.45570-03	0.11660-12	0.48400-03	60000-05	11200-12	0.46300-01		
5	0.35530-03	0.11120-03	0.11120-03	0.45570-03	0.11660-12	0.48400-03	60000-05	11200-12	0.46300-01		
6	-78530-03	0.35000-04	0.35000-04	0.11570-04	0.72720-13	0.30000-03	0.10700-03	0.10700-03	0.10700-03		
7	-12670-06	0.35630-03	0.35630-03	0.11570-04	0.90100-09	0.32000-03	0.19500-05	0.19500-05	0.19500-05		
8	0.34920-06	-0.21010-03	-0.21010-03	0.11570-04	0.10300-06	0.20100-03	0.19500-05	0.19500-05	0.19500-05		
9	-15850-06	0.34500-03	0.34500-03	0.11570-04	0.14400-06	0.43370-05	0.16200-06	0.16200-06	0.16200-06		
10	0.22330-03	0.16060-05	0.16060-05	0.11570-04	0.21720-03	0.10900-06	0.10900-07	0.10900-07	0.10900-07		
11	0.16310-05	0.16310-05	0.16310-05	0.11570-04	0.66330-06	0.15190-06	0.12200-03	0.12200-03	0.12200-03		
12	0.71330-03	-0.15570-03	-0.15570-03	0.11570-04	-46900-06	0.15190-06	0.12200-03	0.12200-03	0.12200-03		
13	0.23570-05	0.67310-03	0.67310-03	0.11570-04	-10500-03	0.15190-06	0.12200-03	0.12200-03	0.12200-03		
14	-10570-05	0.23620-03	0.23620-03	0.11570-04	-47340-06	0.121360-03	0.10600-03	0.10600-03	0.10600-03		
15	-15750-05	0.15180-03	0.15180-03	0.11570-04	-14680-03	0.97030-05	0.616230-04	0.14390-03	0.14390-03		
16	-15750-05	0.14130-05	0.14130-05	0.11570-04	-26970-04	0.20470-02	0.66410-04	0.20470-02	0.20470-02		
17	0.27230-04	-0.27770-02	-0.27770-02	0.11570-04	-10770-05	0.311670-05	0.34760-05	0.34760-05	0.34760-05		
18	0.25250-05	-0.49760-06	-0.49760-06	0.11570-04	-10730-04	0.10730-06	0.16930-06	0.16930-06	0.16930-06		
19	0.11510-04	-0.22170-05	-0.22170-05	0.11570-04	0.12270-13	0.22750-14	0.1940-14	0.1940-14	0.1940-14		
20	0.35730-03	-0.35100-16	-0.35100-16	0.11570-04	0.13630-04	0.22750-01	0.1770-01	0.1770-01	0.1770-01		
21	0.32370-04	0.13770-03	0.13770-03	0.11570-04	0.10550-03	0.10550-03	0.12750-06	0.11770-03	0.11770-03		
22	0.13150-03	0.27740-05	0.27740-05	0.11570-04	0.44650-03	0.44650-03	0.55310-05	0.27660-03	0.27660-03		
23	0.45550-05	-0.45550-05	-0.45550-05	0.11570-04	0.26030-05	0.26030-05	0.4750-03	0.3920-03	0.3920-03		
24	-0.45550-05	0.45550-03	0.45550-03	0.11570-04	0.45330-05	0.45330-05	0.55920-14	0.19150-14	0.19150-14		
25	-0.13010-13	-0.61310-15	-0.61310-15	0.11570-04	0.21010-13	0.64610-07	0.86610-07	0.86610-07	0.86610-07		
26	-0.31950-04	-0.70130-05	-0.70130-05	0.11570-04	0.31950-04	0.15850-15	0.11140-15	0.11140-15	0.11140-15		
27	0.10950-14	0.2750-16	0.2750-16	0.11570-04	-10500-14	0.15160-15	0.15160-15	0.15160-15	0.15160-15		
28	0.42550-01	-0.17710-02	-0.17710-02	0.11570-04	0.17710-02	0.17710-02	0.24430-04	0.14060-06	0.14060-06		
29	0.12750-03	0.31310-05	0.31310-05	0.11570-04	0.1330-03	0.1330-03	0.2250-05	0.11770-02	0.11770-02		
30	0.12750-03	0.59350-02	0.59350-02	0.11570-04	0.2850-03	0.2850-03	0.33230-02	0.13030-02	0.13030-02		
31	-0.55150-04	-0.15150-02	-0.15150-02	0.11570-04	0.15300-01	-0.1660-01	-0.64910-02	0.15300-01	0.15300-01		
32	0.14410-04	0.7750-07	0.7750-07	0.11570-04	0.27070-08	0.27070-08	0.36310-06	0.20977-05	0.20977-05		
33	0.37570-05	0.67750-05	0.67750-05	0.11570-04	0.1590-02	-0.2650-02	-0.79670-03	0.28530-02	0.28530-02		
34	0.18750-03	0.38520-03	0.38520-03	0.11570-04	0.11350-01	0.11350-01	0.16420-03	0.11350-01	0.11350-01		
35	0.10750-01	-0.10750-01	-0.10750-01	0.11570-04	0.47770-05	0.55350-03	0.1030-04	0.53310-03	0.53310-03		
36	0.30970-04	0.76750-03	0.76750-03	0.11570-04	-10500-04	0.35750-06	0.38420-06	0.38420-06	0.38420-06		
37	0.71420-03	-0.10110-01	-0.10110-01	0.11570-04	0.37940-02	0.21090-02	-0.12860-02	0.43010-02	0.43010-02		
38	0.39210-02	0.59350-02	0.59350-02	0.11570-04	0.10450-01	0.27510-02	0.10010-01	0.10010-01	0.10010-01		
39	-0.16140-01	0.532130-01	0.532130-01	0.11570-04	0.62600-02	0.16160-02	0.14470-01	0.14470-01	0.14470-01		
40	0.190970-02	0.14410-02	0.14410-02	0.11570-04	0.20708-01	0.20708-01	0.20708-01	0.19740-02	0.19740-02		
41	0.9700-02	-0.22500-02	-0.22500-02	0.11570-04	0.11350-02	-0.1540-02	-0.1540-02	0.11350-02	0.11350-02		
42	0.38510-02	-0.95580-02	-0.95580-02	0.11570-04	0.47770-05	0.55350-03	0.1030-04	0.53310-03	0.53310-03		
43	0.11130-02	-0.61750-02	-0.61750-02	0.11570-04	-10500-03	0.59350-02	0.1120-03	0.1120-03	0.1120-03		
44	0.2-240-02	-0.11660-02	-0.11660-02	0.11570-04	0.37940-02	0.60000-02	0.78500-02	0.10530-02	0.10530-02		
45	-0.64350-03	-0.14640-01	-0.14640-01	0.11570-04	0.16150-02	0.64100-03	0.20630-01	0.16210-01	0.16210-01		
46	-0.22660-01	0.14640-01	0.14640-01	0.11570-04	0.72150-02	0.22430-01	0.20570-01	0.19190-01	0.19190-01		
47	0.39710-02	0.37110-01	0.37110-01	0.11570-04	-10500-02	0.58200-01	0.20070-01	0.16370-01	0.16370-01		
48	0.24561-03	0.142070-01	0.142070-01	0.11570-04	0.33170-02	0.61960-02	0.33330-01	0.20860-01	0.20860-01		
49	0.14020-01	-0.10420-01	-0.10420-01	0.11570-04	-10500-02	0.59600-02	0.30400-01	0.16070-01	0.16070-01		
50	0.5-160-34	-0.62570-14	-0.62570-14	0.11570-04	-10500-01	-0.16170-01	-0.16170-01	-0.16170-01	-0.16170-01		

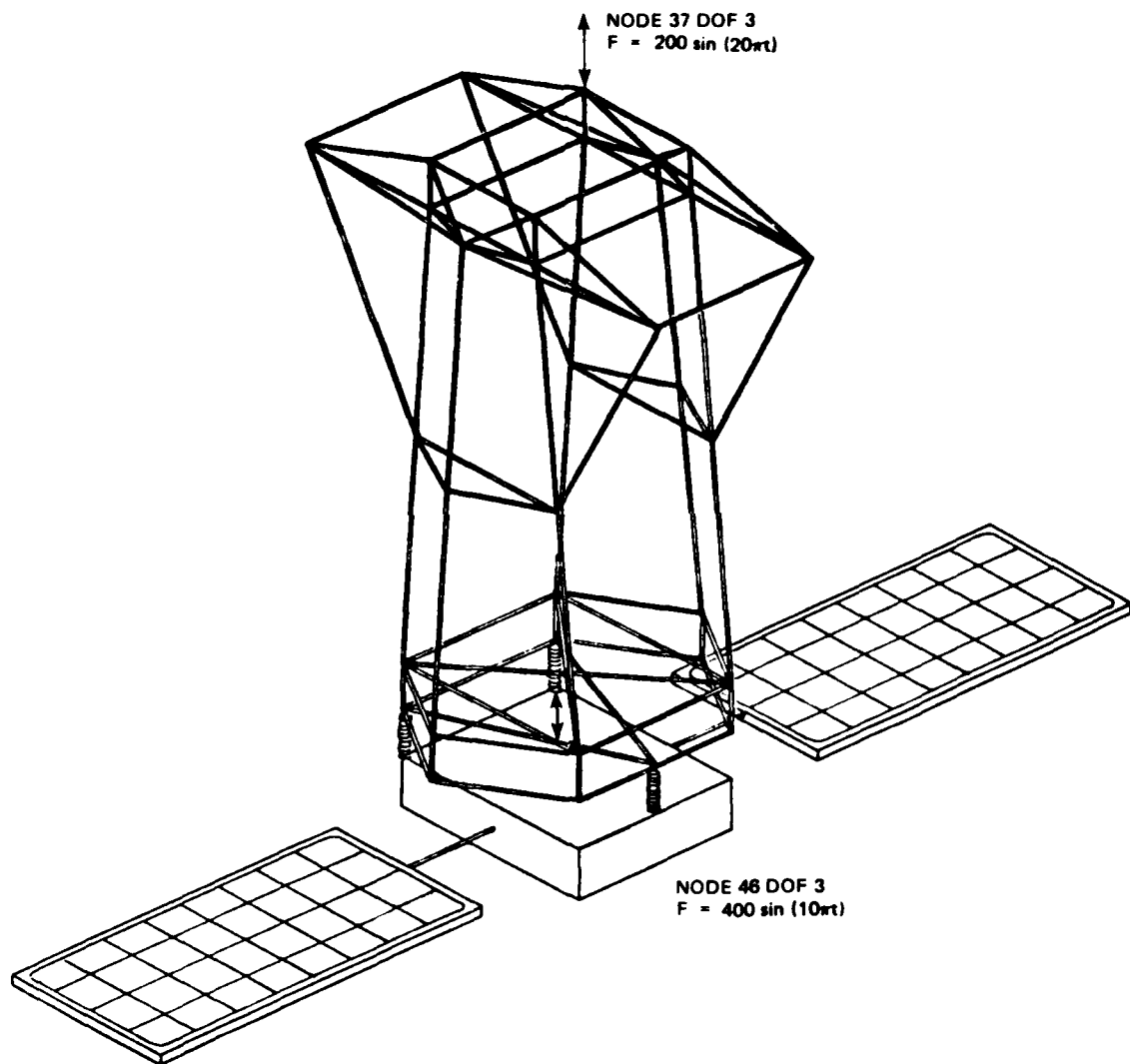


Figure 9-8.

### 9.6.2 Open Loop Performance

To demonstrate that structural control is required, the open loop performance is shown in Figure 9-9. In this analysis each mode is assumed to have 0.1% critical damping and there is no additional isolator damping.

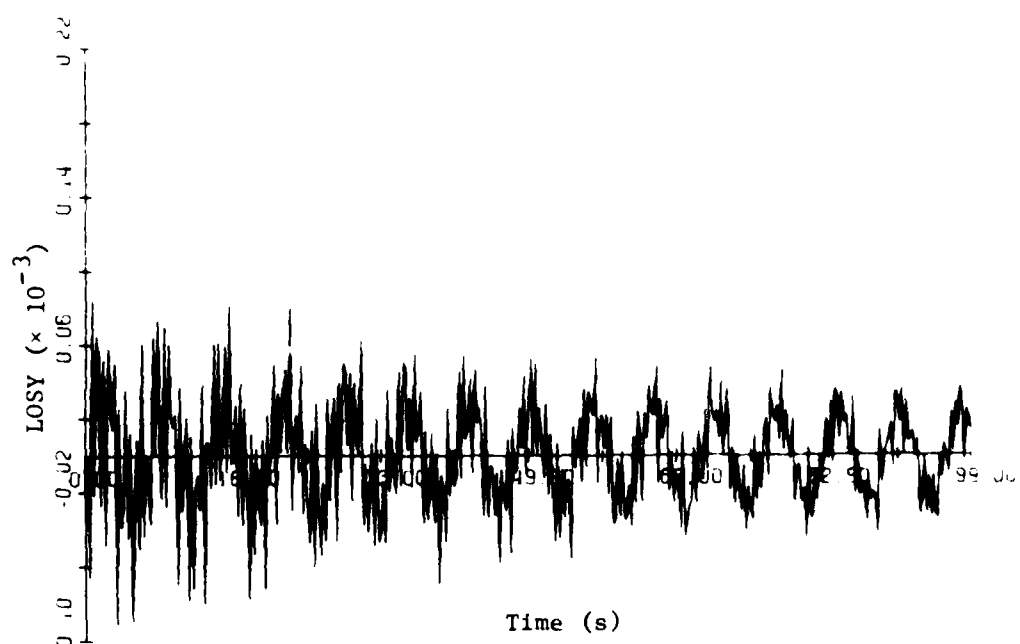
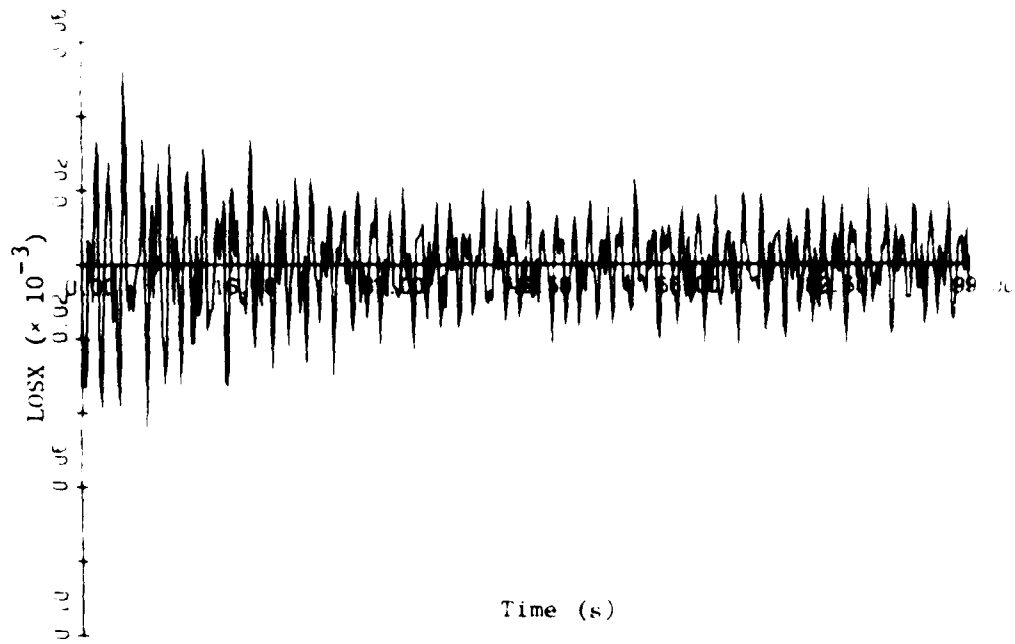


Figure 9-9. Open-loop response.

SECTION 10  
PRELIMINARY ASSESSMENT OF DRAPER MODEL

10.1 Introduction

The Draper model described in Section 9 was analyzed with respect to the two given sinusoidal disturbance functions. The steady state line-of-sight, LOS, amplitude error is determined and then compared to the LOS performance requirements. The amount of modal damping required to meet the LOS performance is determined. The preliminary results show that modal damping alone is not sufficient to suppress the sinusoidal disturbance impact on the LOS error.

10.2 Steady State LOS Error

The amplitude of the steady state LOS error is determined by evaluating the modal response at  $t = \infty$ . The modal equation is

$$\eta_i + 2\zeta_i \omega_i \eta_i + \omega_i^2 \eta_i = \phi_{i,d}^T f$$

where

$\eta_i$  is the modal amplitude for the  $i$ th mode

$\omega_i$  is the modal frequency of the  $i$ th mode

$\zeta_i$  is the damping ratio of the  $i$ th mode

$\phi_{i,d}$  is the disturbance influence at location 'd' to the  $i$ th mode

$f$  is the disturbance forcing function

For this particular case, the disturbance forcing function is assumed sinusoidal.

$$f = A \sin \Omega t \quad t \geq 0$$

Evaluation of the modal response at  $t = \infty$  yields the steady-state solution

$$\eta_i = \frac{A \phi_{i,d}}{\sqrt{(2\zeta_i \omega_i \Omega)^2 + (\omega_i^2 - \Omega^2)^2}} \sin(\Omega t + \beta)$$

where

$$\beta = \tan^{-1} \left( -\frac{2\zeta_i \omega_i \Omega}{\omega_i^2 - \Omega^2} \right)$$

The steady state amplitude of the modal response is defined as

$$AMPL = \frac{A\phi_{i,d}}{\sqrt{(2\zeta_i \omega_i \Omega)^2 + (\omega_i^2 - \Omega^2)^2}} \quad (10-1)$$

The steady state LOS error amplitude is obtained by multiplying the above, AMPL, by the LOS error influence ( $\phi_{i,LOS}$ ) for the  $i$ th mode.

$$\epsilon_{LOS} = \phi_{i,LOS} AMPL \quad (10-2)$$

### 10.3 Sinusoidal Disturbance Impact on LOS Error

As described in Section 9, two sinusoidal disturbance functions were used to degrade the LOS

$$f_1 = A_1 \sin \Omega_1 t \quad \left\{ \begin{array}{l} A_1 = 200 \text{ N} \\ \Omega_1 = 10 \text{ Hz} \\ \text{at node \#37} \end{array} \right.$$

$$f_2 = A_2 \sin \Omega_2 t \quad \left\{ \begin{array}{l} A_2 = 400 \text{ N} \\ \Omega_2 = 5 \text{ Hz} \\ \text{at node \#46} \end{array} \right.$$

The performance requirement for the LOS error is

$$\bar{\epsilon}_{i,LOS} = \begin{pmatrix} 1 \mu \text{ radian} \\ 1 \mu \text{ radian} \\ 500 \mu \text{ meters} \end{pmatrix} \quad \left\{ \begin{array}{l} \text{LOS error about X-axis} \\ \text{LOS error about Y-axis} \\ \text{defocus error in Z-direction} \end{array} \right.$$

The asterisk in Table 10-1 shows that 19 of 50 modes have a steady-state LOS amplitude greater than the performance requirement. Note that modes 1 to 6 are the rigid body modes. The defocus error always meets the performance. The definitions for the headings in Table 10-1 are as follows:

LOSX<sub>j</sub> = LOS error about X-axis due to disturbance  $f_j$  ;  
 $j = 1, 2$  (see equation (10-1,2))

LOSY<sub>j</sub> = LOS error about Y-axis due to disturbance  $f_j$  ;  
 $j = 1, 2$  (see equation (10-1,2))

Table 10-1. Steady-state line-of-sight amplitude as functions of  $f_1$ ,  $f_2$ .

MODE	FREQ (Hz)	LOSS1 (H)	LOSS1 (m)	DEFOCUS1 (H)	DEFOCUS1 (m)	LOSS2 (H)	LOSS2 (m)	DEFOCUS2 (H)	DEFOCUS2 (m)
1	0.000382	-1815D-08	-2534D-07	-6210D-13	-2561D-07	-1511D-07	-2110D-06	-5202D-12	-2116D-06
2	0.000409	-8328D-08	-4442D-09	-9819D-11	-8340D-08	-6633D-07	-3564D-08	-7819D-10	-6692D-07
3	0.000420	-2936D-07	-1866D-08	-5726D-13	-2944D-07	-4316D-06	-2746D-07	-6172D-12	-4327D-06
4	0.000436	-4854D-08	-4498D-08	-1852D-14	-6859D-08	-4917D-07	-4917D-07	-1878D-13	-7086D-07
5	0.000460	-6217D-08	-1446D-08	-4831D-12	-1441D-06	-5073D-07	-1175D-05	-3394D-11	-1176D-05
6	0.000472	-1057D-06	-6309D-08	-9424D-13	-1059D-06	-1343D-05	-8016D-07	-1198D-11	-1346D-05
7	0.914426	-2026D-10	-2503D-07	-3765D-11	-2503D-07	-6616D-09	-8175D-06	-1225D-09	-8175D-06
8	1.653911	-1426D-10	-8750D-08	-4491D-10	-8750D-08	-1530D-10	-8339D-08	-4225D-07	-8235D-08
9	1.993596	.3947D-09	.9050D-10	.1374D-08	.4050D-09	.4586D-09	.1046D-09	.1567D-08	.4676D-09
10	2.091605	-1202D-07	-231CD-10	-7688D-11	-1200D-07	-1132D-06	-2521D-09	-8393D-10	-1312D-06
11	2.784732	.2415D-08	.4261D-09	.6230D-08	.2452D-08	.1242D-07	.2122D-08	.3205D-07	.1295D-07
12	3.630822	-1118D-06	-1065D-09	-3000D-09	-1158D-06	-1190D-07	-3353D-08	-1300D-05	-1300D-05
13	3.653243	-4191D-09	-1571D-06	-7692D-10	-1571D-06	-5063D-09	-1897D-06	-9293D-10	-1897D-06
14	7.689052	-7318D-11	-1663D-05	-3441D-12	-1653D-08	-9889D-08	-2255D-05	-4612D-09	-2255D-05
15	8.169507	-6024D-10	-2454D-06	-1244D-09	-2455D-09	-4660D-09	-1721D-07	-8797D-09	-1739D-07
16	8.466874	-1077D-07	-9578D-10	-6349D-09	-1078D-07	.3560D-05	.3112D-07	-2062D-06	.3560D-05
17	10.613030	-1136D-08	-1213D-06	-2163D-08	-1213D-06	-1335D-08	-2388D-10	-1213D-06	-1213D-06
18	11.427218	-1641D-10	-2001D-11	-1055D-10	-1061D-10	-3721D-08	-7168D-09	-3794D-08	-3799D-08
19	11.427431	-3828D-10	-7855D-11	-1825D-11	-3995D-10	-5489D-08	-1127D-08	-2618D-09	-5662D-08
20	11.869940	-4175D-27	-4081D-28	-3514D-26	-4193D-27	-2895D-24	-2631D-25	-2435D-25	-2900D-24
21	14.850253	-1618D-05	-9949D-05	-6535D-05	-9940D-05	-1265D-07	-7792D-07	-5114D-08	-1264D-04
22	18.703530	-32700D-08	-6621D-10	-3666D-09	-32700D-05	-7311D-05	-1481D-06	-6202D-06	-7311D-05
23	19.955063	-8102D-10	-4341D-08	-4651D-10	-4641D-08	-4911D-09	-2934D-07	-2819D-09	-2935D-07
24	21.2322791	-1443D-10	-1175D-07	-11103D-10	-1175D-07	-2003D-07	-1930D-04	-1575D-07	-1630D-04
25	32.431671	-2891D-23	-7007D-30	-4146D-29	-2892D-28	-1376D-23	-3356D-25	-1973D-24	-1377D-23
26	33.051529	-9710D-16	-2002D-10	-1357D-10	-9710D-10	-2870D-05	-5925D-07	-4012D-06	-2671D-05
27	49.492233	-7110D-31	-4975D-32	-6585D-32	-6585D-32	-1165D-27	-7726D-25	-1023D-28	-1106D-27
28	50.999069	-32710D-05	-13010D-05	-1492D-06	-1340D-05	-1929D-08	-7675D-08	-8800D-09	-7914D-08
29	52.527542	-3935D-08	-6456D-05	-4913D-10	-3935D-08	-2574D-05	-4214D-05	-3210D-07	-2574D-05
30	53.859615	-12331D-04	-7301D-08	-7062D-06	-1233D-04	-2722D-05	-1605D-08	-1556D-06	-2712D-05
31	55.376602	-2852D-10	-2217D-12	-2217D-11	-2217D-10	-2691D-07	-6086D-10	-7635D-09	-7974D-08
32	55.376602	-1227D-09	-2211D-11	-2713D-11	-1227D-09	-2691D-07	-6465D-10	-5717D-09	-2691D-07
33	71.290451	-6336D-11	-1527D-10	-8890D-12	-1652D-10	-1157D-09	-12630D-13	-16360D-13	-1652D-10
34	72.242966	-4566D-06	-7572D-06	-1610D-06	-9052D-06	-9733D-05	-1455D-07	-3163D-08	-9054D-06
35	79.958420	-7615D-07	-3930D-05	-1106D-04	-7620D-05	-3661D-06	-1899D-08	-5344D-06	-7636D-05
36	85.346527	-9733D-09	-3466D-07	-3185D-08	-3466D-07	-9185D-07	-3272D-05	-3005D-06	-3274D-05
37	86.168518	-4465D-06	-6331D-05	-7135D-06	-6333D-05	-2217D-06	-3135D-05	-3546D-06	-3146D-05
38	88.972687	-3934D-06	-5905D-06	-1079D-06	-1079D-06	-1105D-06	-1663D-06	-3036D-07	-1992D-06
39	98.346039	-1135D-05	-2575D-06	-3986D-06	-1140D-05	-1735D-06	-3944D-06	-1636D-05	-3045D-12
40	100.965977	-1246D-06	-6824D-06	-1499D-07	-6937D-05	-2025D-07	-11110D-06	-2440D-08	-1178D-06
41	103.828430	-8C56D-06	-2900D-06	-1846D-05	-9322D-06	-3611D-07	-1165D-07	-7522D-07	-9330D-06
42	105.214050	-7375D-06	-2321D-06	-3345D-05	-9655D-06	-1666D-07	-4132D-08	-5953D-07	-1715D-05
43	107.791077	-2335D-07	-1735D-05	-3592D-06	-1735D-05	-6057D-09	-1225D-07	-5663D-07	-1737D-05
44	112.016387	.5690D-06	-1204D-06	.1255D-05	.6044D-06	-1572D-07	.5662D-08	-3477D-07	.6051D-06
45	119.623278	-8265D-07	-1655D-06	-1857D-05	-1857D-05	-3003D-07	-6095D-07	-3210D-08	-1857D-05
46	149.361545	-5245D-07	-3865D-07	-1205D-06	-6518D-07	-6748D-08	-4972D-08	-1554D-07	-8381D-08
47	153.397614	-16310D-06	-75010D-06	-4635D-06	-7722D-06	-1074D-07	-4339D-07	-2715D-07	-4522D-07
48	162.729466	-7762D-03	-3460D-06	-9577D-07	-3431D-06	-7232D-10	-3235D-05	-8907D-09	-3481D-06
49	163.646686	-5252D-05	-2343D-05	-5366D-06	-4010D-05	-7255D-08	-5246D-08	-1197D-08	-5953D-08
-50	166.053479	-1004D-29	-16672D-30	-1504D-30	-1200D-29	-7161D-31	-1875D-31	-1214D-29	-1435D-30

DEFOCUS<sub>j</sub> = LOS defocus error in Z-direction due to disturbance  $f_j$ ;  $j = 1, 2$  (see equation (10-1,2))

$$\text{LOS}_j = \sqrt{(\text{LOSX}_j)^2 + (\text{LOSY}_j)^2} ; j = 1, 2$$

$$\text{LOS} = \sqrt{(\text{LOS1})^2 + (\text{LOS2})^2}$$

#### 10.4 Modal Damping Requirements

The damping requirements for each mode are determined by solving equations (10-1), (10-2) for  $\zeta_i$  and specifying the desired performance amplitude,  $\epsilon_{\text{LOS}}$ .

$$\zeta_i = \frac{1}{2\omega_i \Omega} \sqrt{\left( \frac{A\phi_{i,d}\phi_{i,LOS}}{\epsilon_{\text{LOS}}} \right)^2 - (\omega_i^2 - \Omega^2)^2}$$

Table 10-2 shows the results for the disturbance  $f_1$  at node #37 while Table 10-3 is for disturbance  $f_2$  at node #46. Ignoring the rigid body, modes 1 to 6, it can be seen that there are numerous damping ratios  $\gg 1$ . In order to obtain some insight, a frequency response was determined (Fig. 10-1) between disturbance  $f_1$  and the LOSX. Note the solid line at 62.8 rad/sec (10 Hz). Since this line intersects the frequency response at a location removed from the peaks, just adding damping will only affect the magnitude of the response peaks and not the general shape of the frequency response in the neighborhood of the disturbance frequency.

#### 10.5 Summary

Preliminary results show that the defocus error is not degraded by the two sinusoidal disturbances. Ignoring the rigid body, 17 modes degrade the LOS error about the X and Y axes. Furthermore, the addition of damping to individual modes is not sufficient to suppress a sinusoidal disturbance impact on LOS error.

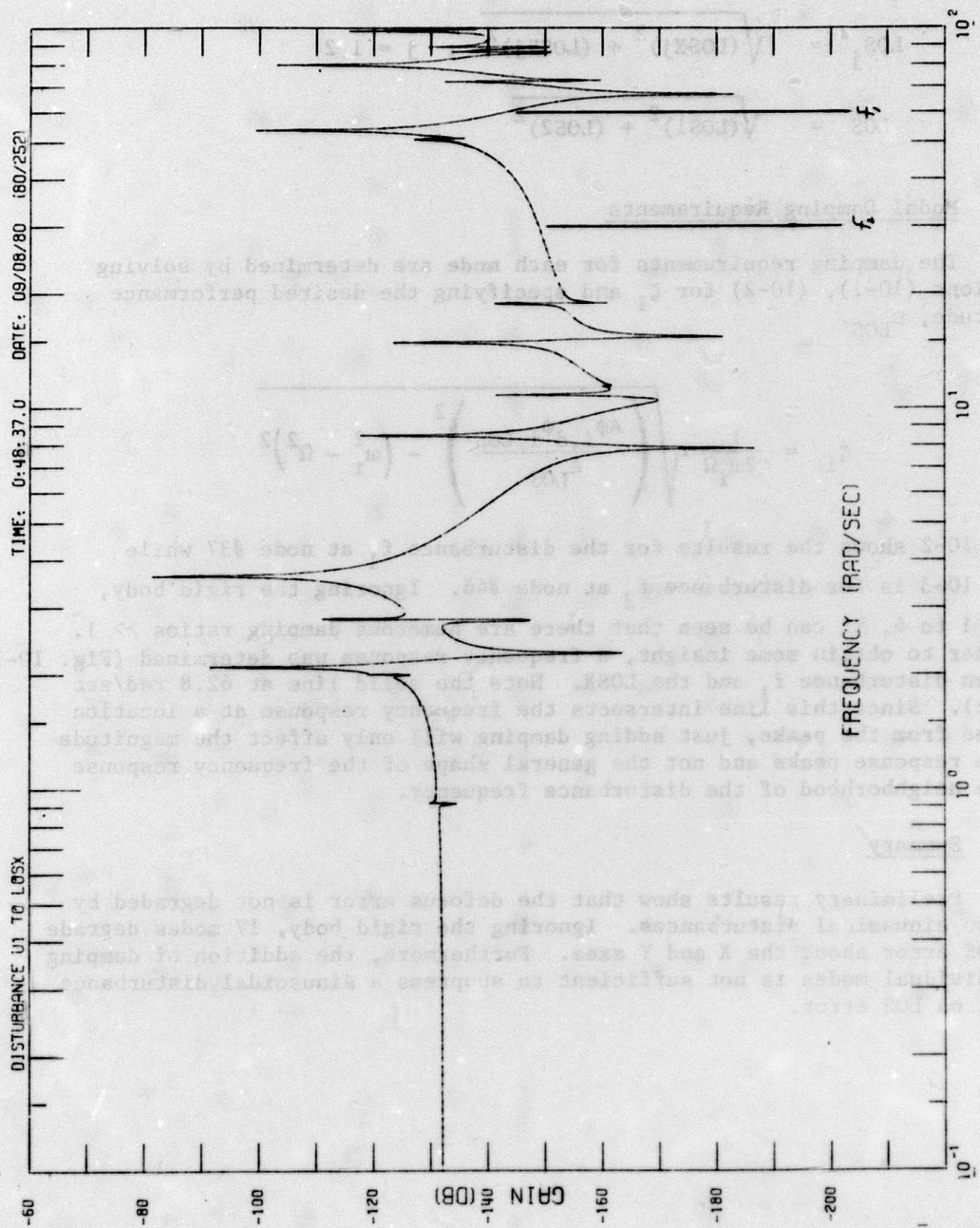


Figure 10-1. Frequency response (disturbance  $f_1$  to LOSX).

Table 10-2. Damping ratio required to meet LOS performance ( $f_1$ ).

MODE	FREQ (r/s)	AMPL	LOSSX (r)	LOSSY (r)	DEFOCUS (m)	X	DAMPING RATIO Y	Z
1	0.000382	- .67080-04	- .18150-08	- .25340-07	- .62470-13			
2	0.000409	.52710-03	- .83280-08	.44480-09	- .98190-11			
3	0.000420	- .59880-04	- .29380-07	.18680-08	.57260-13			
4	0.000436	- .41970-04	- .48940-08	- .48480-08	- .18320-14			
5	0.000460	.17750-03	- .62170-08	- .14400-06	- .48310-12			
6	0.000472	.13480-03	- .10570-06	.63090-03	.94240-13			
7	0.914406	- .76780-04	.20260-10	- .25030-07	.37630-11			
8	1.653811	.40860-04	.14260-10	- .87500-08	- .44910-10			
9	1.993596	- .06220-03	.39470-09	.90560-10	.13740-08			
10	2.091605	.52410-04	- .12020-07	.23100-10	- .76680-11			
11	2.784732	.39970-03	.29150-08	.46610-09	.62300-08			
12	3.630302	- .15740-03	- .11580-06	.10650-08	- .50000-09			
13	3.653243	- .17970-03	- .41910-09	- .15710-06	.76900-10			
14	7.689052	.71230-05	.73180-11	- .16830-08	- .34410-12			
15	8.169607	- .16020-04	.60240-10	.24340-08	.12440-09			
16	8.466874	.67800-04	- .10770-07	- .95780-10	.63480-09			
17	10.813030	.43660-04	.11960-08	- .12130-06	.21630-08			
18	11.427218	.40210-05	.10410-10	- .20010-11	.10590-10			
19	11.427431	- .33220-05	- .38260-10	.78560-11	.18250-11			
20	11.869740	.11600-13	- .41730-27	- .40510-03	.35140-28			
21	14.850258	- .72330-03	- .16180-07	- .99470-05	- .65300-08	19.77		
22	18.793630	- .24300-04	- .32700-09	- .66110-10	.36680-09			
23	19.955063	.18600-04	- .81820-10	- .45410-08	.45510-10			
24	21.292791	.25900-04	.14430-10	- .11750-07	- .11030-10			
25	32.431671	.15930-14	- .28910-28	- .70070-30	.41440-29			
26	33.051529	.28600-05	- .97100-10	- .20090-11	.13570-10			
27	49.492233	- .68520-16	- .71100-31	.49780-32	.65880-32			
28	50.999039	.76520-03	- .32710-06	- .13010-05	- .14900-06	.1750		
29	52.527542	- .13510-04	- .39390-08	- .64500-11	.49130-10			
30	53.870315	- .65680-03	- .12310-04	.73010-08	- .70620-06	1.899		
31	55.376602	.74620-06	- .06520-10	- .21780-12	- .28020-11			
32	55.376617	.28410-05	- .12770-09	.22110-12	.27130-11			
33	71.070451	- .16970-05	- .63540-11	- .15270-10	.68940-12			
34	72.242966	.40490-03	- .49600-06	.75720-06	.16120-06			
35	79.988420	- .69410-03	- .76190-05	.39300-06	.11060-04	1.838		
36	85.345627	- .46400-04	- .97330-09	- .34680-07	.31850-08			
37	86.168518	.62470-03	- .44630-06	- .63170-05	.71350-06	2.003		
38	88.972687	- .99510-04	- .39340-06	- .59300-06	.16740-06			
39	98.346039	- .80270-04	.11350-05	- .25780-06	.39860-06	.2490		
40	100.935977	- .65340-04	- .12460-06	- .63840-06	.14990-07			
41	103.822430	.13070-03	- .88500-06	- .29020-06	.13460-05			
42	105.014050	- .24330-03	- .93750-06	.23210-06	.33450-05			
43	107.791077	- .20660-03	- .23390-07	.17360-05	.35920-06	.8038		
44	112.016337	.17540-03	.56900-06	- .20490-06	.12590-05			
45	119.828278	.12830-03	- .80600-07	- .18550-05	- .19630-06	1.080		
46	149.3b1542	- .23160-05	.52490-07	- .38550-07	- .12080-06			
47	153.397614	.20210-04	.18310-06	.75010-06	- .46350-06			
48	162.790466	- .28870-04	- .77620-08	- .34300-06	.95790-07			
49	165.640686	- .22530-03	.30550-05	.23480-05	- .53660-06	3.492		
50	166.056479	.10660-15	.10040-29	- .66720-30	- .15840-30	2.398		

Table 10-3. Damping ratio required to meet LOS performance ( $f_2$ ).

MODE	FREQ (r/s)	AMPL	LOSX (r)	LOSY (r)	DEFOCUS (m)	X	Y	Z	DAMPING RATIO
1	0.000382	- .5586D-03	- .1511D-07	- .2110D-06	- .5202D-12				
2	0.000409	.4230D-02	- .6683D-07	.3564D-08	- .7079D-10				
3	0.000420	- .8763D-03	- .4318D-06	.2746D-07	.6417D-12				
4	0.000436	- .4303D-03	- .5017D-07	- .4970D-07	- .1878D-13				
5	0.000460	.1449D-02	- .5073D-07	- .1175D-05	- .3942D-11				.2105D+05
6	0.000472	.1714D-02	- .1343D-05	.6916D-07	.1198D-11				.2983D+05
7	0.914426	.2505D-02	- .6618D-09	.8175D-06	- .1229D-09				
8	1.653511	- .3847D-04	- .1343D-10	.8239D-09	.4228D-10				
9	1.993596	- .3029D-03	.4558D-09	.1046D-09	.1567D-08				
10	2.091605	.5721D-03	- .1312D-06	.2851D-09	- .8391D-10				
11	2.784732	- .2058D-02	- .1242D-07	- .2192D-08	- .3205D-07				
12	3.630822	- .1759D-02	- .1294D-05	.119C0-07	- .3353D-08	3.508			
13	3.653243	- .2173D-03	- .5063D-09	- .1897D-06	.9293D-10				
14	7.659052	.9547D-02	- .9805D-08	- .2255D-05	- .4612D-09				3.883
15	8.169607	.1133D-03	.4260D-09	- .1721D-07	- .8797D-09				
16	8.466874	- .2202D-01	.3500D-05	.3112D-07	- .2062D-06	5.771			
17	10.813030	- .4819D-06	- .1320D-10	.1538D-08	.2385D-10				
18	11.427218	- .1440D-02	- .3731D-08	.7162D-09	- .3794D-08				
19	11.427431	.4766D-03	.5488D-09	- .1127D-09	- .2618D-09				
20	11.869940	- .8046D-11	.2895D-24	.0831D-25	- .2438D-25				
21	14.850258	- .5665D-03	- .1268D-07	- .7792D-05	- .5114D-08				6.348
22	18.783630	.5434D-01	.7311D-05	.1481D-06	- .8202D-06	3.891			
23	19.955063	.1113D-03	- .4911D-09	- .2934D-07	.2815D-09				
24	21.282791	- .3593D-01	- .2003D-07	.1630D-04	.1530D-07				6.497
25	32.431671	- .7585D-10	.1376D-23	.3336D-25	- .1975D-24				
26	33.051529	- .8453D-01	.2870D-05	.5929D-07	- .4012D-06	.1366			
27	49.492233	.1064D-12	.1104D-27	.7726D-29	- .1023D-28				
28	50.999669	- .4513D-05	.1922D-08	.7675D-08	.8800D-09				
29	52.527542	.8325D-02	.2574D-05	.4214D-08	- .3210D-07	1.273			
30	53.850815	- .1452D-03	- .2712D-05	.1609D-08	- .1555D-06	1.425			
31	55.376602	.2085D-03	- .7973D-08	- .6089D-10	- .7834D-09				
32	55.376617	- .5986D-03	.2691D-07	- .4659D-10	- .5717D-09				
33	71.290451	- .3123D-07	- .1175D-12	- .2809D-12	.1636D-13				
34	72.242966	.7944D-05	- .9733D-08	.1486D-07	.3163D-08				
35	79.953420	- .3354D-04	- .3681D-26	.1699D-07	.5344D-06				
36	85.345627	.4378D-02	.9182D-07	.3272D-05	- .3005D-06				3.659
37	86.168518	.3104D-03	- .2217D-06	.3139D-05	.3546D-06				3.538
38	88.972687	.2801D-04	.1108D-06	.1663D-06	- .3032D-07				
39	98.346039	.1227D-04	- .1736D-06	.3943D-07	- .6095D-07				
40	100.965977	- .1064D-04	- .2028D-07	- .1111D-06	.2440D-08				
41	103.808430	- .5326D-05	.3611D-07	.1182D-07	- .7523D-07				
42	105.214050	.4330D-05	.1668D-07	- .4130D-08	- .5952D-07				
43	107.791077	.7116D-05	.8059D-09	- .5983D-07	- .1238D-07				
44	112.018387	- .4643D-05	- .1572D-07	.5662D-08	- .3477D-07				
45	119.826278	- .2077D-05	.1337D-08	.3003D-07	.3210D-08				
46	149.361542	.2978D-06	- .6746D-08	.4970D-08	.1555D-07				
47	153.397614	- .1105D-05	- .1074D-07	- .4399D-07	.2716D-07				
48	162.790466	- .2685D-06	- .7218D-10	.3236D-08	.8907D-09				
49	165.640636	- .5027D-06	.7252D-08	.5240D-08	- .1197D-08				
50	166.059479	- .1265D-16	- .1191D-30	.7916D-31	.1879D-31				

TR Distribution List

ADDRESSES	NUMBER OF COPIES	LINE NUMBER
R. Carman RADC/OCSE	5	
RADC/TSLD Griffiss AFB NY 13441	1	2
RADC/DAP Griffiss AFB NY 13441	2	3
Administrator Def Tech Inf Ctr Attn: DTEC-DDA Cameron Sta Bg 5 Alexandria Va 22314	12	5
Charles Stark Draper Lab 555 Technology Square Cambridge, MA 02139	5	2
ARPA/MIS 1400 Wilson Blvd Arlington, VA 22209	1	3
ARPA/STO 1400 Wilson Blvd Arlington, VA 22209 Attn: Dr. C. Thomas	1	4
Charles Stark Draper Lab 555 Technology Square M.S. - 95 Cambridge, MA 02139 Attn: Dr. Keto Soosar	1	5
Charles Stark Draper Lab 555 Technology Square M.S - 95 Attn: Dr. J. B. Linn	1	6
Charles Stark Draper Lab 555 Technology Square M.S. - 95 Cambridge, MA 02139 Attn: Mr. R. Strunce	1	7
Riverside Research Institute 1701 N. Ft. Myer Drive Suite 711 Arlington, VA 22209 Attn: Dr. R. Kappesser	3	8

Itek Corp Optical Systems Division 10 Maguire Road Lexington, MA 02173	1	9
Perkin Elmer Corp Electro Optical Division Main Avenue Norwalk, CT. 06856 Attn: Mr. H. Levenstein	1	10
Hughes Aircraft Company Culver City, CA 09230 M.S. B-156 Attn: Mr. George Speak	1	11
Air Force Institute of Technology Wright-Patterson Air Force Bas, Oh 45433 Attn: Prof. R. Calico/ENY	1	12
Aerospace Corporation 2350 E. El Segundo Blvd El Segundo, CA 90245 Attn: Dr. G. T. Tseng	2	13
SD/YCD P.O. Box 92960 Worldway Postal Center Los Angeles, CA 90009 Attn: Lt Col T. May	1	14
SD/YCD P.O. Box 92960 Worldway Postal Center Los Angeles, Ca. 90009 Attn: YCPT/Capt Gajewski	1	15
Grumman Aerospace Corp South Oyster Bay Road Bethpage, NY 11714 Attn: Dr. A. Mendelson	1	16
Jet Propulsion Laboratory 4800 Oak Grove Drive Pasadena, CA 91103 Attn: Mr. D.B. Schaechter	2	17
MIT/Lincoln Laboratory P.O. Box 73 Lexington, MA 02173 Attn: S. Wright	1	18

MIT/Lincoln Laboratory P.O. Box 73 Lexington, MA 02173 Attn: Dr. D. Hyland	1	19
MIT/Lincoln Laboratory P.O. Box 73 Lexington, MA 02173 Attn: Dr. N. Smith	1	20
Control Dynamics Company 221 East Side Square, Suite 1B Huntsville, AL 35801 Attn: Dr. Sherman Seltzer	1	21
Lockheed Space Missile Corp 3460 Hillview Ave. Palo Alto, CA 94304 Attn: M. Lyons Bldg. 580 Organ. 52-56	1	22
Air Force Weapons Lab/DYP Kirtland AFB, NM 87117 Attn: Lt Col Donald Washburn	1	23
Air Force Flight Dynamics Laboratory Wright-Patterson AFB, Ohio 45433 Attn: Dr. Lynn Rogers	1	24
General Dynamics Convair Division 5001 Keary Villa Rd. San Diego, CA 92123 Attn: Ray Halstenberg	1	25
STI 20065 Stevens Creek Blvd Cupertino, CA 95014 Attn: Mr. R. C. Stroud	1	26
NASA Langley Research Ctr Langley Station Bldg 1293B M/s 230 Hampton, VA 23665 Attn: Dr. G. Horner Attn: Dr. Card	2	27
McDonald Douglas Corp Douglas Missile Space Systems Div 5301 Balsa Ave Huntington Beach, CA 92607 Attn: Mr. Read Johnson	1	28
Integrated Systems Inc P.O. Box 3702 Stanford, CA 94305 Attn: Dr. Narendra Gupta	1	29

Boeing Aerospace Company P.O. Box 3999 Seattle, WA 98124 Attn: Mr. Leo Cline MS 8W-23	1	30
NASA Johnson Space Center Ms. EA Houston, TX 77058 Attn: Robert Piland	1	31
TRW Defense Space Systems Group Inc Bldg 82/2054 One Space Park Redondo Beach, Ca 90278 Attn: Ralph Iwens	1	32
Department of the Navy Naval Research Laboratory Code 7920 Washington DC 20375 Attn: Dr. K.T. Alfriend	1	33
ARPA/STO 1400 Wilson Blvd Arlington, VA 22209 Attn: Lt Col A. Herzberg	2	34
Aerospace Corporation 2350 E. El Segundo Blvd El Segundo, CA 90245 Attn: Mr. J. Mosich	1	35
Aerospace Corp./Bldg 125/1054 Advanced Systems Technology Division 2400 E. El Segundo Blvd El Segundo, CA 90245 Attn: Mr. Steve Burrin	1	36
Airesearch Manufacturing Company of California 2525 West 190th Street Torrance, CA 90509 Attn: Mr. Oscar Buchmann	1	37
Analytic Decisions, Inc. 1401 Wilson Blvd Arlington, VA 22209 Attn: Mr. Gary Glaser	1	38
Analytic Decisions, Inc. 5336 West Rosecrans Ave Suite 203 Lawndale, CA 22209 Attn: Mr. Richard Mollicone	1	39

Center for Analysis 13 Corporate Plaza Newport Beach, CA 92660 Attn: Mr. Jim Justice	1	40
Air Force Wright Aeronautical Laboratory FIEE Wright Patterson AFB, OH 45433 Attn: Mr. Joseph Johnson	1	41
General Research Corporation P.O. Box 3587 Santa Barbara, CA 93105 Attn: Mr. G.R. Curry	1	42
General Research Corporation 7655 Old Springhouse Road McLean VA 22101 Attn: Mr. Thomas Zakrzewski	1	43
Hughes Aircraft Company Centinela Teale Streets Culver City, CA 90230 Attn: Mr. Ken Beale	1	44
Institute of Defense Analysis 400 Army Navy Drive Arlington, VA 22202 Attn: Dr. Hans Wolfhard	1	45
Kaman Sciences Corporation 1500 Garden of the Gods Road P.O. Box 7463 Colorado Springs, CO 80933 Attn: Dr. Walter E. Ware	1	46
Lockheed Missiles Space Company 3251 Hanover Street Palo Alto, CA 94304 Attn: Mr. Paul Williamson	1	47
MRJ, Inc 10400 Eaton Place Suite 300 Fairfax, VA 22030	1	48
Photon Research Associates P.O. Box 1318 La Jolla, CA 92038 Attn: Mr. Jim Myer	1	49
Riverside Research 1701 N. Fort Myer Drive Arlington, VA 22209 Attn: HALO Library, Mr. Bob Passut	2	50

Rockwell International 12214 Lakewood Blvd Downey, CA 90241 Attn: Russell Loftman (Space Systems Group) (Mail Code - SL56)	1	51
Science Applications, Inc. 3 Preston Court Bedford, MA 01730 Attn: Mr. Richard Ryan	1	52
TRW Bldg. R-5, Room 2031 Redondo Beach, CA 90278 Attn: Mr. Len Pincus	1	53
U.S. Army Missile Command Redstone Arsenal, AL Attn: DRSMI-RAS/Mr. Fred Haak	1	54
Naval Electronic Systems Command PME-106-4 National Center I Washington, DC 20360 Attn: Mr. Charles Good	1	55
Naval Research Laboratory EOTPO 4555 Overlook Ave., SW Washington, DC 20375 Attn: Dr. John McCallum	1	56
U.S. Army/DARCOM AMC Bldg 5001 Eisenhower Ave Alexandria, VA 22333 Attn: Mr. Bernie Chasnov	1	57
Grumman Aerospace Corporation Plant 25 Bethpage, NY 11714 Attn: Mr. Art Bertapelle	1	58
ARPA/STO 1400 Wilson Blvd Arlington, VA 22209 Attn: Mr. J. Larson	1	59
Sensor System Group 181 West Street Waltham, MA 02154 Attn: Joseph S. Titus	1	60

ARPA/STO  
1400 Wilson Blvd  
Arlington VA 22209  
Attn: Maj E. Dietz

1

62

**MISSION**  
**of**  
**Rome Air Development Center**

RADC plans and executes research, development, test and selected acquisition programs in support of Command, Control Communications and Intelligence (C<sup>3</sup>I) activities. Technical and engineering support within areas of technical competence is provided to ESD Program Offices (POs) and other ESD elements. The principal technical mission areas are communications, electromagnetic guidance and control, surveillance of ground and aerospace objects, intelligence data collection and handling, information system technology, ionospheric propagation, solid state sciences, microwave physics and electronic reliability, maintainability and compatibility.